DESIGN AND DEVELOPMENT OF A TEST RIG FOR

HYDRAULIC REGENERATIVE BRAKING SYSTEM

NORHIRNI BINTI MD ZAHIR

DISSERTATION SUBMITTED IN FULFILMENT
OF THE REQUIREMENTS FOR THE
DEGREE OF MASTER OF ENGINEERING SCIENCE

FACULTY OF ENGINEERING
UNIVERSITY OF MALAYA
KUALA LUMPUR

MARCH 2012

UNIVERSITI MALAYA

ORIGINAL LITERARY WORK DECLARATION

Name of Candidate: **NORHIRNI BINTI MD ZAHIR**

Registration/Matric No: **KGA090062**

Name of Degree: **Master of Engineering Science**

Title of Project Paper/ Research Report / Dissertation /Thesis ("this Work"):
Design And Development Of A Test Rig For Hydraulic Regenerative Braking System

Field of study: **Product Design and Advance Manufacturing Technology**

I do solemnly and sincerely declare that:

(1)   I am the sole author/writer of this Work;
(2)   This Work is original;
(3)   Any use of any work in which copyright exists was done by way of fair dealing and for permitted purposes and any excerpt or extract from, or reference to reproduction of any copyright has been disclosed expressly and sufficiently and the title of the Work an its authorship has been acknowledge in this Work;
(4)   I do not have any actual knowledge nor do I ought reasonably to know that the making of this work constitutes an infringement of any copyright work;
(5)   I hereby assign all and every rights in the copyright of this Work to the University of Malaya ("UM"), who henceforth shall be owner of the copyright in this Work and that any reproduction or use in any form or by any means whatsoever is prohibited without the written consent of UM having been first had and obtained;
(6)   I am fully aware that if in the course of making this Work. I have infringed any copyright whether intentionally or otherwise, I may be subject to legal action or any other action as may be determined by UM.

Candidate's Signature   Date

Subscribed and solemnly declared before,

Witness's Signature   Date

Name:
Designation:

ABSTRACT

In the effort to reduce the consumption of fossils fuels and consequently the release of greenhouse gasses into the atmosphere, there has been a growing interest in the automotive industry to develop and produce hybrid vehicles. Most of the attention on hybrid vehicles nowadays has been on electrical-based hybrids. However, the implementation of electrical-based hybrids on large, heavy vehicles is impractical, due to the size and cost of the batteries required. Additionally, the amount of energy that has to be regenerated for a large vehicle is also huge and this is unsuitable for electrical based systems, which has lower rate of energy transfer. Therefore application of hybrid technology for large vehicles using hydraulic systems has received recent attention. Hydraulic regenerative braking system (HRBS) is a system that reduces the vehicle speed by converting its kinetic energy into potential energy using axial piston pump, and storing it inside a hydro-pneumatic accumulator for future use. When the vehicle accelerates, pressurized working fluid discharges from the accumulator, which in turn converts the stored potential energy into kinetic energy by rotating the driveshaft, thus moving the vehicle.

This project is about using a test rig system to investigate the actual behavior of the newly designed HRBS. Concept selection has been conducted to select the most suitable components for the HRBS. Structural analysis by calculation and Finite Element Analysis (FEA) of the test rig chassis and some other parts is done by ABAQUS software. The test rig system is assembled and a simple controller is developed and integrates with the test rig to test the function of the test rig system. This study will have some limitation due to the situation where the chassis is existing from previous research and some of the parts are only an imitation of an actual 5-ton lorry condition during

cycle test. The result shows that the system is able to capture and release energy during operation which is an important characteristic in HRBS. It is also discovered that, the smaller the swash plate angle (plate inside axial piston pump), the longer the flywheel spins and the more pressure supplied from the accumulator to the system, the faster the flywheel can spin. With the result of this work, further installation of HRBS system onto an actual 5-ton lorry can be planned.

ABSTRAK

Dalam usaha untuk mengurangkan penggunaan bahan api fosil dan pembebasan gas-gas yang menyebabkan kesan rumah hijau ke atas atmosfera, timbul kesedaran terhadap industri automotif untuk mencipta dan menghasilkan kenderaan hibrid. Namun tumpuan banyak diberikan kepada kenderaan berasaskan hibrid-elektrik. Walaubagaimanapun, penggunaan kenderan hibrid elektrik keatas kenderaan yang berat adalah tidak praktikal kerana saiz dan kos bateri yang diperlukan. Selain itu, jumlah tenaga yang perlu dijana semula untuk kenderaan berat adalah banyak dan ini menyebabkan kenderaan jenis hibrid elektrik tidak sesuai untuk kenderaan berat. Maka baru-baru ini penggunaan teknologi hibrid untuk kenderaan berat yang menggunakan system hidraulik telah mendapat perhatian. *Hydraulic Regenerative Braking System* (HRBS) merupakan satu sistem yang mengurangkan kelajuan kenderaan dengan menukar tenaga kinetik kepada tenaga potensi dengan menggunakan pam omboh paksi dan menyimpannya dalam penumpuk hidropneumatik untuk kegunaan masa depan. Apabila kenderaan memecut cecair bertekanan dilepaskan dari penumpuk lalu menukarkan tenaga potensi yang disimpan kepada tenaga kinetik dengan memutarkan aci pacuan dan seterusnya mengerakkan kenderaan.

Projek ini mengenai pengujian sistem rig bagi megetahui keadaan sebenar sistem HRBS yang baru direka. Pemilihan konsep telah dijalankan untuk memilih komponen yang paling sesuai untuk HRBS. Analisis struktur dilakukan melalui pengiraan dan Analisa Unsur Terhingga (FEA) bagi struktur sistem rig dan beberapa bahagian lain dilakukan menggunakan perisian ABAQUS. Sistem rig dipasang dan kawalan yang ringkas dibina dan diintegrasikan dengan sistem rig bagi menguji keberkesanan sistem rig tersebut. Kajian ini mempunyai beberapa batasan disebabkan oleh struktur sistem rig merupakan warisan dari penyelidikan terdahulu dan beberapa bahagian adalah hanya peniruan

keadaan sebenar lori 5 –tan semasa ujian kitaran. Hasil kajian mendapati sistem mampu bertindak sebagai HRBS apabila sistem dapat menyimpan dan membebaskan tenaga semasa operasi, dimana ia merupakan satu ciri penting dalam HRBS. Kajian juga menunjukkan semakin kecil sudut condong omboh (plat di dalam pam omboh paksi), semakin lama roda tenaga dapat berputar dan lebih banyak tekanan yang dibekalkan dari penumpuk ke sistem, lebih laju roda tenaga boleh berputar. Dari hasil kajian ini, pemasangan sistem HRBS ke dalam lori sebenar 5-tan dapat dirancang.

ACKNOWLEDGEMENT

...........THANK YOU..........

The Future of Renewable Energy

CONTENTS

LIST OF FIGURES

LIST OF TABLES

NOMENCLATURE

Symbol		Description	Unit
A	=	Area where force is acting	m^2
D	=	Displacement, cubic centimeter per revolution	$cc.rev^{-1}$
d	=	Piston diameter	cm
D_a	=	Actual displacement	$cc.rev^{-1}$
D_{FW}	=	Flywheel diameter	feet
D_T	=	Theoretical displacement	$cc.rev^{-1}$
E	=	Young modulus of beam	$N.m^{-2}$
E_{mat}	=	Young Modulus of material	GPa
E_m	=	Mechanical Efficiency (0 – 1.0)	-
E_v	=	Volumetric efficiency (0-1.0)	-
F	=	Force acting	N
F_{DB}	=	Force of drum brake	N
F_{FW}	=	Force of flywheel	N
g	=	Gravity, 9.81	-
I_{Total}	=	Total inertia on rotational axis	$kg.m^2$
I	=	Moment inertia of beam	m^4
L	=	Total length of system	mm
m	=	Mass of Lorry	kg
m_{DB}	=	Mass of drum brake	kg
m_{FW}	=	Mass of flywheel	kg
N	=	Maximum angular velocity	RPM
P	=	Reacting force	N
P_F	=	Fluid pressure	k.Pa

P_{out}	=	Mechanical power output	watt
Q	=	Volume flow rate	$L.min^{-1}$
R	=	Distance between the piston axis and the cylinder barrel axis	cm
R_A	=	Reaction force acting on point A	N
R_B	=	Reaction force acting on point B	N
R_C	=	Reaction force acting on point C	N
T	=	Torque	N.m
v	=	Speed of lorry	$m.s^{-1}$
Z	=	Total number of piston	-
α	=	Fraction of distance A and B to total length	-
α_{max}	=	Maximum swash plate angle	θ
σ_y	=	Yield shear stress	MPa
ω	=	Angular velocity	RPM
ρ	=	Density	$kg.m^{-3}$

ABBREVIATION

ABAQUS	=	Finite Element Analysis Software
AC	=	Alternating Current
CATIA	=	Computer Aided Three-Dimensional Interactive Application
CNC	=	Computer Numerical Control
CO_2	=	Carbon Dioxide
CVT	=	Mechanical Variator
DAQ	=	Data Acquisition System
DC	=	Direct Current
ECU	=	Engine Control Unit
EPA	=	Us Environmental Protection Unit
FEA	=	Finite Element Analysis
FMVSS	=	Federal Motor Vehicle Safety Standards
HC	=	Hydrocarbon
HEV	=	Hybrid Electric Vehicle
HHV	=	Hydraulic Hybrid Vehicle
HRBS	=	Hydraulic Regenerative Braking System
KERS	=	Kinetic Energy Recovery Systems
MHV	=	Mechanical Hybrid Vehicles
NGV	=	Natural Gas Vehicle
NKR 71 E	=	Isuzu 5 Ton Lorry
NO_X	=	Nitrogen Oxide
PC	=	Personal Computer
PHHV	=	Parallel Hydraulic Hybrid Vehicle
ROS	=	Remote Optical Sensor
RPM	=	Rotation Per Minute
SCADA	=	Supervisory Control And Data Acquisition
UPS	=	Uninterruptible Power Supply
3D	=	Three Dimensional

CHAPTER 1

INTRODUCTION TO HRBS

1.1   Background

The present production and use of non-renewable energy sources especially fossil fuels pose a serious threat to the global environment, particularly in relation to emissions of greenhouse gases (principally, carbon dioxide – CO_2) and the consequent climate change. As a consequence, the auto industry has embarked on many improvements within the automotive industry which has led many researchers to develop vehicles that consume less fuel, require lower cost of maintenance, as well as emit less emission of noxious fumes into the environment. This has resulted in the development of various green technologies and innovation in vehicle technologies in several types of vehicles such as solar, electric, hydrogen fueled and hybrids including hydraulic hybrids.

Hydraulic regenerative braking system (HRBS) or also known as Hydraulic Hybrid Vehicle (HHV) proves to offer better green solution in the short-term as the system and maintenance is cheaper particularly for heavy vehicles. The HRBS energy storage mechanism concept is similar to Mechanical Hybrid Vehicles (MHV), which use flywheels to store energy. However in the HRBS, the kinetic energy of a vehicle in braking which is usually lost as heat is captured into hydropneumatic accumulators. The energy is then reused to accelerate the vehicle. This technology has been reconsidered these past few years as an alternative green technology, particularly for the application on larger vehicles.

The sustainability of the system lies on the working principle which is achieved by using a hybrid hydraulic pump/motor device, which can function both a hydraulic pump and a hydraulic motor. During braking, when the driver steps on the brake pedal (slowing the vehicle), the HRBS will be activated in pump mode. The hydraulic pump will pump hydraulic fluid into the accumulator, using the energy from the rotating driveshaft of the vehicle, thus capturing kinetic energy. Then during acceleration, as the system receives the input from the throttle pedal the system will activate acceleration mode and the previously operation through the control system. Previously stored energy in the accumulator is reconverted into kinetic energy via the hydraulic motor, which then provides accelerating torque to the driveshaft. These processes that occur in HRBS will therefore create renewable energy.

The HRBS will be most beneficial in urban driving cycles where frequent acceleration /braking cycles occur. Therefore, with this system, total energy needed from the engine is reduced and the kinetic energy which would have been lost as heat is effectively recovered. Hence, fuel requirement and exhaust emissions are reduced.

1.2   Research Question

As of 2011, the human population across the globe owns around 775 Million motor vehicles to fuel, repair, park and run, almost exclusively using petroleum and natural gas (McKillop, 2011). With the reduction of fuel supply and the increase in of fuel prices worldwide, vehicle manufacturers are moving towards making sustainable vehicles where hybrid electrical vehicles (HEV) have become the most popular choice. However, HEV is not suitable for heavy vehicles. In this situation, a hydraulic hybrid vehicle (HHV) is more "sustainable" compared to HEV. This is explained by the

situation whereby larger HEV vehicles require more batteries thus making the cost not viable besides taking longer, in terms of time, for charging. Furthermore, the reliability and predictability of lead acid batteries are costly and if not installed and maintained correctly, thus causing failures during operation (Bitterlin, 2010). Therefore, HHV is one of the better solutions in producing sustainable heavy vehicles.

The benefit of HRBS is well known now, however, all the research is from outside Malaysia. The knowledge on how to develop a hydraulic hybrid vehicle has not been explored fully within the country. Therefore it is important for this research to be conducted in order to fill-in the knowledge gap. This study will focus on large, heavy vehicles. This is because large vehicles such as buses and trucks require substantial amounts of energy to operate; hence the kinetic energy that could be saved would also be significant. This would be more evident especially for vehicles operating in urban areas, where repeated stop-go driving patterns are more typical.

A major problem when it comes to designing a hybrid car is the necessary modifications required on the existing vehicle. Most hybrid vehicles produced today have totally different configurations from normal cars making it impossible for consumers to retrofit the system onto their existing vehicle. Conversely, the new design HHV for a 5 ton lorry suggested in this research should be able to be installed on a vehicle without the need for major modifications.

A test rig setup is constructed instead of using an actual lorry to test the HRBS idea as it would be considered inefficient in terms of space and cost. The existing chassis of the test rig used in this study is modified to better suit the requirement to prove the HRBS concept. Safety measurement must be taken as this test involves moving load of

flywheel and high pressure accumulator which can be explosive if safety precautions are not taken during commissioning test.

1.3   Objective of Study

i.   To design a Hydraulic Regenerative Braking System (HRBS) for a 5 ton lorry with little modification required.

ii.   Design and fabrication of a test rig that can be used to simulate the HRBS design.

iii.   Modification of existing test rig chassis that can withstand the load of new flywheel and shaft.

iv.   Modeling and analysis of structural geometry of important parts on test rig system.

v.   To perform commissioning test of the test rig system to observe the actual response of the system during testing.

1.4   Scope and limitation of Study

1.4.1   Scope

This research is focused on the development of HRBS test rig based on a 5-ton lorry. The lorry used in this study is the ISUZU NKR 71-E. The calculation for components selection is therefore selected based on this lorry's specifications. The test rig system design includes the existing chassis from a previous study by Chan (Chan, 2010). The design and structural analysis of test rig components (accumulator stand, power pack stand and test rig chassis) will be presented. Design consideration includes material selection, fabrication process, interaction between components and ease of assembly.

The components in 3D model will be analyzed for its structural geometry using ABAQUS software to optimize the design in terms of safety.

1.4.2 Limitation

The design is limited to the purchased equipment's geometry and its function. The functions of equipment will determine its position in the test rig system. Design of the component parts is also limited based on the fabrication process available which is mostly by welding and CNC milling. Simplicity of design is needed to reduce cost and fabrication time. This study will have some limitations due to the situation where some of the parts are only an imitation of actual lorry condition during cycle test. The chassis of the test rig is existing from previous research and therefore limitations on the work that can be done exist, as some parts were already pre-fixed on the chassis. The controller for commissioning is also a simple controller to test the functioning of the test rig system.

1.5 The Structure of Thesis

In general this thesis report contains 6 chapters briefly described as below:

Chapter 1 Introduction to HRBS:

Introduction to HRBS contains the general introduction on the current scenario and research questions posed that gives motivation in wanting to conduct this research. The objective, scope and limitation of the research are presented.

Chapter 2 Literature Review:

In this chapter, literature reviews of related technologies on HRBS are presented. This chapter will provide some information to the reader in order to better understand the subject matter throughout the thesis.

Chapter 3 Design of HRBS System:

Chapter 3 presents the detail on the steps taken to develop the HRBS. Based on the literature review, the HRBS configuration was decided and detailed concept of the HRBS was expanded on until and including the HRBS configuration stage on a 5 ton lorry.

Chapter 4 Development of Test Rig:

The chapter begins with a brief introduction of the chapter. Optimization results of chassis and Finite Element Analysis (FEA) of important parts are presented. The final assembly of the test rig and controller integration preparation are presented.

Chapter 5 Commissioning of HRBS test rig:

This chapter describes the commissioning test performed to evaluate the test rig system. Sets of data will be presented and the efficiency of the system will be discussed.

Chapter 6 Conclusion:

Chapter 6 includes the summary and recommendation for improvement on this subject will be presented for future work.

CHAPTER 2

LITERATURE REVIEW

2.1 Introduction

This chapter will start with the description on hybrid vehicles followed by the HRBS system. Past researches on HRBS systems and work related to the development of the test rig are presented, beginning with i) Background on hybrid vehicle; ii) introduction to HRBS and its application; iii) HRBS major components and calculation to select the component; iv) HRBS components on lorry; v) introduction to test rig and finally; vi) commissioning test of test rig.

2.2 Hybrid vehicle

The introduction of hybrid vehicles in the automotive industry has given rise to much interest from buyers. There are various types of hybrid vehicles such as electric hybrid, electric combined with solar hybrid, kinetic energy recovery system (KERS) and also hydraulic hybrid as shown in Figure 2.1. An electrical hybrid vehicle is usually a vehicle fitted with a regenerative system that captures kinetic energy during braking and stores it electrically inside a battery to be reused later when the vehicle starts to accelerate. Next, an electrical hybrid combined with solar's works similarly in principle to electric vehicles. The difference of this type of hybrid vehicle is that the energy to propel the car from stop is by electric generated from the solar panel located on the roof

of the vehicle. This type of car is most suitable in countries with substantial sunlight coverage and the energy captured is limited by the size of the solar panel.

Toyota Prius- Hybrid Electric
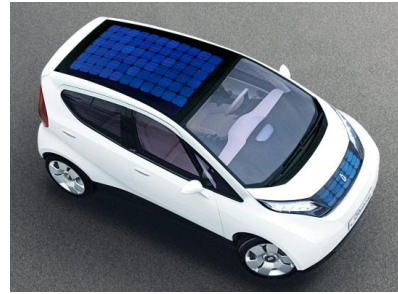
Blue Car- Hybrid Electric & Solar

Lightning,Beacon Power New York- Hydraulic Hybrid

Renault and Williams F1 Teams- Kinetic Energy Recovery Systems (KERS)

Figure 2.1 Various hybrid vehicles in the market (Boretti, 2010).

Additionally, KERS also captures kinetic energy during braking and stores it in a reservoir (either in a flywheel or a battery) (Boretti, 2010). The earlier development of KERS was seen in F1 cars. The Formula 1 racing, where it was introduced in 2009 was implemented by the Ferrari, Renault, BMW and McLaren teams. This technology however has been discontinued from F1 as the technology adds on weight to the racing vehicle which raises the vehicle's center of gravity.

The last type of hybrid vehicle is the hydraulic hybrid vehicle. This type of hybrid system also captures kinetic energy during braking, and the energy is stored inside pressurized accumulators. An accumulator is a special tank filled with inert gas, usually nitrogen that can be compressed and decompressed. The biggest advantage in comparing this technology to electric hybrid and KERS is the rate of charging which is much faster as compared to a battery or flywheel. Although there are many types of

hybrid vehicles, each type has its own advantages and disadvantages, which depends on the user's needs and situation.

2.2.1   Hydraulic Hybrid Vehicle

While the electric hybrid vehicle uses the battery for energy storage (BMW, 2007), the hydraulic hybrid uses an accumulator to store the energy, with the help of an axial piston pump (Vint & Gilmore, 1988). Figure 2.2 illustrates the difference between these two types of hybrid systems. The question as to why choose hydraulic over electric hybrid is simply based on the concerns of vehicle size. The larger the vehicle, more batteries will be needed for operation. This will not be viable in terms of cost and will not attract buyers. Furthermore, the hydraulic system is able to store more energy at a faster rate compared to electrical system (Hui & Junqing, 2010). The hydraulic hybrid systems are much larger than the electric hybrid, which is why it is more suitable for heavy vehicles compared to the electrical systems, which are more reasonable for small cars (Hui, Ji-hai, & Xin, 2009; Swing, 2008a, 2008b).
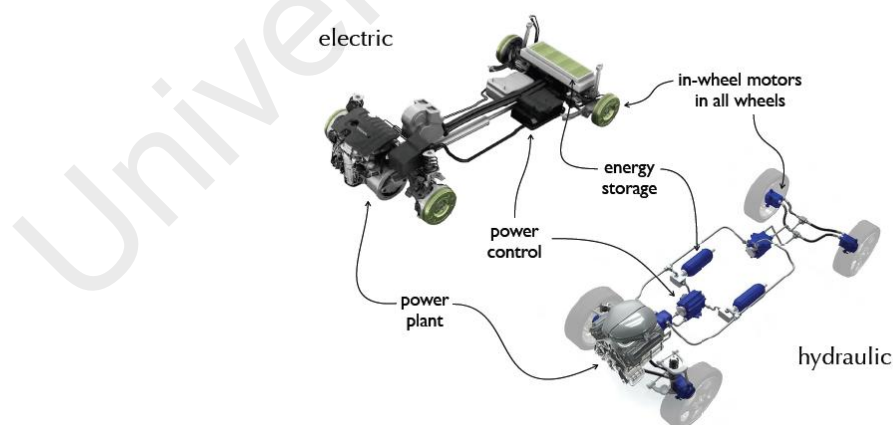
Figure 2.2 Electric hybrid and hydraulic hybrid vehicle (Hui, Lifu, Junqing, & Yanling, 2010b).

The hydraulic hybrid systems will benefit the most, especially for heavy vehicle operations, when stop and go mostly occurs. This is because the possibility of saving more energy in a hydraulic accumulator is higher in a short time (high power density) (Lindzus & Contact, 2010). Simulations done by the company UPS on a 20 ton garbage truck shows that during operation, the regenerated energy from previous braking can provide driving torque up to 2500 Nm, which can move the vehicle in third gear on level ground (Bracht, Ehret, & Kliffken, 2009). Figure 2.3 shows the performance graph of storage loading versus brake energy for three different types of vehicles (Lindzus & Contact, 2010). The graph shows that only the refuse truck using the hydraulic accumulator can absorb complete braking energy in a short time. This is because the hydraulic hybrid system uses hydraulic accumulator that can capture the braking energy faster compared to battery.

Refuse Truck 25 to, 10 km/h, 1,5 m/s²	Delivery Vehicle 7 to, 30 km/h, 2,5 m/s²	Passenger Car 1,5 to, 50 km/h, 2 m/s²
Only the hydraulic accumulator is sufficient fast to absorb the complete breaking energy	The hydraulic accumulator is suitable and the lithium battery can largely recover the braking energy	The Lithium Battery fits well, however the lead battery is never sufficient to recover a part of the braking energy

Hydraulic Bladder Accumulator, Lithium Battery, Lead Battery and **real Breaking Energy**

Figure 2.3 Storage loading speed vs. brake energy (Lindzus & Contact, 2010).

2.3   Hydraulic Regenerative Braking System (HRBS)

The hydraulic regenerative braking system (HRBS) is a mechanism that reduces vehicle speed by converting some of the kinetic energy into potential energy by storing it inside a hydraulic accumulator for future use (Lin, Hu, & Gong, 2010). The system is made up of four main components: working fluid, reservoir, pump/motor (variable-displacement, axial-piston type pump), and accumulator, to power a vehicle at low speeds and to augment the gasoline engine (Achten). Normally, when the driver presses on the brake pedal, friction force is applied on the disc brakes. In this situation, the vehicle's kinetic energy is transferred as heat energy and wasted into the air (Vint & Gilmore, 1988). In order to make the system work and capture the kinetic energy, the hydraulic axial piston pump has to work in dual mode. Previous research conducted on bent-axis piston pump showed that it is capable of operating in dual function. The bent-axis piston pump/motor has been designed for hydraulic hybrid vehicles by the US Environmental Protection Agency (EPA) (Abuhaiba & Olson, 2010). In an axial piston the major part is the swash plate angle because it determines the mode of the pump (pump or motor mode) (Kaliafetis, 1995).

During braking, the hydraulic axial piston pump installed in the system operates as a pump and starts charging the high–pressure accumulator. The charging takes place when the system reverses the direction of the fluid, with pressure normally drawn from high –pressure accumulator to low-pressure accumulator to move forward. When this happens, the hydraulic fluid moves in the opposite direction, or in other words trying to move the vehicle in the reverse direction. Therefore instead of using friction to stop the vehicle, the rear wheels move in the reverse direction, which is opposite to the direction where it currently moves to slow down the vehicle (Stecki & Matheson, 2005). This

operation will take the pressure off the engine and thus helps to extend the life of the engine (Carnago, Koch, Pawlik, & Smith, 2007). Supposing that the accumulator reaches maximum capacity before the vehicle has stopped, conventional brakes are then used to bring the vehicle to a stop. When the vehicle accelerates from stationary mode, pressurized working fluid discharges from high-pressure accumulator. The pressurized fluid converts potential energy into kinetic energy (pump/motor) and rotates the driveshaft to move the vehicle (Norhirni, 2011). This can be illustrated by referring to Figure 2.4 (Norhirni, 2011).
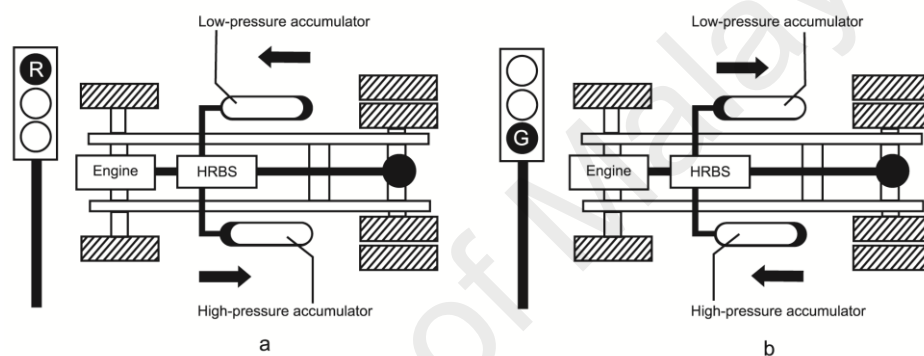
Figure 2.4 (a) System during braking (b) System during acceleration (Norhirni, 2011).

When the vehicle starts to move, the wheels will rotate. The rotational motion of the wheel (on stock brake and regenerative brake) is measured using position transducer i.e. rotational sensors (Figure 2.5). The sensors will rotate with the wheel (Carnago, et al., 2007) and register an input as a mechanical movement, creating an electrical signal as an output through voltage to the Engine Control Unit (ECU) (Carnago, et al., 2007). This will determine the amount of fuel and ignition timing. It is important that the sensor is placed in the right position as the result will determine the efficiency of the system.
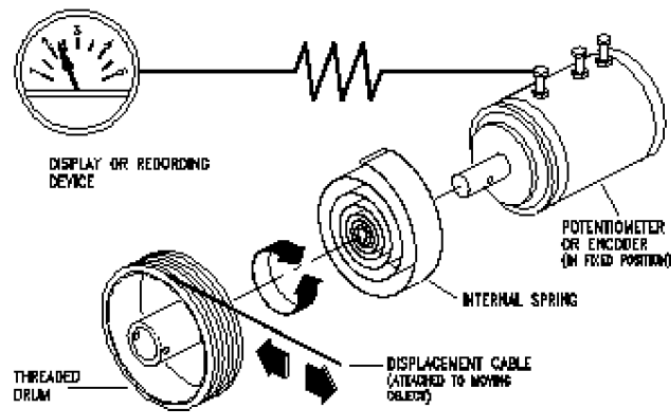
Figure 2.5 Angular position sensors (Carnago, et al., 2007).

Compared to a normal vehicle, a combination of pump/motor with engine will have higher efficiencies at higher load. When the required power needed to propel the vehicle exceeds the maximum power provided by the pump/motor, the engine will work exclusively while at the same time the hydraulic pump is used to adjust engine working load. This is done by changing pressure function and keeping propulsion component in the high load/high efficiency region. However, the configuration of HRBS should also be considered as it affects the energy regeneration efficiency.

Basically, there are two types of configuration for the system which is the series (Figure 2.6) (Achten) and parallel type. The series type replaces conventional transmission and driveline with hybrid hydraulic powertrain (Achten). The energy is transferred from the engine to the drive wheels through fluid power. However, major modification needs be made on an existing the vehicle driveline to obtain the series type configuration.

① constant displacement hydrostatic pump/motor
② hydraulic transformer
③ common pressure rail: high pressure
④ common pressure rail: low pressure
⑤ hydraulic accumulator
⑥ first, smaller power plant
⑦ second, larger power plant
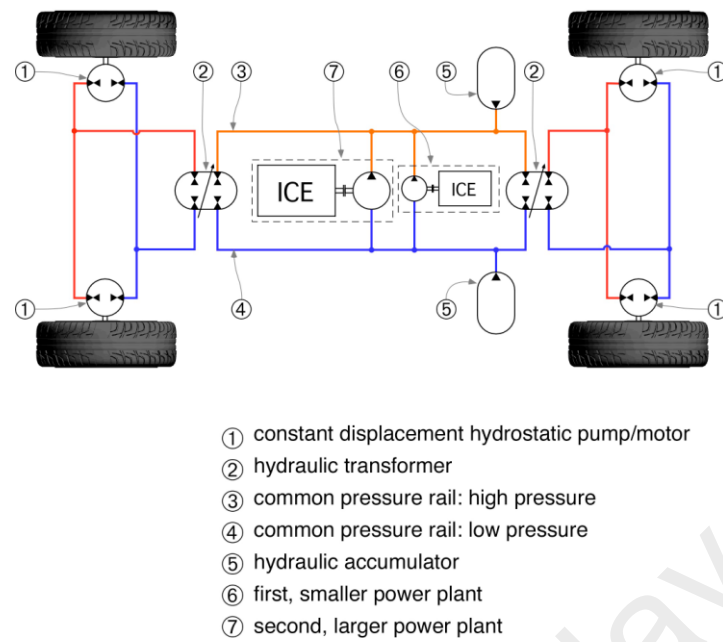
Figure 2.6 Schematic of Serial Hydraulic Hybrid Propulsion System (Achten).

For the parallel type, the existing driveline of the vehicle is used together with the hydraulic system requiring comparatively less modification to install the necessary components. In past research, simulation and experimental results show that parallel hydraulic hybrids can effectively regenerate and reused recovered braking energy, therefore improved the working performance of vehicle and reduced fuel consumption (Hui & Junqing, 2010). Figure 2.7 (a) (Hui, et al., 2009) and (b) (BMW, 2007) are examples of schematic design of parallel hydraulic hybrid propulsion system that has been produced by other research.
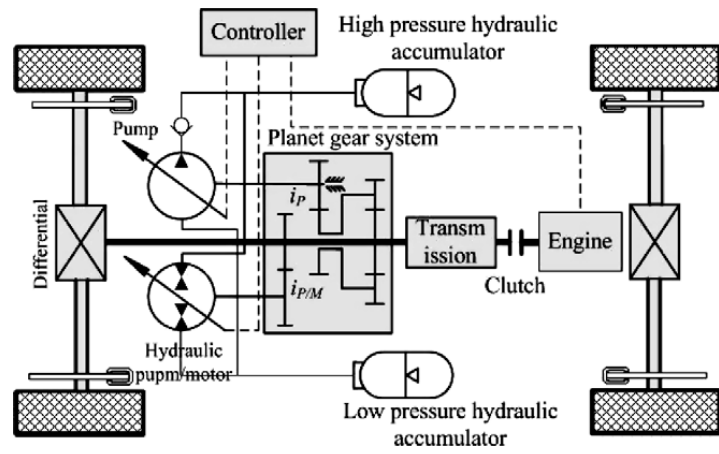
(a)
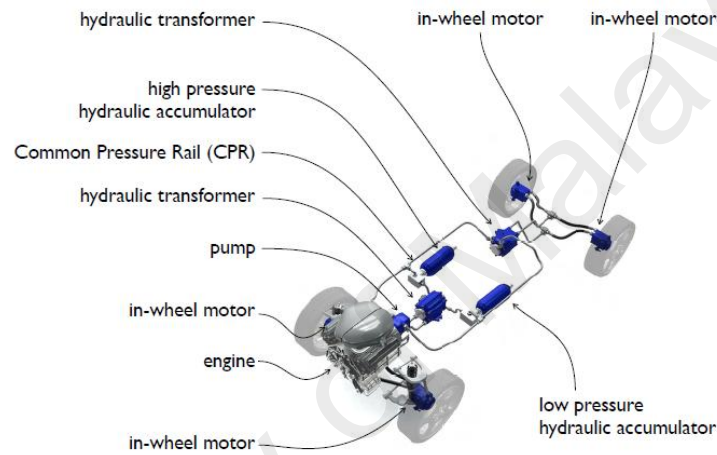
(b)

Figure 2.7 Schematic of Parallel Hydraulic Hybrid Propulsion System, (a) (Hui, et al., 2009)and (b) (BMW, 2007).

Although many researches have been done on this type of configuration, the controller for the system varies depending on the researcher. An example for controller development can be referred to a work done by a group of researchers from University of Colorado (Swing, 2008a). The controller is designed using Matlab software and tested on diesel truck.

2.3.1 HRBS Application

The design of HRBS is made to be applicable for various types of vehicle and also for energy storage system (B. Rexroth, 2011). Figure 2.8 shows some example where the system can be applied. Accordingly, industrialized countries are examining a whole range of new policies and technology issues to make their energy futures 'sustainable' (Della & Rand, 2001). The test rig can also function as an uninterruptible power supply (UPS) to provide emergency power when the utility main source fails (Bitterlin, 2010). The system can be considered as a system that can produce sustainable energy for future usage.

| Truck Crane | Forklift | Bus |

| Truck | Auto Tram | Refuse Truck |

Hybrid Injection Molding Machines, Bosch Rexroth, German

Uninterruptible power supply (UPS)

Figure 2.8 Various application of the system.

2.4   HRBS Major Components

There are two major components in HRBS namely the axial piston pump (to capture the kinetic energy and to propel the vehicle) and the accumulator (to store the energy captured).

2.4.1   Axial Piston Pump

Hydraulic axial piston units are widely used for industrial application, mobile machinery and hydraulic hybrids. Current designs of hydraulic axial piston units are limited to operate in one or two quadrants (single mode). Classical solutions of four quadrant operation (dual mode), requires extra hydraulic axial piston units that are complex, bulky, heavy and expensive. In order to make the system work and collect the kinetic energy, the hydraulic axial piston unit has to be able to store more energy and work in dual mode. However, most hydraulic axial piston units available off-the-shelf are made with fixed displacement-static control with small flow rates, which are not suitable to implement on heavy vehicles. Besides, the hydraulic axial piston units available are in the form of pumps or motors, which can only function as single mode device.

With the development of variable displacements axial piston pump, the dual mode function is possible. The swash plate feature inside the pump, as shown in Figure 2.9 is the main part of the pump. The pump is controlled by its swash plate angle; therefore, by varying swash plate angle, the flow and pressure of an axial piston can be controlled. The pump is an assistant power source in this system which minimizes the lower energy density of the accumulator. This will help to make the engine work in high efficiency during charging time (Hui, et al., 2009). Furthermore, variable displacement pump is

adjustable via the changes in the swash plate inclination whether to capture (pump mode) or to produce desired torque (motor mode). The shaft will transmit the torque from engine of the vehicle to the driven axle to propel the vehicle (Thompson, 1980).
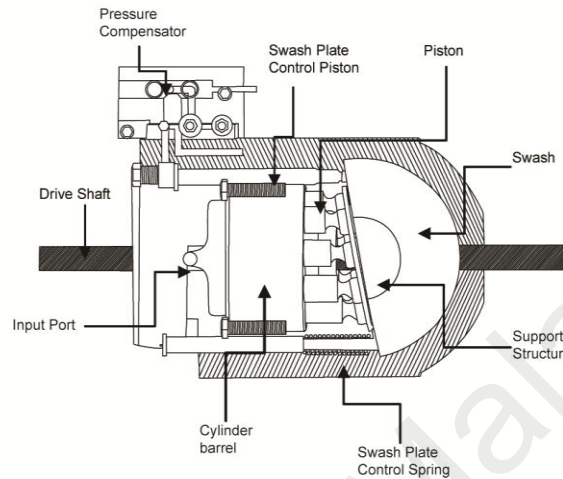
Figure 2.9 Pressure compensator and hydraulic axial piston pump (Norhirni, 2011).

When system pressure reaches the preset levels of the pressure compensator, the hydraulic system will be constrained and therefore stop operating. The position of the swash plate with zero swash plate angle means the hydraulic component is in idle position and does not functions as neither pump nor motor. Pressure compensator is connected to the hydraulic component through the swash plate control piston and directional control valve that connect through the hydraulic component output port. During braking, hydraulic pump/motor functions as pump to stop vehicle. Nitrogen gas in the accumulator bladder is compressed, hydraulic fluid flows out of tank into hydraulic pump, then enters high pressure accumulator. When it functions as pump mode, swash plate directional control piston will be pushed to the right by a servo motor which in turn pushes the swash plate to the counterclockwise direction (Norhirni, 2011) as illustrated in Figure 2.10.
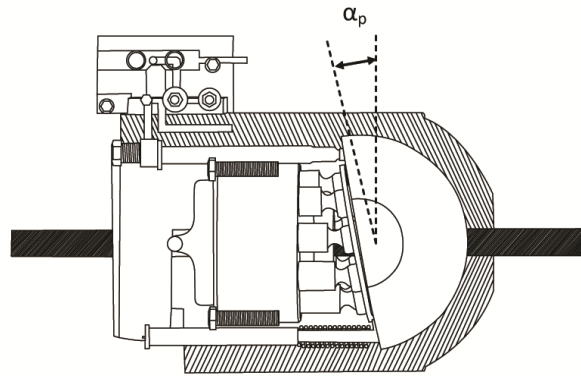
Figure 2.10 Swash plate position and swash plate angle at hydraulic axial piston unit operating as pump (Norhirni, 2011).

During acceleration, hydraulic pump/motor functions as a motor to propel the vehicle. Nitrogen gas in accumulator bladder is expanded, hydraulic fluid flows out of accumulator into hydraulic motor, then enters low pressure tank. In motor mode function, the swash plate directional control piston will be pulled to the left by a servo motor which eventually pulls the swash plate to the clockwise direction (Norhirni, 2011) as shown in Figure 2.11.
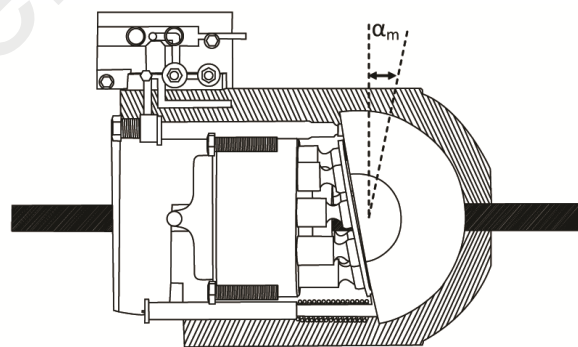
Figure 2.11 Swash plate position and swash plate angle at hydraulic axial piston unit operating as motor (Norhirni, 2011).

During braking, the axial piston pump will works as a pump and start pumping hydraulic fluid flows from the reservoir to the high-pressure accumulator thru hydraulic transmission line. The reservoir is an accumulator working at much lower pressure. The Nitrogen gas (N_2) inside the bladder accumulator is an inert gas making it possible for compression. As the gas is compressed, the internal energy is increased (pumping mode) (Bylsma, 2003). When accelerating, the axial piston pump acts as a motor and the hydraulic fluid flows back in reverse direction. The high pressure accumulator starts emptying and hydraulic fluid flows back to reservoir.

2.4.2 Accumulator

In a hybrid vehicle, the capability of storing energy is the most important factor to determine the efficiency of the system. In a HEV, energy is captured and stored in batteries while for a HHV the energy is stored by the accumulator. Accumulator's main function is to serve as energy storage in a hydraulic system. Besides that the accumulator also function as (Pete, 2008);

i.   To supply oil for high transient flow demands when the pump is at low performance.

ii.   Reduce the pump ripple and pressure transients.

iii. During valve closures or actuator hitting stops, the accumulator will absorb hydraulic accumulator shockwaves.

iv.   At low demand, the accumulator is used as primary power source.

v.   Assist in accommodating thermal expansion of fluid in the system.

There are four types of accumulators; bladder, diaphragm bladder, piston (either spring or gas controlled) and metal bellows. Each type of accumulator has different ways of operating and the choice for a system is based on the given application and depends on required speed of accumulator response, weight, reliability and cost (Pete, 2008). In a hydraulic hybrid vehicle, the choice of accumulator is the bladder type. The advantages of the bladder type is fast response, no hysteresis and not susceptible to contamination. The bladder accumulator reacts very fast to changes in hydraulic system pressure because of the inside structure of the accumulator that uses a bladder instead of a piston. Therefore this type of accumulator is best for pressure pulsation damping (Pete, 2008).

The inside structure of the accumulator consists of a pressure vessel with an internal elastomeric bladder together with nitrogen gas on one side and hydraulic fluid on the other side. Figure 2.12 shows the schematic of bladder accumulator and the stages of operation. Referring to Figure 2.12 (a), when the accumulator not operating, the pressure is at nominal pressure or pre-charged. When the accumulator starts to operate, nominal pressure is applied and the bag will be compressed to its fully compressed state in as in Figure 2.12 (b). The nitrogen pressure and the hydraulic pressure are equal when the bag is fully compressed. As the system pressure drops, the bag expands forcing fluid from the accumulator into the system as in Figure 2.12 (c). Expansion of bag will continue until the bag pressure equals the hydraulic pressure (Figure 2.12 (d)). However this situation is undesirable in maintaining the accumulator live as it will be in over expanded form. Therefore a poppet valve acts to keep the bag in the accumulator from being pulled into the downstream tubing to avoid overexpansion.
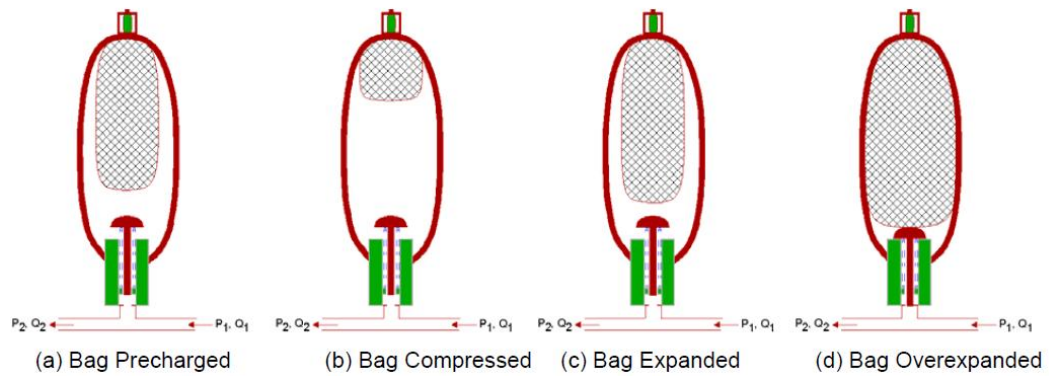
Figure 2.12 Bladder accumulator schematic (Pete, 2008).

The function of bladder accumulator in HHV has been demonstrated by the Eaton Company (Li, Ven, & Sancken, 2007). The braking energy successfully recorded was 380 kJ from a 1 ton (1000kg) vehicle travelling at 100km/h where 50 litres volume is required. Energy captured is stored by pumping pressurized oil into bladder accumulator. When accelerating, the energy inside the accumulator in form of compressed gas pushes the stored oil back into the hydraulic circuit, thus propelling the vehicle (Li, et al., 2007).

2.5 Design Calculation of HRBS Components

The key parameter of HRBS was determined by design calculation which will be presented in the proceeding chapter. The calculation result will be used to determine the proper size of axial piston pump and accumulator for a 5 ton lorry. This subsection is to introduce the equations that will be used to determine the sizing of the components of the system particularly the axial piston, the accumulator and the flywheel.

2.5.1 Pump Sizing Calculation

The mechanical power output for motor (Kirschen, 1985) is given as;

$$P_{out} = \frac{2\pi \times \mathrm{T} \times \mathrm{N}}{60} watt \qquad \text{Eqn. (2.1)}$$

Where;

T = torque, Nm

N = speed, rpm

And the torque output for motor is given as;

$$T = \frac{D \times P \times E_m}{2 \times \pi \times 1000} Nm \qquad \text{Eqn. (2.2)}$$

Where;

D= Displacement, cc/rev

P_F= Fluid pressure, kPa

E_m = Mechanical Efficiency (0-1.0)

Stall torque must be 1.5 times the running torque in designing stage (Gould, 2010). At normal application, the torque (mechanical) efficiency at stall will be between 75% and 95% for most motors (Gould, 2010). Therefore, the assumption for motor minimum efficiency condition taken as;

$E_m = 75\% = 0.75$

Another important detail to consider is the maximum output pressure. The maximum output pressure is assumed to be P = 300 bar = 30, 000kPa which is based on the

assumption that this can be supported by the accumulator. From Equation (2.2), the theoretical displacement equation is derived for the hydraulic pump, D_T;

$$D_T = \frac{T \times 2\pi \times 1000}{P \times E_m}$$

Eqn. (2.3)

By referring to the formula stated by Zhai (Zhai, 1978) for piston diameter, d;

$$d = (1 \sim 1.09) \sqrt[3]{\frac{D_a}{Z}} \quad cm$$

Eqn. (2.4)

Where;

d = Piston diameter

D_a= Actual displacement, cc/rev

Z = Total number of piston

The distance between the piston axis and the cylinder barrel axis, R;

$$R = (0.22 \sim 0.27) Z \sqrt[3]{\frac{D_a}{Z}} \quad cm$$

Eqn. (2.5)

Therefore, theoretical displacement for the design hydraulic pump (Handbook, 2012) express is;

$$D_T = \frac{\pi}{4} d^2 \times 2RZ \tan \alpha_{max}$$

Eqn. (2.6)

Where;

D_T = Theoretical displacement, cc/rev

R = Distance between piston axis and cylinder barrel axis

α_{max} = Maximum swash plate angle

2.5.2 Accumulator Sizing Calculation

To determine the size of a suitable accumulator for the system, the volume flow rate of hydraulic fluid equation, Q (E. M. Rexroth, 2012) is used;

$$Q \ (L/min) = \frac{E_v \times D \times N}{1000}$$
Eqn. (2.7)

Where;

E_v= Volumetric efficiency (0-1.0)

N= Maximum angular velocity

D= Displacement, cc/rev

2.5.3 Flywheel Calculation

The actual situation of the vehicle on the road is done by representing the inertia of the vehicle with a rotating flywheel (Vint & Gilmore, 1988). Modeling capability of flywheels is determined by energy equation;

$$\frac{1}{2}mv^2 = I\omega^2$$
Eqn. (2.9)

Where;

m = mass of lorry

v = speed of lorry

I = Total inertia on rotational axis

ω = angular velocity in rpm

2.6   Configuration of HRBS Critical Component of on Lorry

After deciding on the components for HRBS, the configuration of the components on the lorry is decided. Safety is one of the most important aspects in automobile industry. The automotive manufacturer has developed new passive and active vehicle safety systems to ensure the safety of passengers. Therefore, in any hybrid vehicle design, placement of the auxiliary power source components and its mounting must also satisfy safety guidelines. The most critical design in hydraulic hybrid is the mounting of axial piston pump and accumulator. In the study done by Khoo (Khoo, 2010), the rigidity and safety of mounting design and position of axial piston unit and hydro-pneumatic accumulator is investigated. The frontal crash is performed using ABAQUS according to Federal Motor Vehicle Safety Standards and regulations (FMVSS). The modeling includes the truck frame, engine and transmission, tires, 71cc axial piston unit (Figure 2.13) and its mounting, driving cabin, two 32 liter bladder accumulators (Figure 2.13) and its mounting, oil tank, hydraulic reservoir, transfer casing and transmission shaft of secondary power source. The total weight of hydraulic regenerative braking system is approximately 200kg.

Figure 2.13 Axial piston pump (right), accumulator (left).

2.6.1 Axial Piston Pump Placement

The axial piston pump is located at the end of the transmission line. It will have more potential to capture the energy during braking if it is position behind the front differential (the front-wheel-drive model) because of the increasing dimension of front axle that happen during braking (Hui, et al., 2009). Based on research done by Khoo, an existing 5-ton truck has been modeled into simplified truck with axial piston pump installed (Khoo, 2010). A frontal crash simulation was done and Figure 2.14 illustrated the stress on the pump mounting during the collision process of 50ms.
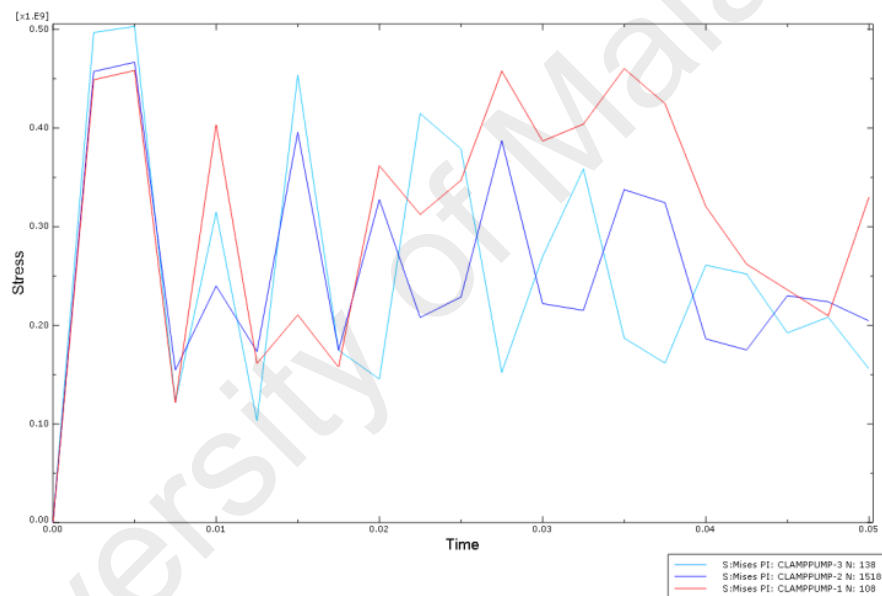
Figure 2.14 Stress distributions at pump mounting during the collision process (Khoo, 2010).

From Figure 2.15, the pump is held firmly to the chassis after the collision process; a little distortion was found on the mounting (Saw, 2010). The maximum Von Mises stress on mountings is about 500MPa. At this condition, the mountings are safe and stay in the plastic zone. The pump will not detach from the chassis after the collision process. The computational results indicate that the axial piston pump safety attached to the vehicle is sufficient to handle the frontal crash (Saw, 2010).

```
S, Mises
(Avg: 75%)
  +5.267e+08
  +4.828e+08
  +4.389e+08
  +3.950e+08
  +3.511e+08
  +3.073e+08
  +2.634e+08
  +2.195e+08
  +1.756e+08
  +1.317e+08
  +8.780e+07
  +4.391e+07
  +1.955e+04
```
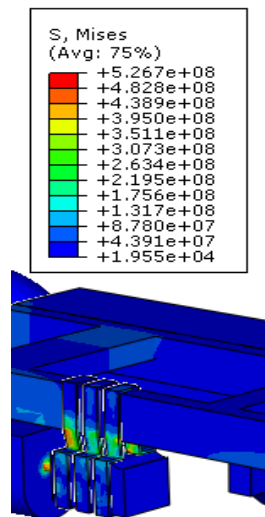
Figure 2.15 Von Mises stress contour plot of pump mounting (Saw, 2010).

2.6.2 Accumulator Placement

The accumulator is an energy storage device and stored high pressure fluids. The pressurized accumulator can achieve pressures as high as 400 bars. Therefore, appropriate measurement and safety design is necessary to reduce the occupant risk before accidents occur. Moreover, the position of the accumulator will also affect the optimum of energy transfer from or into the system. There are three ways of positioning the accumulator; vertical, horizontal or slanting. When installing vertically or at a slant, the oil valve must be at the bottom.The positioning of the accumulator depends on the functions as listed below (International, 2003);

i.   Energy storage: vertical

ii.   Pulsation damping: any position from horizontal to vertical

iii. Maintaining constant pressure: any position from horizontal to vertical

iv.   Volume compensation: vertical

In industry application, vertical position of accumulator is desired and recommended (International, 2003). The frontal crash simulation for accumulator positioning done by Khoo (Saw, 2010) is presented. In the first design, the accumulator is mounted horizontally as shown in Figure 2.16 (b). For the second design, the accumulator is mounted vertically as shown in Figure 2.16 (d). Since crash analysis involves large deformation, ABAQUS/Explicit method was used to analyze the impact collision behavior of the hydraulic hybrid vehicle with the wall (Gholami, Lescheticky, & Pabmann, 2003).

(a)   (b)

Accumulator

(b)   (c)
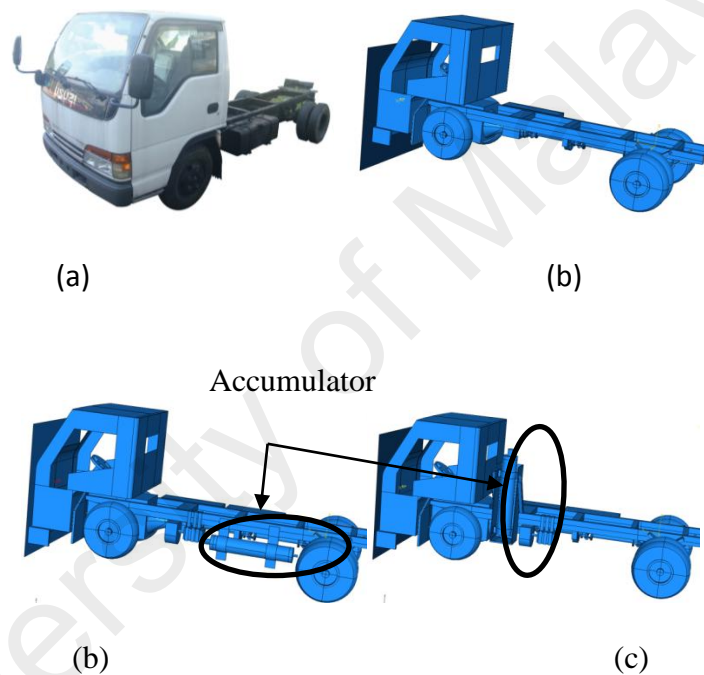
Figure 2.16 (a) The existing truck, (b) Simplified truck , (c) Truck with the accumulator mounted horizontally, (d) Truck with the accumulator mounted vertically (Khoo, 2010).

The result shows that the horizontal positioning for accumulator is most suitable for this application (Saw, 2010). Since the impact analysis of horizontal positioning appear to be the best choice and subject to less stress spike that will probably cause the catastrophic failure of bracket (Saw, 2010). The result of stress analyses of the horizontal (Figure 2.17 and Figure 2.18) and vertical (Figure 2.19 and Figure 2.20) positions of the accumulator is shown. The horizontal mounting design yields a

maximum stress of 360MPa and a displacement of 1.3689×10^{-2} m. The bracket is below yield region and only one highest peak of stress is found during the collision process. On the other hand, three peaks of stress are observed in Figure 2.19 for vertical mounting of accumulator during the collision process. The maximum stress is about 350MPa with maximum displacement of 1.3406×10^{-5} m.
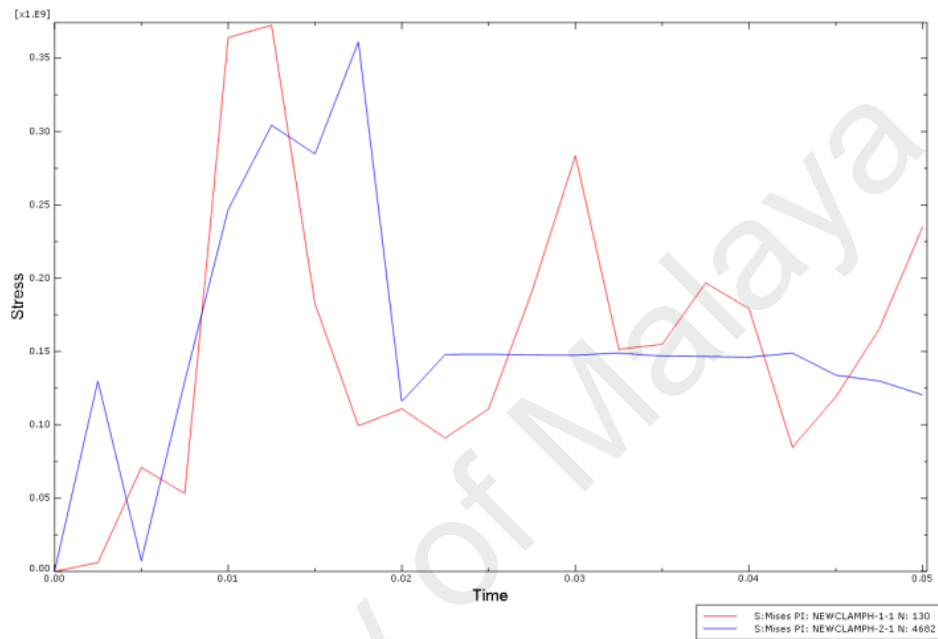
Figure 2.17 Stress plots of the horizontal accumulator mountings(Saw, 2010).
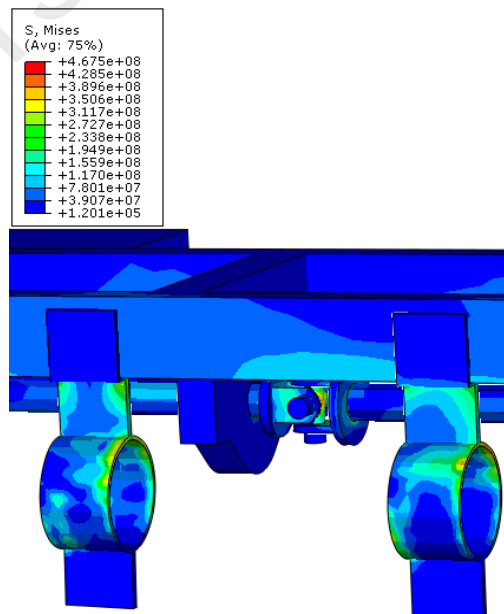
Figure 2.18 Von Mises stress distribution on horizontal accumulator mountings (Saw, 2010).
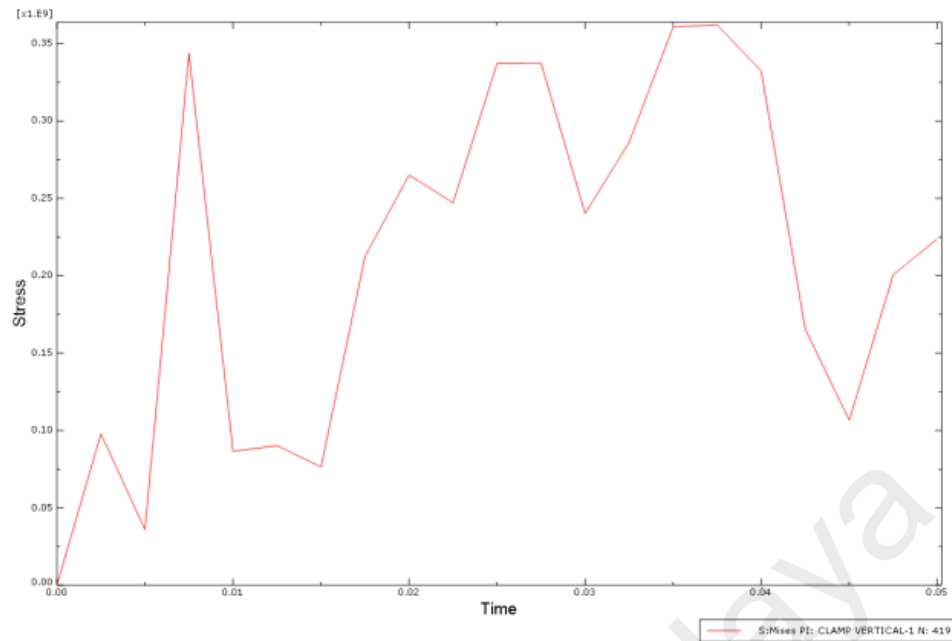
Figure 2.19 Stress plots of the vertical accumulator mountings (Saw, 2010).
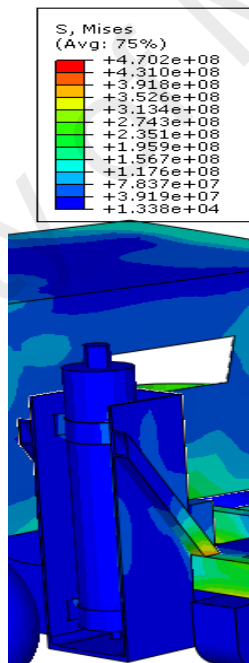
Figure 2.20 Von Mises stress distribution on vertical accumulator mountings(Saw, 2010).

Another study on an ISUZU 5 ton truck (Figure 2.21) for NGV (Natural Gas Vehicle) application also shows similar configuration as the hydraulic hybrid system. Both systems use horizontal positioning for the accumulator (hydraulic hybrid) and the tank (NGV).
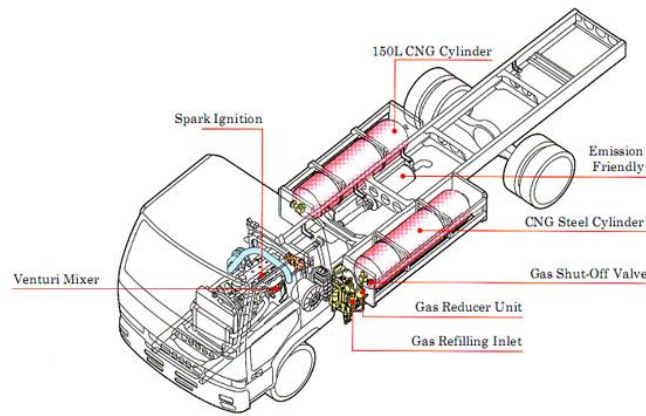
Figure 2.21 ISUZU 5 Ton NGV rigid trucks.

2.7   Test Rig

The test rig design is based on the concept of flywheel system. Improvements on energy density of hydraulic systems are made by using a flywheel-accumulator system. The energy is stored in the flywheel-accumulator by compressing a gas thus increasing the moment of inertia of the flywheel. The moment of inertia is increased by adding hydraulic fluid, and by increasing the angular velocity of the flywheel. Based on past research, the energy storage of the flywheel-accumulator proves to be approximately 10 times greater than a conventional accumulator. Another advantage when combining a flywheel with accumulator is the quantity of energy stored for this hydraulic system pressure can be variable (Ven, 2009).

A flywheel – variator system consists of mechanical variator (CVT) which controls the power flow bi-directionally between flywheel and transmission. This mechanism is reliable, effective, relatively efficient and economical. The main advantage of the system is, it can provide practical basis for hybrid propulsion system. The concept of propulsion using hybrid systems has been seen as an alternative in reaching zero or near

zero emission vehicles. In flywheel system, most are using fuel cell batteries (Bitterlin, 2010). This is a costly technology as it uses batteries which is non-ecological (Suzuki, Koyanagi, Kobayashi, & Shimada, 2005) and needs maintenance. Despite the cost and maintenance factor, there are research being done on producing vehicle on hybrid flywheel system such as Kinetic Energy Recovery Systems (KERS) developed by the Renault and Williams F1 teams. There are also research on implementation of the flywheel system on a bus that integrates with hydraulic accumulator as in Figure 2.22, to effectively recover energy (Vint & Gilmore, 1988).
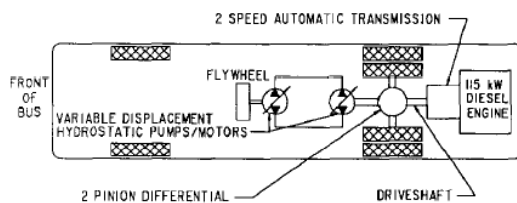
Figure 1. Simplified Schematic of a Flywheel Energy Storage and Braking System installed in a Transit Bus.
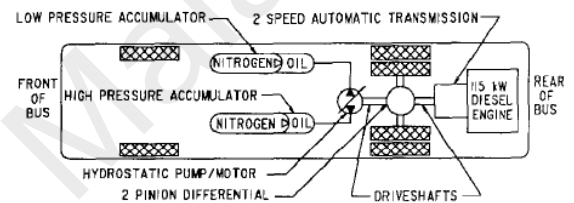
Figure 2. Simplified Schematic of a Regenerative Braking System which incorporates Hydraulic Accumulators For Energy Storage.

Figure 2.22 Flywheel system implement on a bus added with hydraulic regenerative braking system (Vint & Gilmore, 1988).

For energy recovery during braking, the flywheel gives energy buffer storage because of its high power density and cycle life. The system is compact, highly efficient and able to provide constant power. The system is also functional as energy buffer for robust autonomous power supply (Jefferson & Ackerman, 1996). In the experiment performed, it is estimated that when the flywheel moves at 4200 rpm, the energy that can be capture is around 100 kJ when using composite flywheel (Jefferson & Ackerman, 1996). In this study, the flywheel system is implemented in a hybrid hydraulic regenerative braking system where it is used to simulate the inertia of vehicle to determine the actual behaviour of the system on the road (Jefferson & Ackerman, 1996).

In HRBS system however, the flywheel will not be included in the system. The flywheel is only used in test rig to simulate the inertia of the vehicle. The test rig is design to test the HRBS system. The unit is connected to a flywheel by drive shaft in order to simulate vehicle load and also connected to the accumulators (Hui, Lifu, Junqing, & Yanling, 2010a). The test rig is supposed to simulate real lorry conditions during braking and accelerating. Equipment for test rig consist of flywheel, disc brake, variable displacement axial piston pump, high-pressure accumulator and low-pressure tank (or known as power pack in test rig application) where volume of tank must be larger than of accumulator to ensure constant availability of hydraulic fluid supplied to accumulator.

Research on test rig development is shown in Figure 2.23 (Chan, 2010). For the initial testing, the accumulator is fully charged by external hydraulic power supply (power pack). During acceleration, the accumulator then discharges and potential energy is converted into kinetic energy to rotate the flywheel. The fluid flows from the accumulator to the pump, rotates the pump shaft, and then flows to the tank. During braking, rotational energy of the flywheel is restored back by means of the charging accumulator. Hydraulic fluid flows from tank to pump, and then back again to accumulator. The process continues as long as the system is running (Norhirni, 2011). The initial testing for the test rig is using normal induction motor which can rotate the flywheel at maximum around 1010 rpm.

(a)
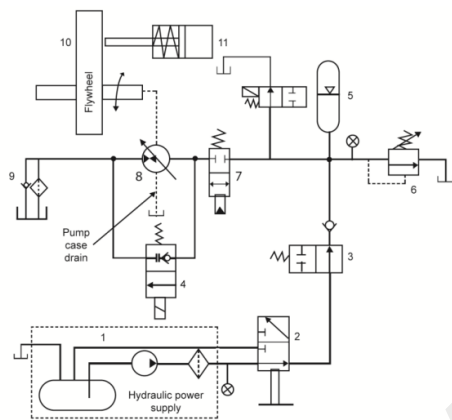
1	-	Hydraulic power supply
2	-	Manually operate 3 ways valve
3	-	Hydraulic actuated valve
4	-	Normally close solenoid check valve
5	-	Accumulator
6	-	Relief valve
7	-	Two way solenoid check valve
8	-	Variable displacement axial piston pump
9	-	Tank and filter
10	-	Flywheel
11	-	Drum brake

(b)

Figure 2.23 (a) Connection of hardware and (b) Hydraulic schematic (Chan, 2010).

Another work done by students from Colorado State University is shown in Figure 2.24. The mechanical part of the test rig has been successfully attached on a heavy diesel truck (Figure 2.25) (Swing, 2008a). The controller of the test rig on truck has been developed in parallel to control the system operation.

Figure 2.24 Test rig without cover (left), test rig with cover (right) (Swing, 2008a).

Figure 2.25 the heavy diesel truck attaches with the hydraulic system (Swing, 2008a).

Research has been done to develop a supervisory control and data acquisition (SCADA) system for data acquisition instrument control software of AC servo motor in Taiwan (Horng, 2008). This research uses a configuration as in Figure 2.26 and using this configuration; a user can operate the system from far which adds safety value during testing of a system.
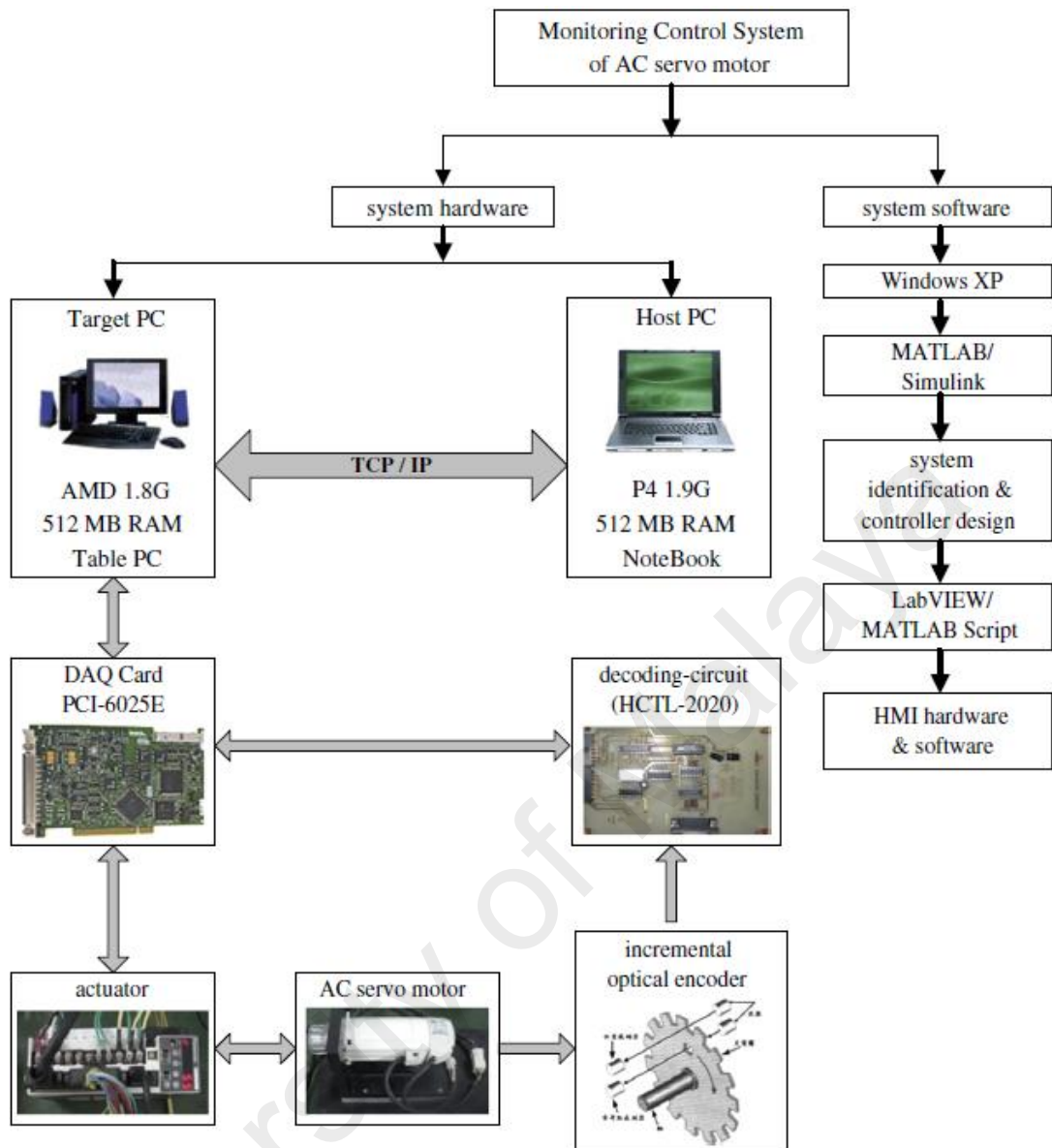
Figure 2.26 Configuration of AC servo motor systems (Horng, 2008).

2.8 Commissioning Test

The commissioning test for flywheel is to define the system constants such as the control wheel setting and output speed. The speed range of the test is 1000-2500 rpm. The flywheel is driven at constant speed while the power from and to the motor is monitored (Jefferson & Ackerman, 1996). The maximum safe speed, N is calculated to make sure the speed set is not over the limit (Hoffma & McCauley, 2001).

$$N = \frac{7425}{D} \qquad \text{(Hoffma \& McCauley, 2001)} \qquad (2.10)$$

Where;

N   = maximum safe speed, rpm

D_{FW} = flywheel diameter, feet

2.9   Conclusion

In summary, the literature on the relevant findings will be used as a guide in designing the HRBS and fabrication of the test rig flywheel. Chapter 3 will elaborate more on the detail of the HRBS design.

CHAPTER 3

DESIGN OF HRBS

3.1   Introduction

Basically, this chapter will describe the process of designing a HRBS for a 5 ton lorry. At the end of this chapter, a HRBS concept will be introduced and verified by constructing and commissioning of a test rig. The HRBS design is based on literature review which has been presented in chapter 2.

3.2   HRBS Design Process

The chapter begins with an introduction on the description of HRBS and selected configuration based on the literature review. The configuration will include the component that will be used in the HRBS. After selection of components, each component function is described. The major component for the system is the pump and the accumulator and therefore design calculation is performed to determine the proper size of pump and accumulator for a 5 ton lorry. After determining the specifications for pump and accumulator, the selection for other components used in the HRBS is done using the morphological analysis. At the end of the chapter, the specification of the HRBS is listed out and placement of HRBS on actual lorry is presented. Figure 3.1 shows the flow of the designing step of HRBS.

```
┌─────────────────────────────────────────────┐
│   Understanding of HRBS working principle    │
└─────────────────────────────────────────────┘
                      │
                      ▼
┌─────────────────────────────────────────────┐
│       Sizing of components in HRBS           │
└─────────────────────────────────────────────┘
                      │
                      ▼
┌─────────────────────────────────────────────┐
│    Morphological analysis of HRBS component  │
└─────────────────────────────────────────────┘
                      │
                      ▼
┌─────────────────────────────────────────────┐
│              Prioritize Matrix               │
└─────────────────────────────────────────────┘
                      │
                      ▼
┌─────────────────────────────────────────────┐
│              Concept selection               │
└─────────────────────────────────────────────┘
                      │
                      ▼
┌─────────────────────────────────────────────┐
│             HRBS control system              │
└─────────────────────────────────────────────┘
                      │
                      ▼
┌─────────────────────────────────────────────┐
│             HRBS layout on lorry             │
└─────────────────────────────────────────────┘
                      │
                      ▼
┌─────────────────────────────────────────────┐
│     Final specification of HRBS component    │
└─────────────────────────────────────────────┘
```
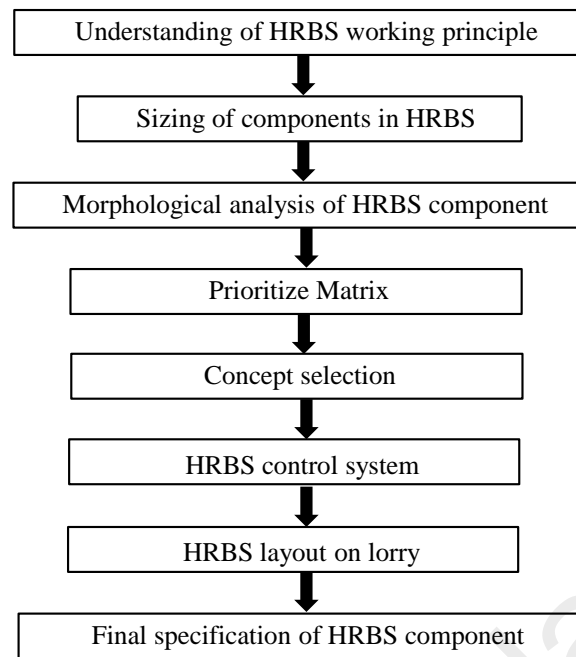
Figure 3.1 Design step in HRBS development.

Based on literature review, the parallel type of configuration is chosen. In this study, the parallel configuration is selected as this types requires less modification on an existing lorry, while series configuration will need major modification on the existing lorry structure. The details on the HRBS are shown in HRBS description. In order to design a HRBS system, the principle idea of HRBS is introduced and must be comprehend to gain the understanding of the working concept.

3.3   HRBS Working Principle

After reviewing other works, a set of working flow for braking and acceleration is constructed as in Figure 3.2. Initially, the accumulator is fully charged by an external hydraulic power supply. It receives input from the throttle pedal and activates the operation through the control system. While braking, when the driver steps on the brake pedal (slowing the vehicle), the HRBS will be activated in pump mode. Rotational energy of the flywheel is captured thus charging accumulator. The vehicle then operates

the braking unit and hydraulic fluids from the reservoir will be transferred into a high-pressure accumulator thus compressing the Nitrogen gas inside. The braking unit provides normal braking and stores the otherwise wasted energy.

During acceleration, when a driver presses the throttle pedal to accelerate the vehicle, the braking unit will be activated in motor mode. The fluid flows from the accumulator to the pump, rotates the pump shaft, and then flows to the reservoir. The accumulator then discharges and potential energy is converted into kinetic thus rotating the flywheel. The previously stored energy during braking is released back to the vehicle. Pressurized hydraulic fluid will be transferred back into the reservoir through the braking unit.

The system operates by giving direction to the hydraulic control circuit. The hydraulic control circuit will vary the swash plate angle. By varying the swash plate angle, the flow and pressure of an axial piston can be controlled. The proper swash plate motion is related to the forces and movements acting along the parts. However, during operation, reaction torque always acts on the swash plate about the titling shaft; it tends to rotate the swash plate to a position perpendicular to the drive shaft. This reaction is directly proportional to the swash plate angle and is substantially independent of the drive shaft rotational speed (Kaliafetis P. & et al., 1995). Therefore, in order to change the swash plate angle during operation, the plate must be moved against the reaction force and torque (Norhirni, 2011).

The next subsection will be on design calculation for two major components in HRBS which is pump and accumulator.
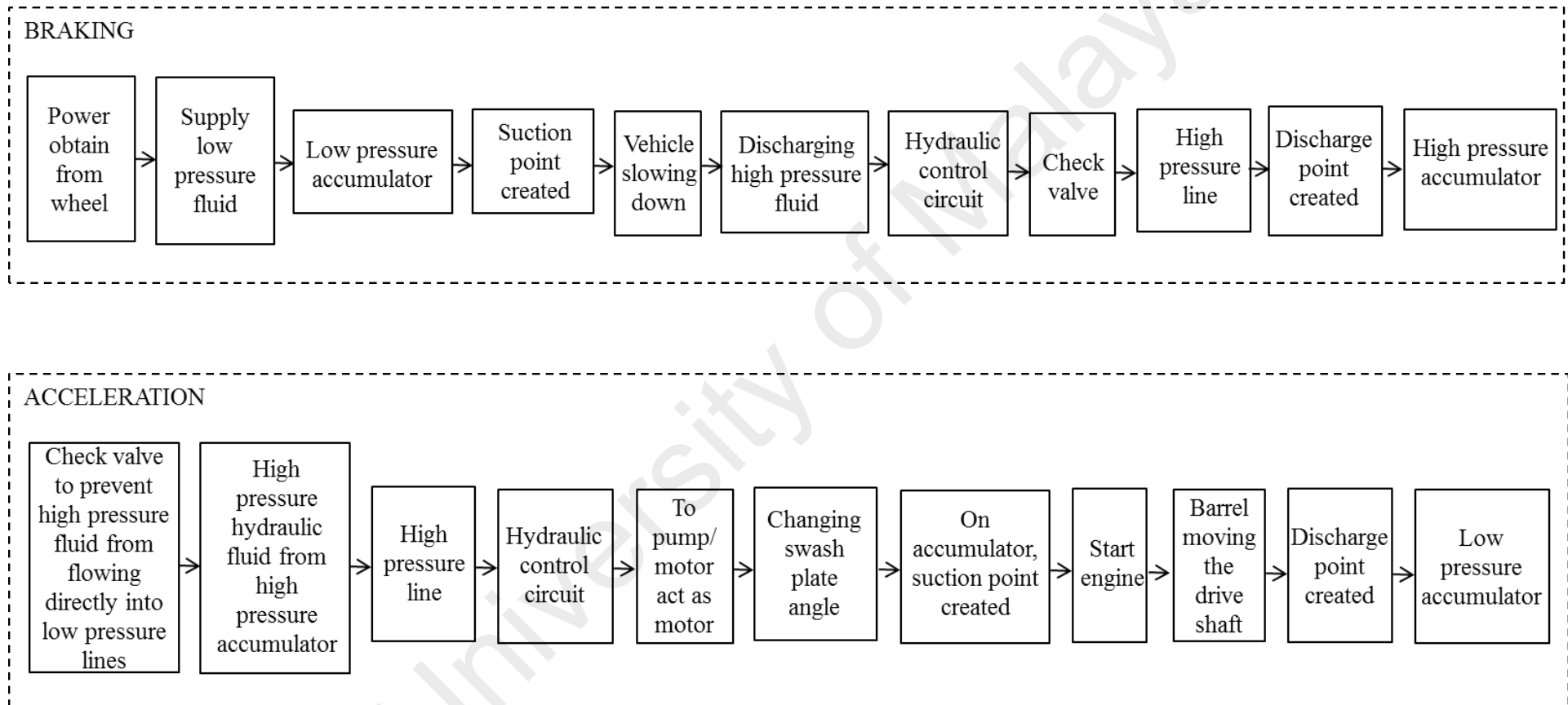
Figure 3.2 Working flows of HRBS during braking and acceleration.

3.4   Sizing of HRBS Components

The mathematical modelling steps are done in order to guide the selection of the proper size of two major components in HRBS which is the pump and accumulator. Calculations are made based on speeds of 20km/h (low speed) and mass of lorry, m= 5000kg.

3.4.1 Lorry Specification

Basic concept for this positive bi-directional variable displacement axial piston pump is applied on the vehicle as regenerative braking system. Therefore the following calculation, NKR 71 E, 5 ton lorry will be used as standard reference (ISUZU, 1999). Base on this data, the size of the axial piston pump is calculated.

Table 3.1 Isuzu NKR 71 E specification.

Type	:	Isuzu NKR 71 E- 7419185
Configuration and number of cylinders	:	Direct injection, in-line 4 cylinder diesel
Tire radius	:	0.04064 m
Maximum power output	:	90kW @ 3000r/min
Maximum torque	:	304 Nm @ 1800r/min

3.4.2   Axial Piston Pump Sizing

Referring to Equation (2.1), calculation for mechanical power output for motor is;

$$P_{out} = \frac{2\pi \times T \times N}{60} watt \qquad \text{Eqn. (2.1)}$$

Where,

T = torque, Nm

N = speed, rpm

and the torque output for motor is;

$$T = \frac{D \times P \times E_m}{2 \times \pi \times 1000} Nm$$
Eqn. (2.2)

Where,

D= Displacement, cc/rev

P_F= Fluid pressure, kPa

E_m = Mechanical Efficiency (0-1.0)

Referring to Table 3.1, the maximum power output, P_{out} = 90 kW at speed, N = 3000 r/min.

Substitute in Equation (2.1),

$$P_{out} = \frac{2\pi \times T \times N}{60} watt$$
Eqn. (2.1)

$$90 k = \frac{2\pi \times T \times 3000}{60}$$

T = 286.479 Nm

Therefore torque output, T= 286.479Nm. At the design point, stall torque must be 1.5 times the running torque. Therefore the required torque for hydraulic pump, T $_{pump}$ (Gould, 2010),

$$T_{pump} = 286.479 \times 1.5 = 429.7185 Nm$$

Normally torque (mechanical) efficiency at stall will be between 75% and 95% for most motors, therefore the assumption is that the motor is at minimum efficiency condition, E_m;

$E_m = 75\% = 0.75$

Besides that, assume the maximum output pressure, P = 300 bar = 30000kPa. This is based on the assumption for pressure that the accumulator can support. As a result, from Equation (2.3), the theoretical displacement for the hydraulic pump, D_T;

$$D_T = \frac{T \times 2\pi \times 1000}{P \times E_m}$$ Eqn. (2.3)

$$\frac{429.7185 \times 2\pi \times 1000}{30000 \times 0.75}$$

$$D_T = 120 cc/rev$$

From Equation (2.4), the piston diameter is given as;

Piston Diameter, $d = (1 \sim 1.09)\sqrt[3]{\dfrac{D_a}{Z}}$ cm Eqn. (2.4)

Where;

D_a = Actual displacement, cc/rev

Z = Total number of piston

and from Equation (2.5), the distance between the piston axis and the cylinder barrel axis, R is expressed as;

$$R = (0.22 \sim 0.27)Z\sqrt[3]{\frac{D_a}{Z}}$$ cm Eqn. (2.5)

Where;

D_a = Actual displacement, cc/rev

Z = Total number of piston

and the theoretical displacement from Equation (2.6), D_T for the design hydraulic pump expressed as;

$$D_T = \frac{\pi}{4}d^2 \times 2RZ\tan\alpha_{max} \qquad \text{Eqn. (2.6)}$$

Where;

d = Piston Diameter, cm

R = Distance between piston axis and cylinder barrel axis, cm

Z = Total number of piston

α_{max} = maximum swash plate angle = 20deg

Substitute Equation (2.4) and (2.5) into Equation (2.6);

$$D_T = \frac{\pi}{4}d^2 \times 2RZ\tan\alpha_{max} \qquad \text{Eqn. (2.6)}$$

$$D_T = \frac{\pi}{4}\left(1.09\sqrt[3]{\frac{D_a}{Z}}\right)^2 \times 2\left(0.27 \times Z\sqrt[3]{\frac{D_a}{Z}}\right)Z\tan\alpha_{max}$$

$$= 0.933\left(\sqrt[3]{\frac{D_a}{Z}}\right)^2 \times 0.54Z^2\sqrt[3]{\frac{D_a}{Z}}\tan\alpha_{max}$$

From Equation (2.3), D_T = 120cc/rev and there are 9 piston in the pump. Therefore;

$$120 = 0.933\left(\sqrt[3]{\frac{D_a}{9}}\right)^2 \times 0.54 \times 9^2\sqrt[3]{\frac{D_a}{9}}\tan 20°$$

46

$$120 = 14.855\left(\sqrt[3]{\frac{D_a}{9}}\right)^3$$

$$\frac{D_a}{9} = \frac{120}{14.855}$$

$$D_a = \frac{120}{14.855} \times 9 = 72.7 cc/rev$$

Thus, the required displacement for the hydraulic pump is 72.7cc/rev.

3.4.3   Accumulator Sizing

Accumulator sizing is calculated based on the gas charge of the accumulator (Bylsma, 2003). The determination of how much fluid can be stored and released is based on the changes of volume and pressure. In order to select the proper size of the accumulator, the volume flow rate of hydraulic fluid for pump must be calculated using Equation (2.7);

$$Q \text{ (L/s)} = \frac{E_v \times D \times N}{1000} \qquad\qquad \text{Eqn. (2.7)}$$

Where;

E_v= Volumetric efficiency (0-1.0)

D = Displacement, cc/rev

N= Maximum angular velocity

By referring to Equation 2.7, the value of maximum angular velocity must be determined by calculating the total inertia of components on the rotating axis of shaft. On the test rig structure, the flywheel is attached to a connecting shaft with couplings, and the connecting shaft is connected to a drum brake and other features, thus the flywheel is not the only rotating object. Total inertia of rotating components about the

rotational axis is determined to identify the angular velocity. The components on rotating axis shaft as in Figure 3.3 includes;

   i.   Flywheel

  ii.   Drum brake

 iii.   Coupling (i. pump and ii. connecting shaft)
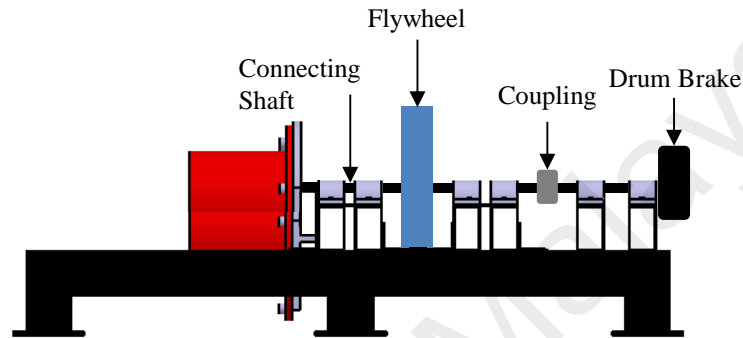
Figure 3.3 Components on rotating axis shaft.

To calculate the inertia Equation (3.1) is used;

$$I = \frac{1}{2}mr^2 \hspace{4cm} \text{Eqn. (3.1)}$$

The inertia for each component is then calculated;

<u>Inertia of Flywheel</u>

$$I_{flywheel} = \frac{1}{2} \times m_{flywheel} \times r_{flywheel}^2$$

$$= \frac{1}{2}(108.33)(0.25 - 0.0175)^2$$

$$= 2.928 \text{ kgm}^2$$

<u>Inertia of Drum Brake</u>

As the total weight of the drum brake cannot be determined due to the constraint that the drum brake was already affixed on the original chassis, the mass of the drum brake

is determined using calculation where mass is equal to density over volume. The construction material of the drum brake is AISI 4000 Series steel with density of 7850 kg/m^3. Thus, the inertia of drum brake is;

$$I_{drumbrake} = \frac{1}{2} \times m_{cover\ without\ holes} \times r^2_{drumbrake}$$

$= 0.5\pi(\rho_{steel})[(0.273)(0.0175^2)^2 + (0.02)(0.0305^2)^2 + (0.07)(0.04^2)^2 + (0.013)(0.0875^2)^2]$
$\qquad + \quad (0.5\text{-}0.3)\pi(\rho_{steel})(0.015)(0.0465^2)^2 \quad + \quad 6\pi(\rho_{steel})[(0.5)(0.00595^2)^2(0.03) \quad +$
$\qquad (0.03)(0.00595^2)(0.07^2)]$

$= 0.0133$ kgm^2

Inertia of Coupling

    i.   Pump Coupling

$$I_{pump\ coupling} = \frac{1}{2} \times m_{pump\ coupling} \times r^2_{pump\ coupling}$$

$$= \frac{1}{2}(1.0417)(0.064 - 0.0175)^2$$

$= 1.1262 \times 10^{-3}$ kgm^2

    ii.   Connecting Shaft Coupling

$$I_{shaft\ coupling} = \frac{1}{2} \times m_{shaft\ coupling} \times r^2_{shaft\ coupling}$$

$$= \frac{1}{2}(1.6212)((0.0575 - 0.0175) + (0.0405 - 0.0175))^2$$

$= 3.2173 \times 10^{-3}$ kgm^2

Therefore total inertia on rotating axis shaft is;

$I_{Total} = I_{flywheel} + I_{drumbrake} + I_{pump\ coupling} + I_{shaft\ coupling}$

$= 2.928 + 0.0133 + (1.1262 \times 10^{-3}) + (3.2173 \times 10^{-3})$

$= 2.9456$ kgm^2

After calculating the total inertia, Equation (3.2) is used to determine the initial angular velocity of the system. The minimum kinetic energy which can propel the lorry from stationary is calculated.

Minimum velocity, v = 10km/h = 2.7778m/s.

$$\text{Kinetic energy of lorry} = \frac{1}{2}mv^2 = \frac{1}{2}(5000)(2.7778)^2 = 19\,290.4321\text{J} \qquad \text{Eqn. (3.2)}$$

As flywheel is used to simulate lorry with same amount of energy, referring to Equation (2.9) therefore;

Kinetic energy of lorry = Rotational energy of flywheel

$$\frac{1}{2}mv^2 = \frac{1}{2}I\omega^2 \qquad\qquad \text{Eqn. (2.9)}$$

Where I_{Total} = Total inertia and ω is angular velocity of flywheel. Therefore;

$$19\,290.4321\text{J} = \frac{1}{2}I_{Total}\omega^2$$

$$19\,290.4321\text{J} = \frac{1}{2}(2.9456)\omega^2$$

$$\omega = 114.4456 \text{ rad/s}$$

$$= 1092.875 \text{ rpm}$$

Substitute the value into Equation (2.7) to calculate the volume flow rate;

$$Q \text{ (L/min)} = \frac{E_v \times D \times N}{1000} \qquad\qquad \text{Eqn. (2.7)}$$

$$= \frac{1 \times 72.7 \times 1092.875}{1000}$$

$$= 79.4520 \text{ L/min}$$

When the vehicle operates at speeds of 10 km/h, the volume flow rate for a 72.7 cc/rev pump is 79.4520 L/min. As the accumulator flow rate must be larger than the pump flow rate, therefore the selected accumulator must have flow rate larger than 79.4520 L/min to accommodate the system during operation.

After calculating the size for each component, morphological box is constructed for selecting the best concept that suits the system.

3.5   Morphological Analysis

The morphological analysis (Table 3.2) uses the functions identified to select the most suitable component based on the function requirement. Basically, all components listed in this morphology box will be used in the actual lorry except for the hydraulic pack which will be used only on test rig setup to generate start-up power similar to an engine. Based on this analysis, the best concept is selected in the concept selection section.

Table 3.2 Morphological analysis of HRBS components.

Function	Concept 1	Concept 2	Concept 3
Move the shaft and flywheel clockwise and counter-clockwise. Provide the necessary pressure to move liquid.	**Eaton, Hydraulic Motor**	Sauer Danfoss, Pumps & Motors	Bosch Rexroth, Axial piston variable pump A4VSG
Store energy from braking and transmit energy during acceleration.	Epoll, Hydropneumatic Bladder Accumulators	Hydac Hydropneumatic Bladder Accumulator	
Transmit power to pump and pressure adjustment.	Preston Hydraulics	Bosch Rexroth	FMC Technologies
Measure the flywheel speed during cycle test.	Honeywell S&C	Monarch ROS-W	
Measure pressure capture and release by accumulator.	GEMS Sensor	HYDAC Pressure transducer	
Transmit fluid from low-pressure accumulator to high-pressure accumulator and vice versa.	Fixed Carbon Steel Hydraulic Pipe	Good Year High pressure flexible hydraulic hose	

3.6   Prioritize Matrix

The score is given based on the priority set for each component. The total score for each function will determine the selection of the component. Rating used in this matrix is from 1 to 5 which are from not important (1) to most important (5).

Function 1

Move the shaft and flywheel clockwise and counter clockwise. Provide the necessary pressure to move liquid.

As the pump is the most important component in the system, the price is also the most expensive. Therefore, price should be one of the main things to consider when selecting the best pump. In this priority matrix, it is shown that the pump from Sauer Danfoss can be a potential concept to select based on the price. However, the Sauer Danfoss pump did not have technical support available or guides in installation to a HRBS system. For Bosch Rexroth Axial Piston Pump, purchasing will include service of technical assistant for installation.

The advantage of using variable pump is that a slight decrease of pressure will cause an increase in flow rate, and a slight increase in pressure causes a decrease in flow rate. Using this variable displacement pump, a pre-set of desired pressure can be done. However there is a disadvantage to this type of pump where the pump response is much slower than fixed displacement pump. Large power systems usually use the variable displacement pump because the power absorbed by the pump varies continuously with the power demanded by the system and the losses in pipeline are small (Stringer, 1976). Therefore, a variable displacement pump will be given priority for pump selection.

Table 3.3 Prioritize Matrix for axial piston pump.

Priority	Concept 1 Eaton, Hydraulic Motor (Eaton Heavy Duty Motor Series)		Concept 2 Sauer Danfoss, Series 90 Closed Circuit High Power Piston Pumps & Motors		Concept 3 Bosch Rexroth, Axial piston variable pump A4VSG	
	Detail	Score	Detail	Score	Detail	Score
Weight (kg)	38	5	90	3	60	4
Displacement	60	4	55	3	71	5
Mode	Motor mode	1	Pump and	5	Pump and	5
Displacement	Fixed	1	Variable	5	Variable	5
Price (RM)	18,500.00	5	19,000.00	4	19,500.00	4
Availability	6 month	1	3 month	3	3 month	3
Technical	Not	1	Not available	1	Available	5
Total Score	**NO**	**18**	**NO**	**24**	**YES**	**31**

Function 2

Store energy from braking and transmit energy during acceleration.

A properly designed system which uses an accumulator will benefit in terms of low installation cost, low maintenance and less leakage (Inc., 2012). Hydac's products are well known for its quality and it is a well-established company in Malaysia and advice on accumulator can be acquired easily as compared to Epoll brand. When this research was conducted only the 32 L with 1800 L/min accumulator could be purchased immediately because it is usually purchased for industrial usage. The weight of the accumulator is also important as it will add weight to the system. Therefore the priority is given to the accumulator with less weight.

Table 3.4 Prioritize Matrix for accumulator.

Priority	Concept 1 Epoll, Hydropneumatic Bladder Accumulators		Concept 2 Hydac, Hydropneumatic Bladder Accumulator	
	Detail	**Score**	**Detail**	**Score**
Weight (kg)	96	4	90	5
Nominal volume (L)	52	3	32	4
Volume flow rate	3120	3	1800	4
Type	Bladder	5	Bladder	5
Availability	3 month	1	Immediately	5
Technical support	No	1	Available	5
Total Score	**NO**	**17**	**YES**	**28**

Function 3

Transmit power to pump and pressure adjustment.

The size of the tank and the power from the motor must be sufficient for the test rig commissioning. Time for purchasing the pack is also important to make sure it can be received within the time for testing.

Table 3.5 Prioritize Matrix for power pack.

Priority	Concept 1 Preston hydraulics		Concept 2 Bosch Rexroth		Concept 3 FMC Technologies	
	Detail	**Score**	**Detail**	**Score**	**Detail**	**Score**
Motor type	Three	5	Three	5	Three	5
Tank volume (L)	40	3	90	5	50	4
Availability	3 month	4	2 month	5	3 month	4
Technical support	No	1	Available	5	No	1
Total Score	**NO**	**13**	**YES**	**20**	**NO**	**14**

Function 4

Measure the flywheel speed during cycle test.

The Monarch ROS-W sensor can measure the speed of a flat surface using reflective tape. Unlike Honeywell S&C sensor, the surface to measure must have an edge which makes it impossible to measure flywheel surface when it is rotating. The Monarch sensor also comes with a bracket for easy installation on the test rig chassis.

Table 3.6 Prioritize Matrix for speed sensor.

Priority	Concept 1 Honeywell S&C, 58426HV Sensor DiMag Speed 		Concept 2 Monarch ROS-W- Remote Optical Sensor with bracket 	
	Detail	**Score**	**Detail**	**Score**
Attachment	Not included	2	Included	5
Availability	3 month	4	2 month	5
Sensor Marker	Edge of rotating object	1	Reflective tape	5
Total Score	**NO**	**7**	**YES**	**15**

Function 5

Measure pressure capture and release by accumulator.

The HYDAC pressure transducer can fit directly on the accumulator fitting and on pump body without holder. The data transmitted to the DAQ card can be linked to commercially available evaluation systems like Matlab without any need for extra tools to convert the data unlike the GEMS sensor which needs a converter software to translate the output data from the accumulator.

Table 3.7 Prioritize Matrix for pressure transducer.

Priority	Concept 1 GEMS Sensor 170281-Rotor Flow Sensor		Concept 2 HYDAC Pressure transducer HDA 4445-B-250-000	
	Detail	**Score**	**Detail**	**Score**
Sensor output	Analog	5	Analog	5
Attachment	Not included	2	Included	5
Technical support	Not available	1	Available	5
Total Score	**NO**	**8**	**YES**	**15**

Function 6

Transmit fluid from low-pressure accumulator to high-pressure accumulator and vice versa.

The flexibility of the hydraulic hose is an important criterion in choosing the pipeline for the system. Flexibility will ease the fitting process on lorry and on test rig. The hose must withstand the pressure set for the system.

Table 3.8 Prioritize Matrix for pipeline.

Priority	Concept 1 Fixed Carbon Steel Hydraulic Pipe		Concept 2 Good Year High pressure flexible hydraulic hose	
	Detail	**Score**	**Detail**	**Score**
Flexibility	No	2	Yes	5
Withstand high pressure	Yes	5	Yes	5
Availability	Immediately	5	Immediately	5
Coupling included	No	1	Yes	5
Installation support	No	1	Available	5
Total Score	**NO**	**14**	**YES**	**25**

3.7 Final Concept Selection of HRBS Components

In this section, the best concept is selected based on a number of criteria such as its suitability on the system as calculated in Component Sizing section, availability of the product in the market, the price of product and time constraint. The final selection of components is;

i. Concept 3: Bosch Rexroth, Axial piston variable pump A4VSG

Figure 3.4 Axial piston pump.

The displacement of the pump as calculated in design calculation is 71 cc/rev. Based on the spread sheet (Corporation, 2004) by Bosch Rexroth, the maximum speed of the pump is 3200rpm and the maximum torque is 395 Nm.

ii. Concept 2: Hydac, 32 Litre Hydropneumatic Bladder Accumulator

Figure 3.5 Accumulator.

The volume of the accumulator is 32 L. Although this size is larger than the calculated accumulator sizing, it is beneficial to purchase a larger sized accumulator as it can be fit onto a larger vehicle in future tests. Normally pre-charged pressure is 80 - 90% of the minimum system working pressure. This is to allow a small amount of fluid to remain

in the accumulator and prevent the bladder, diaphragm from striking the opposite ends of the pressure vessel resulting in damaged discharge valve or blocking fluid passages. Therefore the pre-set of the accumulator to charge during commissioning is 80 bars.

iii.   Concept 2: Bosch Rexroth 90 Litre tank with three phase motor

Figure 3.6 Power pack.

The power pack from Bosch is selected as this power pack can be purchased within the time frame of research. The three phase motor included is an induction motor to power the pack for charging the accumulator. The tank size is sufficient to cover the whole system during operation. Note that this power pack is only used for test rig system testing. On an actual lorry, the power pack function is replaced by the lorry's engine.

iv.   Concept 2: Monarch ROS-W- Remote Optical Sensor with bracket

Figure 3.7 Remote optical sensor.

The ROS is more convenient to use as it can measure using reflective tape. Therefore the measuring condition is more convenient as the reflective tape can be stuck on any

kind of solid surface including reflective surface. The sensor comes with 8 foot cable, mounting bracket and 12 inches of reflective tape.

v.   Concept 2: HYDAC Pressure transmitter HDA 4445-B-250-000

Figure 3.8 Pressure transducer.

The pressure transducer sensors are interfaced by a pair of twisted wires which enables the system to receive, dispatch and monitor information from hydraulic systems. The output data from the accumulator is sent to target PC and pressure reading is obtained from MATLAB software.

vi.   Concept 2: Goodyear High pressure flexible hydraulic hose

Figure 3.9 Pipeline hose.

The advantage of this type of pipeline is its flexibility. The hose from Goodyear can withstand pressures of up to 200 bars. The pipeline hose contains multi-layered woven copper and steel thread.

After the final concept has been selected for HRBS components, the control system of HRBS is designed.

3.8   HRBS Control System

The flowchart in Figure 3.10 shows how the compensator works. The system pressure is set to 85 bars as maximum and 15 bars as minimum. This is to maintain the system pressure at low conditions to maintain safety during testing. When the output pressure is more than 85 bars, swash plate control piston will move to the right to reduce swash plate angle, therefore causing a reduction in the compensation gap; hence system will be compensated to reduce the output pressure. Then, after the compensation completed, the control spring will push the swash plate to the right which increases the swash plate angle to achieve the preset pressure. The same will happen if the output pressure is less than 85 bars, where control piston spring will push the swash plate to the right increasing the swash plate angle and finally increase the output pressure.

Pressure compensators at the pump are used to maintain the preset pressure differential across a hydraulic pump (Kim, 1987). The objective is to minimize the influence variation on a flow rate passing through the hydraulic circuit. Pressure compensation and load sensing are terms often used to describe pump features that improve the efficiency of the pump. Pressure compensator applied in hydraulic pump to regulate preset pressure differential across a hydraulic pump as well as minimizes the influence of pressure variation on the flow rate passing though the hydraulic circuit. Generally, the pressure compensator is a pointer positioned on the side of the hydraulic pump which controls the swash plate angle.

When system pressure reaches preset pressure of the pressure compensator, the hydraulic system will be constrained and therefore stop operating. The position of swash plate with zero swash plate angle means the hydraulic component is in idle

position and does not function as either pump or motor. Pressure compensator is connected to the hydraulic component through the swash plate control piston and directional control valve that connects through the hydraulic component output port. During braking, hydraulic pump/motor functions as pump to stop vehicle. Nitrogen gas in accumulator bladder is compressed, hydraulic fluid flows out of tank into hydraulic pump, then enters high pressure accumulator. When in pump mode, swash plate directional control piston will be pushed to the right by a servo motor which in turn pushes the swash plate to the counterclockwise direction.

During acceleration, hydraulic pump/motor functions as motor to propel vehicle. Nitrogen gas in accumulator bladder is expanded, hydraulic fluid flows out of accumulator into hydraulic motor, then enters low pressure tank. In motor mode function, the swash plate directional control piston will be pulled to the left by a servo motor which eventually pulls the swash plate to the clockwise direction. The process continues as the system is running.

The next step after designing the control system of the HRBS is to plan the components position on the lorry. Following this subchapter is the description of the HRBS layout on the lorry.
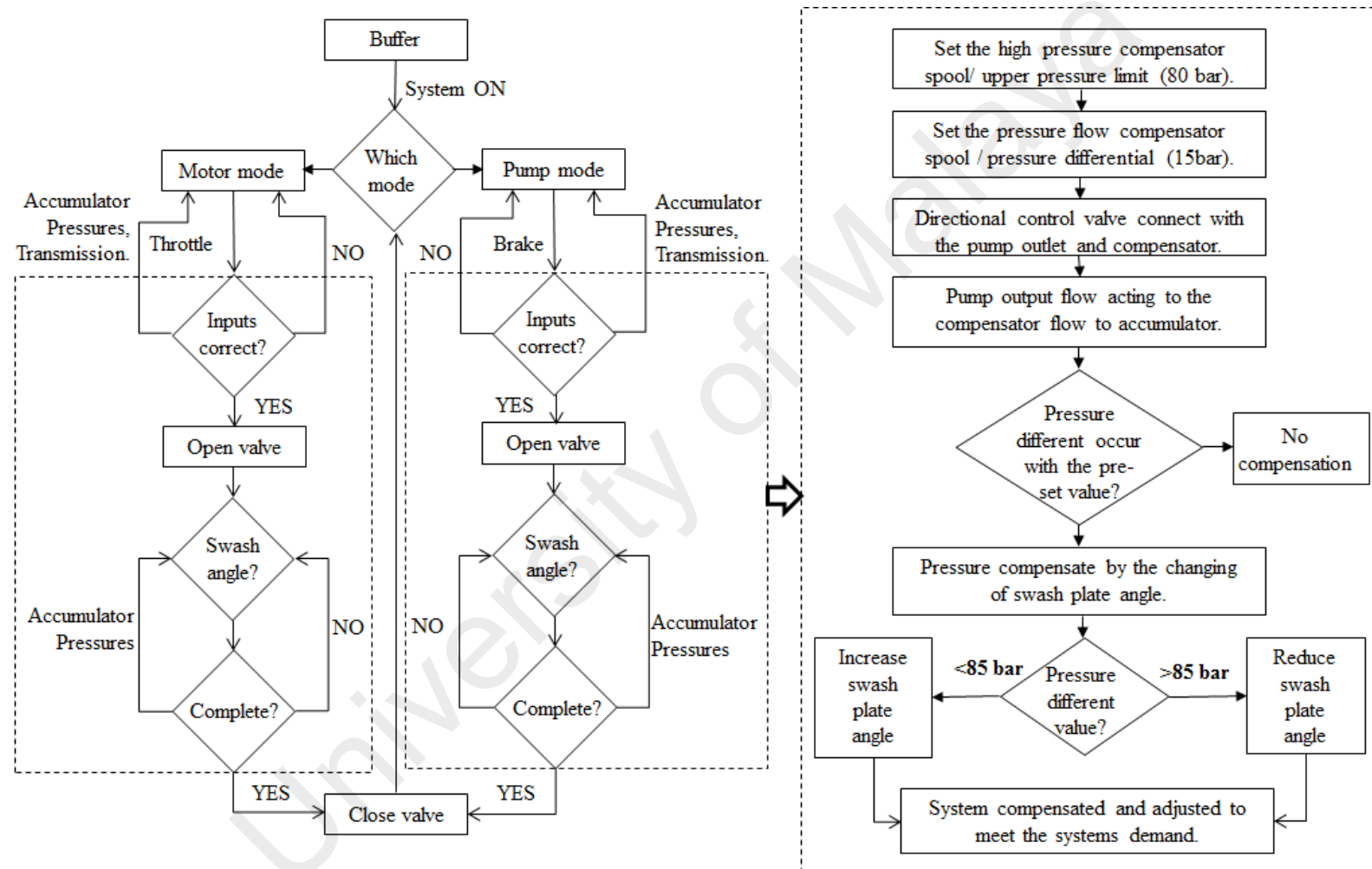
Figure 3.10 Flow chart of HRBS for pump and motor mode (left) with pressure compensator working detail (right).

3.9 HRBS Layout on Lorry

The existing 5 ton lorry for installation of the HRBS is in figure 3.11. Based on this lorry and previous study done (Chan, 2010; Khoo, 2010; Norhirni, 2011) the HRBS components arrangement is designed. The proposed schematic of HRBS is illustrated in Figure 3.12.

Figure 3.11 Picture of actual lorry.

(a)

1 Tyre
2 Drive shaft
3 Two pinion differential
4 Structural body
5 Universal joint

(b)

1 Tyre
2 Drive shaft
3 Two pinion differential
4 Structural body
5 Universal joint
6 Wiring (position sensor)
7 Position sensor (rotational)
8 Pipeline
9 Low pressure accumulator
10 High pressure accumulator
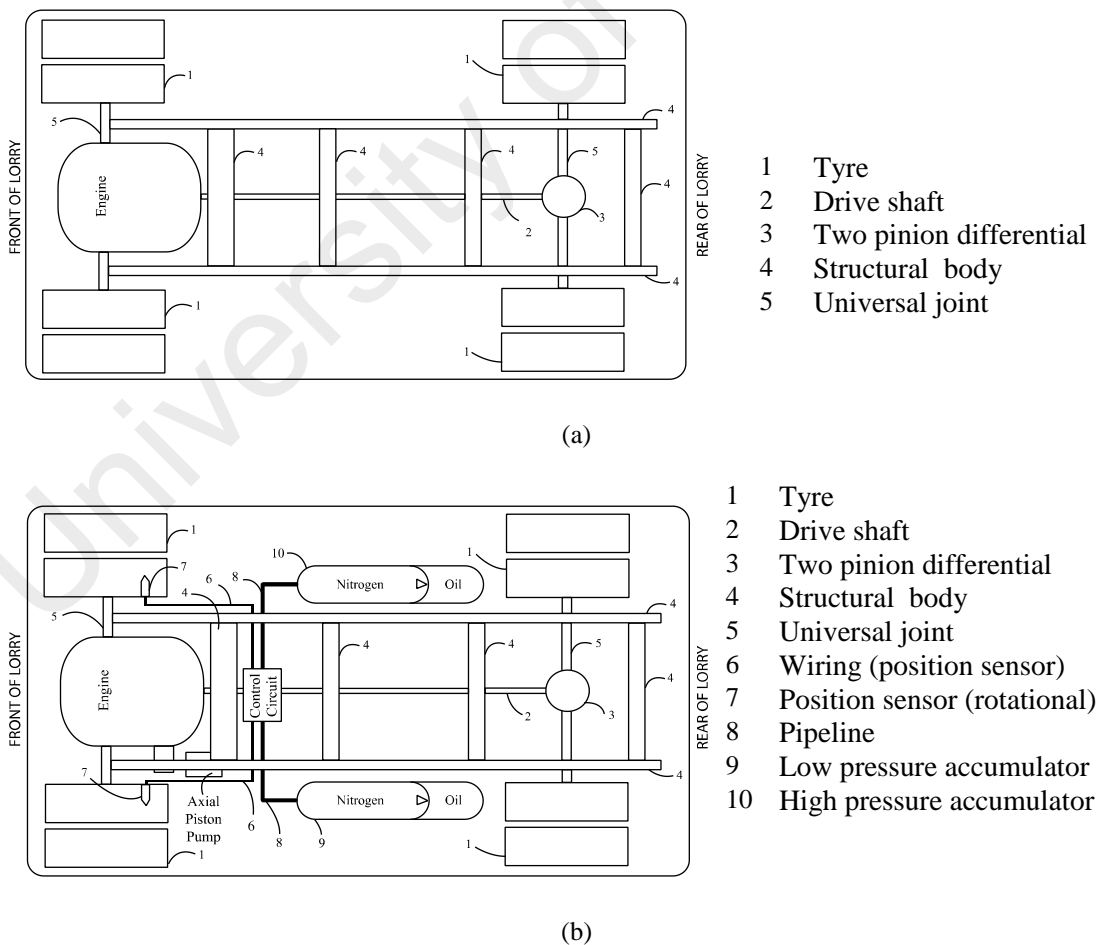
Figure 3.12 (a) Schematic of conventional lorry, (b) schematic of proposed HRBS.

The two pinion differentials are to assist in aiming the engine power of lorry and wheels. It is also as final gear reduction in vehicle. It also slows the transmission rotational speed and at the same time hitting the wheels for braking to occur (Shenron, 2008). Another function of two differential pinions is to transmit the power to the vehicle's wheels while letting the wheels rotate at different speeds. In order to transmit torque at an angle, a Universal Joint is used between the two shafts and usually for automotive applications, a cardan (cross) style universal joint is used (Vista, 2011). It is where shaft coupling is used to transmit torque/ rotary motion between two shafts that are not on a straight line. The components positioned on the lorry are also illustrated in 3D as in Figure 3.13 and Figure 3.14.
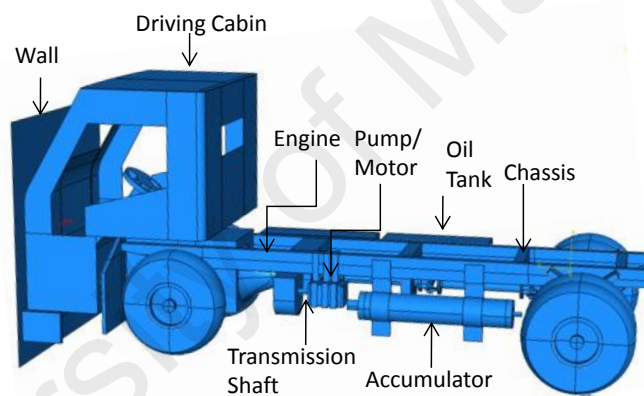
Figure 3.13 Side view of lorry with HRBS.
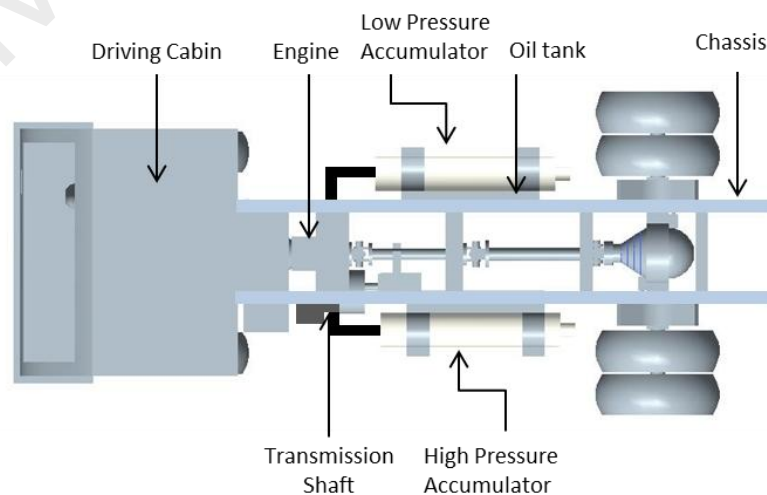
Figure 3.14 Top view of lorry with HRBS.

3.10   HRBS Specification

In summary, the specification of the HRBS is as shown in Table 3.9. The specification is based on the ISUZU NKR-71E lorry, the A4VSG axial piston pump and Hydac 32 L accumulator.

Table 3.9 Specification of HRBS.

Component	Parameter	Symbols	Unit	Value
Vehicle	Total vehicle mass	m	kg	5000
	Front area	A	m²	6
	Wheel radius	r	m	0.4
	Rolling resistance coefficient	f		0.02
	Drag coefficient	C_D		0.65
	Engine power	P_e	kW	90
Axial piston pump	Displacement of hydraulic P/M	D	cc/re	71
	Max speed	v_{max}	rpm	3200
	Max torque	T_{max}	Nm	395
Accumulator	Volume	V	L	32
	Charge pressure	P	Bar	80
	Rated pressure	P_r	Bar	330
	Minimum system working pressure	P_{min}	Bar	15
HRBS	Total weight	m_{HRBS}	kg	350

The HRBS total weight is measured by adding all the key components of HRBS. Table 3.10 summarizes the HRBS components and its weight.

Table 3.10 HRBS total weight

No.	Item	Weight	Unit	Total Weight
1.	Axial piston pump 71cc	60	1	60
2.	Accumulator, 32L	90	2	180
3.	Electronic controller	30	1	30
4.	Position transducer, pressure	2	4	8
5.	Valve control block with accumulator	30	30	30
6.	Linkages, pipeline and bracket	30	NA	42
Approximate total weight of HRBS				350

The total weight of a HRBS is an important factor for a hybrid vehicle since this amount of weight will add towards vehicle weight. Thus the weight percentage of HRBS is calculated and compared to existing system in the market. The weight percentage is calculated as bellow;

Lorry weight without load   = 5 ton (5000 kg)

HRBS on lorry $= m_{lorry} + m_{HRBS}$

     $= 5000 + 350$

     $= 5350 \, kg$

Percentage weight $= \frac{350}{5000} \times 100 = 7\%$

The weight of the system is lower than the weight for hydraulic system developed by Bosch Rexroth. The approximate weight for Bosch system is 500kg which is 43% heavier than the system proposed (Lindzus & Contact, 2010).

3.11 Conclusion

The selected concept and specification of HRBS summarized in table 3.9 will be used as reference for the test rig development in the next chapter which is chapter 4: Test Rig Development.

CHAPTER 4

TEST RIG DEVELOPMENT

4.1   Test Rig Development Process

The objective of this chapter is to describe the development of the test rig system which will be used to test the HRBS concept on 5 ton lorry. The chapter is divided into five sub chapters which are i) modification of test rig which will show the modification done on test rig chassis which has been existing from previous research and flywheel; ii) structural analysis and design calculation of test rig chassis and other components namely the power pack stand and the accumulator stand; iii) the third sub section is hydraulic schematic and description; iv) control system of test rig is where the controller and other electrical components used for operation of test rig system is presented for commissioning test and finally; v) fabrication and installation of test rig component that consist of fabrication of accumulator stand and power pack stand. Figure 4.1 shows the sequence of the development process of test rig;

```
┌─────────────────────────────────────────┐
│         Modification of test rig          │
└─────────────────────────────────────────┘
                    │
                    ▼
┌─────────────────────────────────────────┐
│  Structural analysis of test rig components │
└─────────────────────────────────────────┘
                    │
                    ▼
┌─────────────────────────────────────────┐
│        Hydraulic system of test rig       │
└─────────────────────────────────────────┘
                    │
                    ▼
┌─────────────────────────────────────────┐
│         Control system of test rig        │
└─────────────────────────────────────────┘
                    │
                    ▼
┌─────────────────────────────────────────┐
│   Fabrication and installation of test rig │
│                component                   │
└─────────────────────────────────────────┘
```
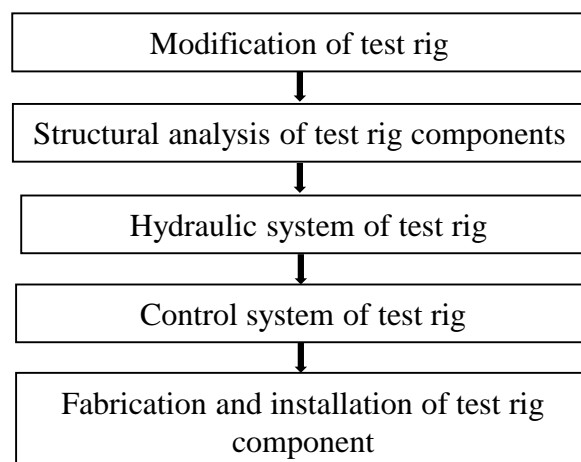
Figure 4.1 Development process of test rig**.**

4.1.2 Introduction to Test Rig

The development of the test rig started in year 2008. At that stage, the test rig developed previously (Chan, 2010) was only to performed initial test and trials to check the flywheel functionality on the chassis constructed. It is basically a three-phase motor connected to two separate second-hand lorry flywheel (to simulate the load of vehicle) by shaft and a lorry drum brake to stop the flywheel manually after each test. In this study, the test rig existing from the previous work is modified and improved to better suit for a 5 ton lorry condition.

The test rig does not really simulate the actual load of the hydraulic system on a lorry as there is limitation since the chassis can only support small load of flywheel which is only 108.33 kg. However it is sufficient enough to test the control system. This existing chassis will help to save cost and time for construction and therefore more time can be spent on understanding and developing the HRBS.

The main components for test rig are variable displacement axial piston pump with maximum displacement, $D_a = 71 cm^3/rev$, high pressure accumulator with 32L, and low pressure tank (hydraulic power pack with 50L) where volume of tank must be larger than of accumulator to ensure availability of hydraulic fluid supplied to accumulator. Before the components for the test rig system is assembled at site, modification on chassis must be done first. Next subsection will show the modification which has been done to the existing chassis.

4.2   Test Rig Modification

The current flywheel setup is a modified version of the existing test rig which was previously developed by Chan (Chan, 2010). The modification has been made to support the new axial piston pump and flywheel. The picture on the left hand side of Figure 4.2 is the setup of the old test rig. Previously a three-phase induction motor and a simple controller to control the speed of the motor were used. The three-phase motor was installed by screwing the base of the motor to a plate which was then welded to the pillow block that was used to support the motor. The pillow block was added at the base of the motor to make the motor shaft the same height as the flywheel shaft. In this setup, the most important issue is to make the whole thing aligned. The motor shaft and the flywheel must be aligned together to reduced internal stress within the test rig (Chan, 2010).

Figure 4.2 Test rig setup, old setup (Left) and new setup (Right).

The modification made to the chassis is to accommodate the new axial piston pump. As mentioned previously, a HRBS needs a pump that can function in dual mode to operate as a regenerative system. Therefore the three-phase induction motor is changed to an axial piston pump. The old chassis design had an open end structure (Figure 4.3). Modification is done by closing the end with a pillow block. This made the structure

more stable and stronger as the structure is all connected by welding. The pillow blocks that hold the journal bearing has been adjusted backward to give space to the bell housing and the axial piston pump. Absorber pad is added at the base of the chassis to absorb vibration when the flywheel is spinning.
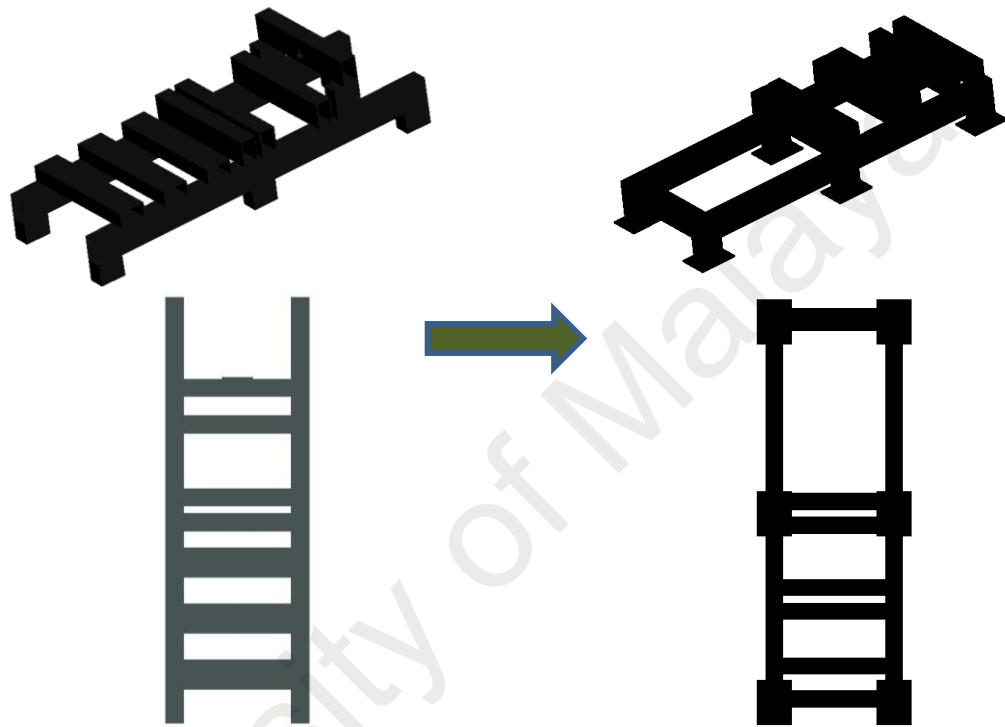
Figure 4.3 Test rig chassis, old chassis (Left) and new chassis (Right).

The old chassis has two flywheels (Figure 4.4). The total weight of the old flywheel was 79.6 Kg. The shaft holding the flywheels was bent during the previous testing. Therefore modification is made to the flywheel by replacing it with a new flywheel fabricated from a solid stainless steel block. The solid block is fabricated into flywheel with hole in the middle for shaft by CNC milling. The weight of the new flywheel is 103.88 Kg. The next subchapter will describe the structural analysis of test rig system components.
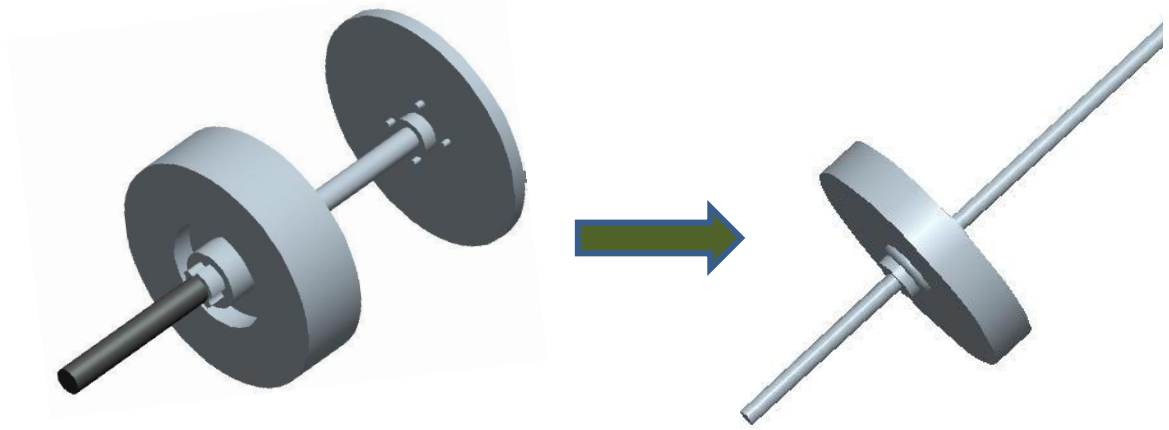
Figure 4.4 Flywheel; old flywheel (Left) and new flywheel (Right).

4.3 Structural Analysis of Test Rig System Components

4.3.1 3D Models of Test Rig Components

The first step before structural analysis is done is to create 3D model of components. The 3D model of 3 parts (test rig structure, accumulator stand and power pack stand) for test rig system was modeled using CATIA V4. 3D model created is to visualize the design and to be used in Finite Element Analysis. The dimension for test rig structure is based on the old chassis in the lab. The accumulator and power pack stand was designed and modeled based on the actual accumulator and the power pack purchased. The 3D model of the components and its description is shown in Figure 4.5, 4.6 and 4.7

4.3.2 Test Rig Chassis

The structure of test rig chassis (Figure 4.5) has a closed end to increase strength. There are 6 chassis base and it is fixed on the lab floor by M8 X 75mm extended anchor bolt. The addition of base in the middle of the structure is to gain stability for the whole structure. A rectangle hollow section 250 x 70 x 4.5mm m/s flat pillow block is used to build this chassis structure.

The modification however does not change the total length of the chassis. Therefore the journal bearing to support the shaft is positioned within the existing length. The shaft that is perpendicular to the flywheel is held by 6 journals bearing positioned along the chassis structure. At the end side of the chassis is where the drum brake is positioned while the pump is held by bell housing (red color) which is located at the opposite end of the chassis.

Isometric view

Top view

Front   Side view
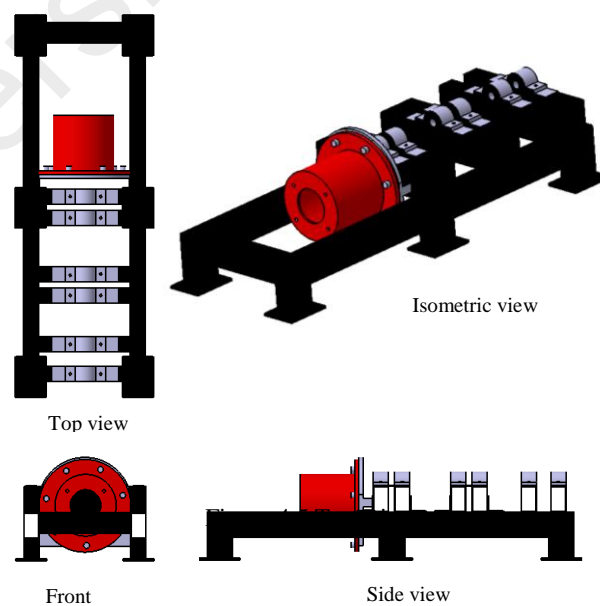
Figure 4.5 Test Rig Chassis

4.3.3   Accumulator Stand

The accumulator is placed in vertical position in this experiment setup. The accumulator can be positioned in three ways; vertical, horizontal and slanted. Each positioning is meant for different usage of the accumulator. For energy storage purpose, it is suggested that the accumulator be positioned vertically. However, in the actual setup the accumulator is positioned horizontally due to safety reasons as the vehicle will be travelling on rough roads. The weight of the accumulator is 90 kg. The design of the accumulator stand (Figure 4.6) is added with belt to hold the accumulator. The belt is hooked to the stand at the plate that holds the accumulator in vertical way. The stand is designed to be higher than the accumulator safety block as the safety block will be positioned under the accumulator. The stand base has 9 holes for affixing to the ground. By fixing the stand to the ground, the stand will be more stable.

Top view

Isometric view

Front view

Side view
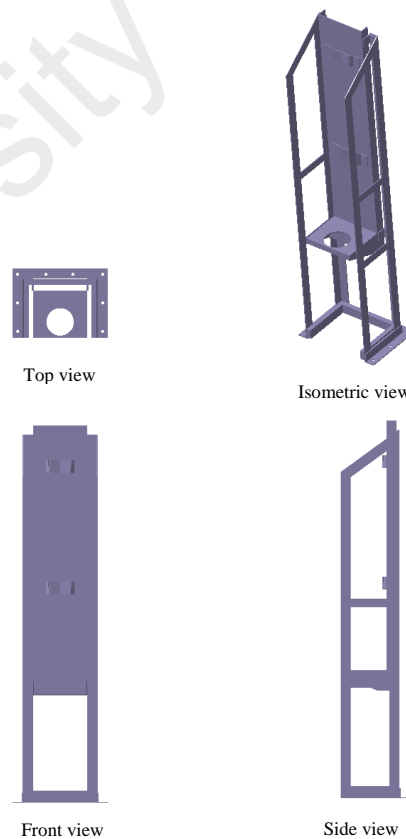
Figure 4.6 Accumulator Stand

4.3.4 Power Pack Stand

The power pack must be positioned as near as possible and above the axial piston pump. Therefore, the stand (Figure 4.7) is designed to hold the power pack at an elevated height so that the hydraulic fluid transfer is flawless by gravity from power pack to the pump (pumping mode) and from pump to power pack (motor mode). At the middle of the stand, there is a square hole for piping purpose.

The surface of the stand must be able to withstand the power pack weight at full tank condition (50 litres). The structure of the stand is added with slanted beam to add strength to the stand. Below the top surface are additionally three beams to support the weight of the power pack. The power pack base is fixed to the stand using bolt and nut. Holes are made at the stand leg to fix the stand to the ground.

Top view   Isometric view

Front view   Side view
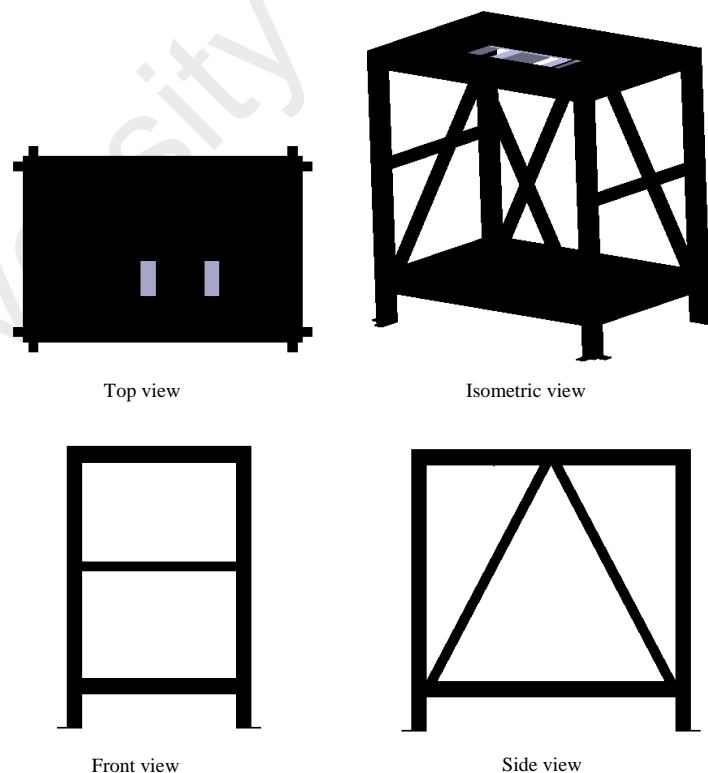
Figure 4.7 Power Pack Stand

4.3.5 Calculation of Test Rig Chassis

There are three supporting locations in test rig, A, B, and C as indicated in Figure 4.8. By using method of Force in Beam (Beer, Johnston, & Jr., 2006), reaction forces on the chassis at those 3 locations due to weight of drum brake and flywheel are calculated. From the illustration in Figure 4.8, a free body diagram (Figure 4.9) is created to calculate the amount of pressure acting on each point. The reason this calculation is done is to determine the value of pressure acting on point R_A, R_B, and R_C. The value obtained from the calculation will be used inside Finite Element Analysis (FEA) to see the reaction of the pressure on the chassis when the flywheel spinning during operation. Note that this calculation is only for chassis structure and does not involve accumulator stand and power pack stand as the force on both component is a primary load (equipment load which is accumulator tank for accumulator stand and power pack tank and motor for power pack stand).
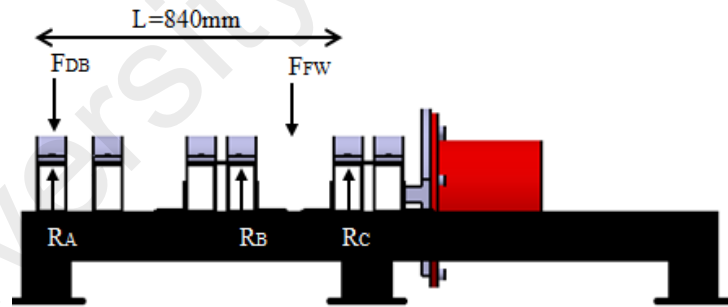
Figure 4.8 Force exerted on the 3D model of chassis.
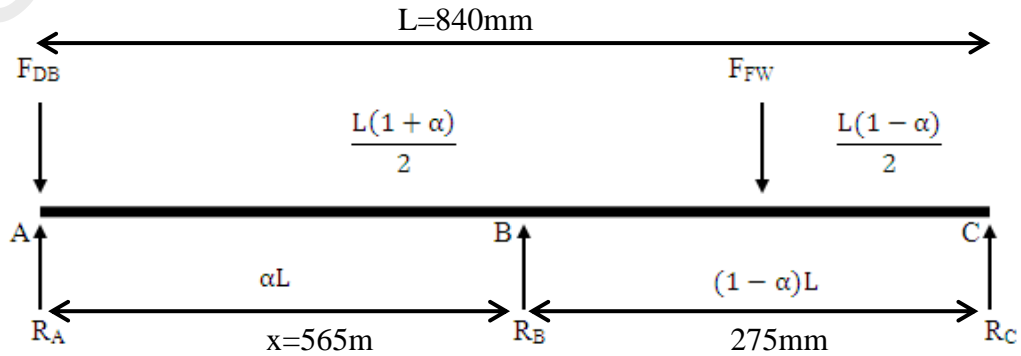
Figure 4.9 Free Body Diagram.

The force of flywheel is calculated using the Equation (4.1);

$$F_{FW} = \text{Mass of flywheel x gravity}$$

$$= m_{FW} \text{ x } g \qquad\qquad\qquad \text{Eqn. (4.1)}$$

$$= 108.33 \text{ x } 9.81$$

$$= 1062.7173 N$$

For drum brake force, the same Equation in (4.1) is used;

$$F_{DB} = \text{Mass of drum brake x gravity}$$

$$= m_{DB} \text{ x } g$$

$$= 17.22 \text{ x } 9.81$$

$$= 168.92 N$$

Since the chassis is existing from the previous research, the total length of the chassis, L, can be measure directly using measuring tape. Therefore the information is added to the list as;

L = Total length of system, 840mm

And α is used to describe the fraction of distance A and B to total length. Therefore;

α = Fraction of distance A and B to total length

R_A, R_B, and R_C, is calculated using Statically Indeterminate Beams (Beer, et al., 2006) as there will be axial loading on the chassis. The properties of the beam with regard to its resistance to bending must then be taken into consideration. The deflection on beam is considered and Method of Superposition (Beer, et al., 2006) is used to compute the slope and deflection separately by each of given loads. The reaction R_B is designated as

redundant and considered as an unknown load. The deflections due to the F_{DB} and F_{FW} and to the reaction R_B are considered separately as shown in Figure 4.10.
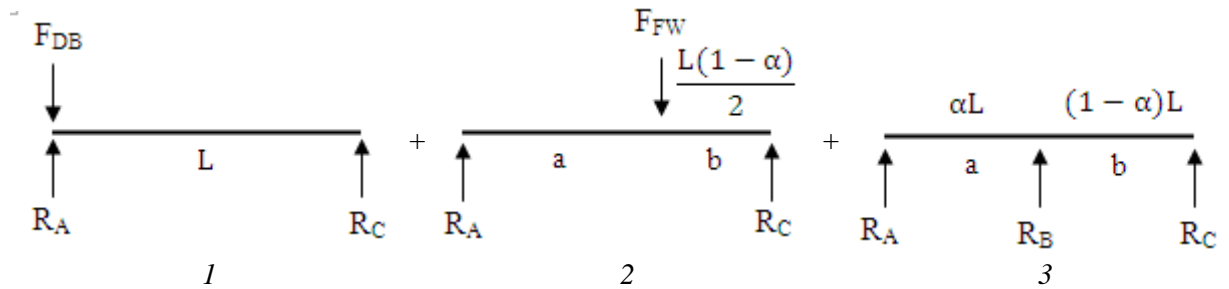
Figure 4.10 Method of Superposition.

The calculation will be based on Figure 4.9. Each section represents different condition listed as bellow;

1: **Deflection at B due to F_{DB};**

$$y_1 = 0 \qquad\qquad\qquad \text{Eqn.(4.2)}$$

2: **Deflection at B due to F_{FW};**

Where x = distance between A and B, since x < a, therefore;

$$y_2 = \frac{Pb}{6EI}[x^3 - (L^2 - b^2)x], \text{ (Beer, et al., 2006)} \qquad \text{Eqn. (4.3)}$$

Where;

P = Reacting force, N

E = Young modulus of beam, Nm^{-2}

I = Moment inertia of beam, m^4

Referring to Figure 4.10;

$P = F_{FW}$

$b = \frac{L(1 - \alpha)}{2}$

$x = \alpha L$

Substitute all this into Equation (4.3) and the simplified form is as Equation (4.4).

$$y_2 = \frac{F_{FW}(-5\alpha^4 + 7\alpha^3 + \alpha^2 + 3\alpha)L^3}{48EI}$$ Eqn. (4.4)

3: Deflection at B due to R$_B$;

When x = a, y_3 is calculated as;

$$y_3 = -\frac{P(a^2)(b^2)}{3EIL}, \text{ (Beer, et al., 2006)}$$

$$= \frac{R_B(\alpha^2 - 2\alpha^3 + \alpha^4)(L^3)}{3EI},$$ Eqn. (4.5)

Where;

$P = -R_B$, as R$_B$ points upward.

To determine R$_B$, recalling that deflection at B, $y_B = 0$ and $y_1 = 0$, hence;

$y_B = y_1 + y_2 + y_3$

$y_3 = - y_2$ Eqn. (4.6)

Substitute Equation (4.4) and (4.5) into Equation (4.6);

$$\frac{F_{FW}(-5\alpha^4 + 7\alpha^3 + \alpha^2 + 3\alpha)L^3}{48EI} = -\left[\frac{R_B(\alpha^2 - 2\alpha^3 + \alpha^4)(L^3)}{3EI}\right],$$

Equation (4.4), (4.5) and (4.6) is simplified into;

$$R_B = \frac{F_{FW}(5\alpha+3)}{16\alpha}$$ Eqn. (4.7)

Since α is always positive as length is positive value, R_B is pointing upward. Thus, the value for R_A, R_B and R_C can be solved by;

$$+ \sum F_y = 0,$$ Eqn. (4.8)

$$R_A + R_B + R_C - F_{DB} - F_{FW} = 0$$ Eqn. (4.9)

Substitute $R_B = \frac{F_{FW}(5\alpha+3)}{16\alpha}$ into Equation (4.9);

$$R_A + R_C = F_{DB} + F_{FW}\frac{(11\alpha-3)}{16\alpha}$$ Eqn. (4.10)

Moment at A is;

$$\sum M_A = 0,$$

$$R_B(\alpha L) + R_C(L) - F_{FW}\frac{L(1+\alpha)}{2} = 0$$ Eqn. (4.11)

$$R_C = F_{FW}\frac{(1+\alpha)}{2} - R_B(\alpha)$$ Eqn. (4.12)

From Equation (4.10), R_A is determined;

$$R_A + R_C = F_{DB} + F_{FW}\frac{(11\alpha-3)}{16\alpha}$$ Eqn. (4.13)

$$R_A = F_{DB} + F_{FW}\frac{(11\alpha-3)}{16\alpha} - R_C$$

Substitute Equation (4.12) into Equation (4.13);

$$R_A = F_{DB} + F_F\frac{(11\alpha-3)}{16\alpha}w - [F_{FW}\frac{(1+\alpha)}{2} - R_B(\alpha)]$$ Eqn. (4.14)

Recall back the information that already been determined before where;

F_{FW} = 1062.7173N

F_{DB} = 168.92N

L   = 840mm

x   = αL

With reference to free body diagram in Figure (4.9), α can be calculated as;

x   = αL = 565mm

α = $\frac{565}{840}$

      = 0.6726

Substitute all the value into Equation (4.14);

R_A = -285.4979 + 0.6726 R_B Eqn. (4.15)

and R_B is calculated using Equation (4.7);

R_B = $\frac{F_{FW}(5\alpha+3)}{16\alpha}$

      = 628.3517 N

Calculate R_A in Equation (4.15) using the R_B value;

R_A = -285.4979 + 0.6726 R_B

      = -285.4979 + 0.6726 (628.3517)

      = 137.1315 N

Using Equation (4.12), R_C is determined;

$$R_C = F_{FW} \frac{(1+\alpha)}{2} - R_B (\alpha)$$

$$= (1062.7173) \frac{(1+0.6726)}{2} - (628.3517) (0.6726)$$

$$= 389.3823 \text{ N}$$

After completion of calculating the reaction force at all three point, pressure on each point is determined. General equation for pressure acting on point is;

$$P = \frac{F}{A}$$ Eqn. (4.16)

Where;

F= Force acting, N

A= area where force is acting, m^2

The area where force is acting is measured directly from chassis body and calculated using area formula (width x height). Summary of calculation for reaction force and corresponding pressure to be used in FEA is shown in Table 4.1;

Table 4.1: Calculation of summary of force and pressure.

Point	Force (N)	Area (m^2)	Pressure (MPa)
A	137.1315	0.00044	0.3117
B	628.3517	0.0175	0.0359
C	389.3823	0.0175	0.0225

4.3.6　Finite Element Analysis (FEA)

The Finite Element Analysis (FEA) in this study is to predict the response of structures and materials to environmental factors which is includes forces and vibration. FEA is commonly used in structural and solid mechanics applications for calculating stresses. These can be used to predict failures (Group, 2012). The software used for FEA was ABAQUS software version 6.10. The completed 3D model is converted into IGS format and imported into ABAQUS. The analysis is done to confirm the stability of constructed structure. The parts are modeled with some simplifications and focused only at the critical part which is important for analysis to reduce the computational time while maintaining the accuracy of the results.

The FEA processes start with the creation of a 3D model of the component. After creating the 3D model, the material property is set into the software. The material property defined is material density, Young's Modulus and Poisson's Ratio. Young's Modulus indicates stiffness of material under uniaxial loading while Poisson's Ratio is when the material is stretched or compressed longitudinally. When the property is set, loading and boundary conditions are applied to the model. The type of loading for this analysis is primary loading which is equipment load. Then the model is subdivided (partitioned and meshed) into small pieces (elements) of simple shapes connected at specific node points. Finally, the model is submitted for Jobs. Jobs is where ABAQUS will analyse the model. When analysis is completed, the output is given in illustration using visualization module.

In this study, two stands will be fabricated to hold accumulator and power pack. Therefore FEA is done to confirm the design ability to hold the components. FEA is also done on the modified design of chassis to check the structure stability.

4.3.7　　　　FEA of Accumulator Stand

In order to assist the simulation, the accumulator stand is modelled into simplified shapes. The focus of this analysis is on the support where the accumulator will be resting (Figure 4.11). The design to hold the accumulator at position higher than accumulator safety block and in vertical position. The accumulator weight is considered as the load for the analysis. Analysis is made to determine whether the design structure of accumulator stand can withstand the accumulator load.
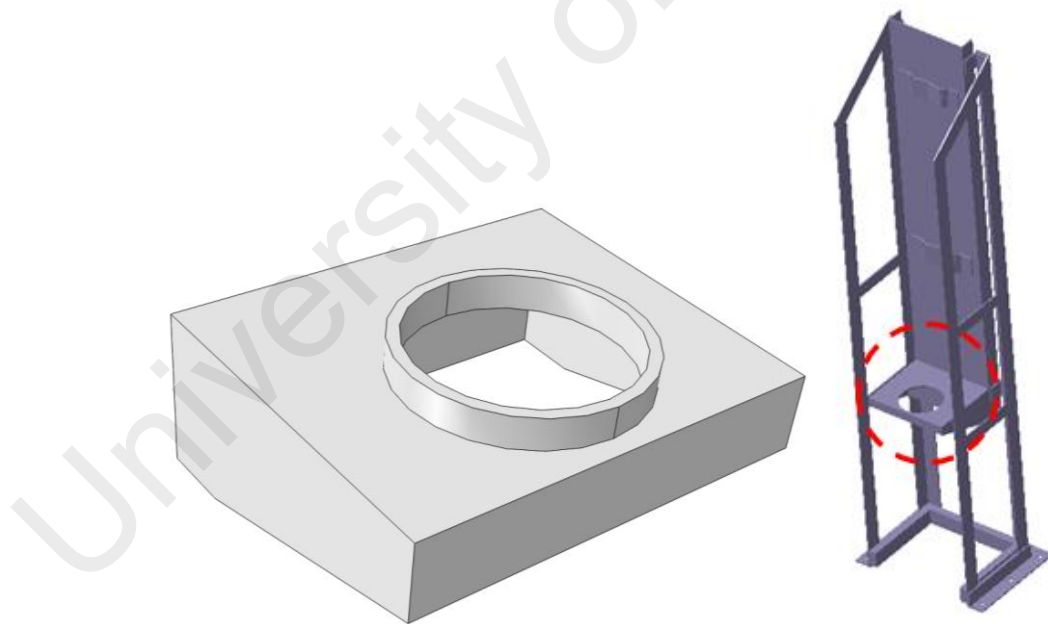
Figure 4.11 Simplified model of accumulator stand.

After importing the 3D model in IGS file from CATIA Software, the property of accumulator stand is set. The material used for this design is stainless steel 304. The value used for analysis is summarized in Table 4.2;

Table 4.2 Material property for accumulator stand.

Property	Unit	Value
Density (ρ)	kg.m^{-3}	7850
Material Young Modulus (E$_{mat}$)	GPa	207
Poisson ratio	-	0.30

Next the boundary condition and loading are set. The side where the support will be welded to the stand (Figure 4.12) is set as "encastre" which mean that the support is fixed and no movement in x, y and z direction will occur. Loading for this analysis as mentioned before is the accumulator weight which is 90kg.
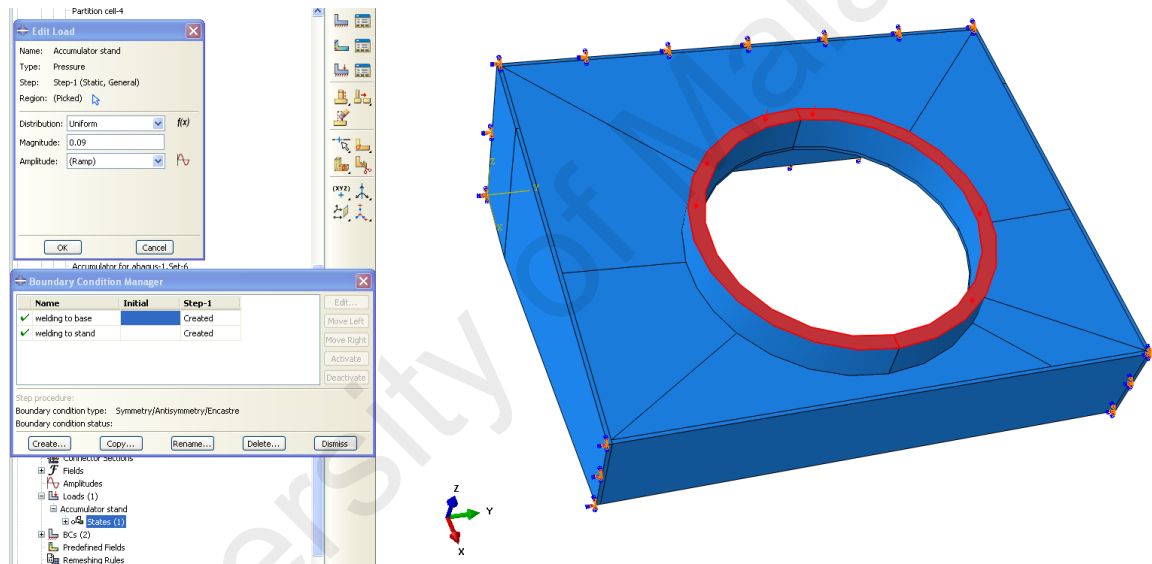
Figure 4.12 Boundary condition and loading for accumulator stand.

Then the stand model dividade segment using partitioned as in Figure 4.13. The objective of partioning the support is to obtain hexagonal type of structed meshing. The seed size and mesh type will influence the result in finite element model. This will lead to difference in result of kinetic energy, strain energy, stress, reaction forces and displacement. Hexagonal element is difficult to assign at complex geometry compared to tetrahedral element. However hexagonal element will yield better quality of results

(Saw, 2010). Hence, hexagonal element mesh technique is adopted for this analysis to reduce the computational time while the quality of result is maintained.
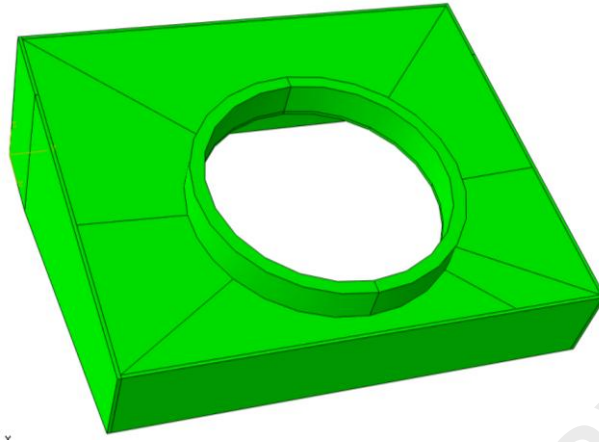
Figure 4.13 Partitioning strategy for accumulator stand support.

Apart of meshing technique, seeding size is also another factor that affects the quality of the results. The small number of elements will increase the computational time. The seeding size used for the support is 0.005. The smaller the seeding size, the more accurate the result will be. The meshing of the accumulator support can be seen in Figure 4.14.
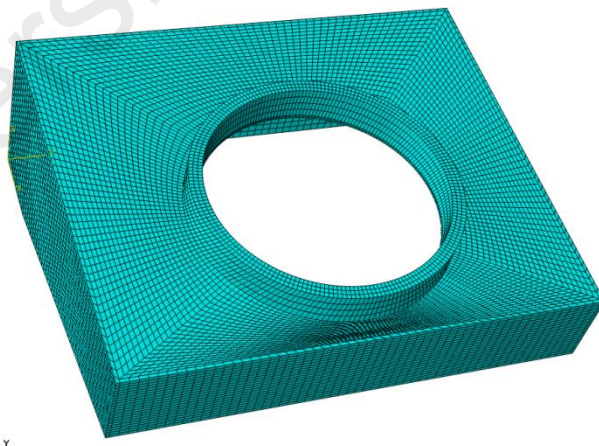
Figure 4.14 Meshing the accumulator stand support.

The last stage before results can be obtained is to create Jobs. Jobs are created after analysis model is completed. This stage is a solver stage where all data input previously is processed and submitted for post processing. The post processor stage is where the

result is read and interpreted into graphic manner. Analysis result of accumulator stand after submitted for Jobs is shown in Figure 4.15 and Figure 4.16. In this analysis, the result for Von Misses is considered. The ABAQUS software does not have measuring unit. Therefore, all value insert into this software must be in standard unit, SI. The Von Misses stress is in MPa value. The stress value is used to calculate the safety factor (FOS). The yielding of constructed material must be determine before actual construction is done as it may fail if it is subjected to excessive loadings that cannot be supported by its structure or material. This is what is called as allowable stress design method (Burdekin, 2007) where the component under maximum loading conditions should nowhere exceed the material yield divided by an appropriate safety factor (Burdekin, 2007).
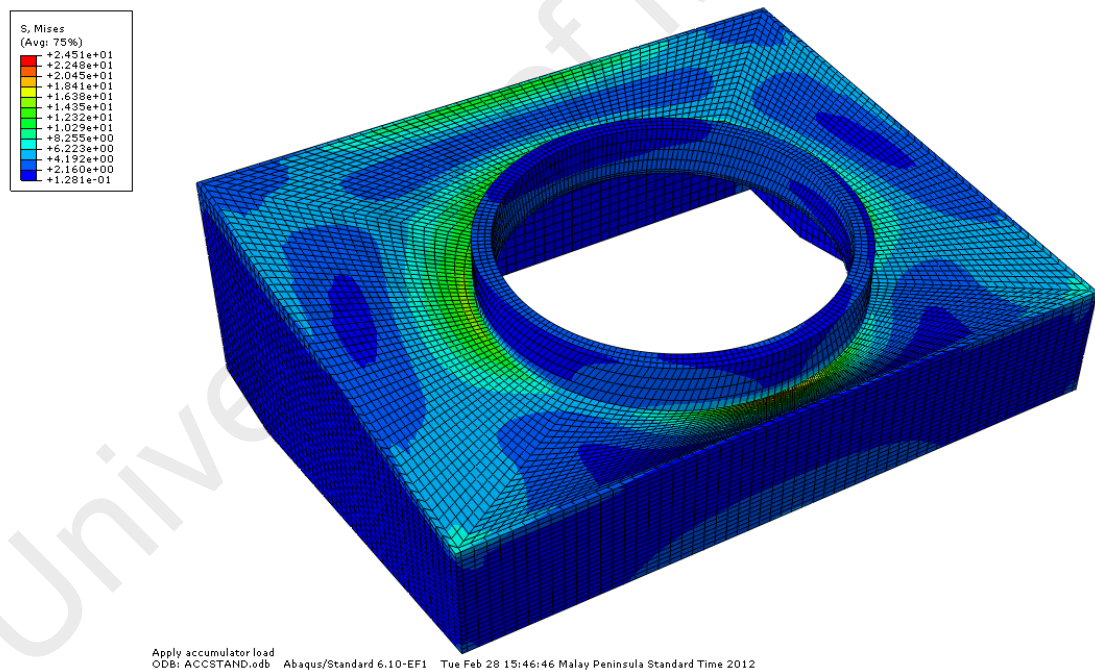
Figure 4.15 Contour plot of Misses stress of accumulator stand (Isometric view).
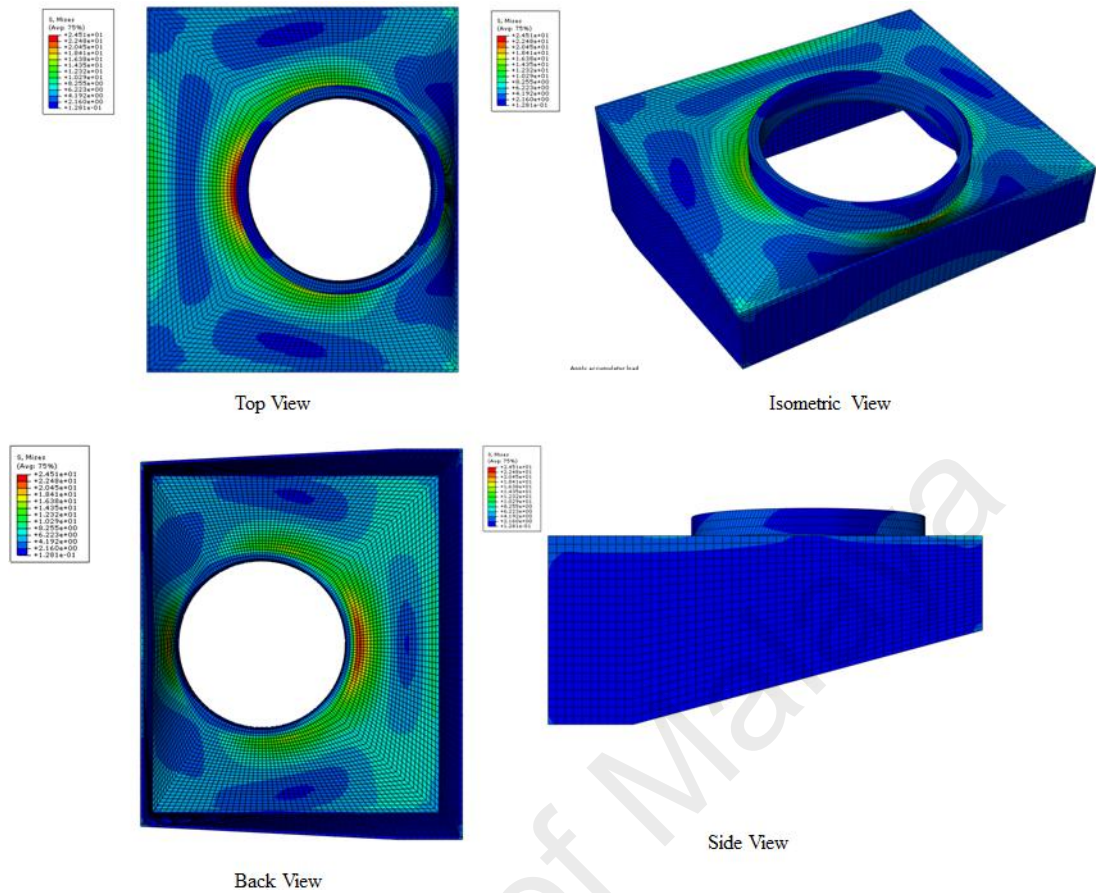
Figure 4.16 Contour plot of Misses stress of accumulator stand (Top, Back, Side and Isometric view).

From the properties table, the yield shear strength for the stainless steel is 276MPa, while the maximum stress exerted on accumulator stand of 24.51 MPa. Therefore, the safety factor for this swash plate design is;

Yield shear stress, σ_y = 276MPa

Maximum stress on accumulator stand = 24.51 MPa

$$\text{Factor of safety} = \frac{\text{Yield shear stress}}{\text{Maximum stress on component}} \qquad (4.16)$$

$$= \frac{276 \times 10^6}{22.51 \times 10^6} = 12.2667$$

This safety value is proven for safety, as the yield strength minus loading effects is larger than 1.5 that is mostly used in engineering application (Burdekin, 2007).

Theoretically, this accumulator design will not face failure when it is positioned on accumulator stand.

4.3.8   FEA of Power Pack Stand

The power pack stand is design to support the power pack tank and motor. The simplified 3D model for the analysis is only the top part of the stand. The top part of the stand is a rectangular shape with rectangular hole for pipeline from the tank to the axial piston pump. The simplified model is shown in Figure 4.17. The concern for this design is whether the stand can support the load of power pack tank and motor.
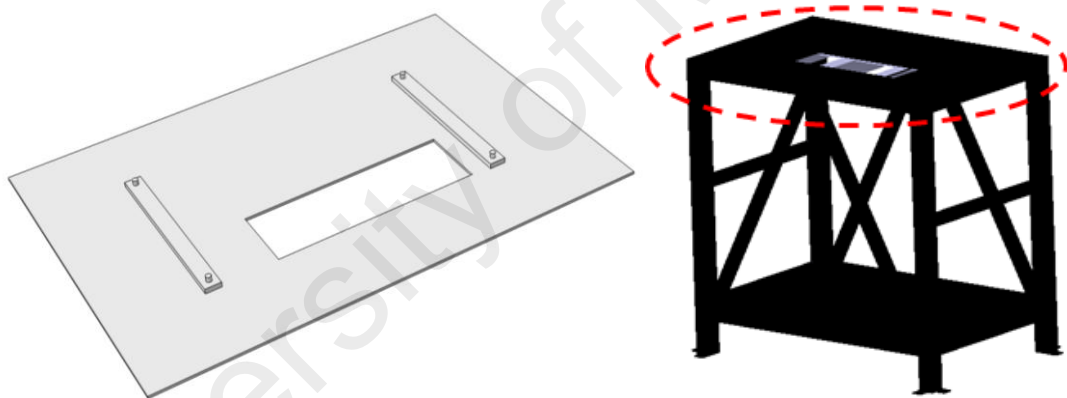
Figure 4.17 Simplified 3D model of power pack stand.

The material used for this stand is stainless steel 304. The property set in ABAQUS is shown in Table 4.3. After setting the property value, loading and boundary conditions are inserted. The boundary condition for the top part of the stand is the same with accumulator support. The rectangular top part of the stand is welded together at all four side. These four sides are set to encastre. Another boundary condition set on the model is the screw used to fix the tank to the top part of the stand. The tank is fixed to the stand to avoid any movement made by vibration of the three phase motor attached to the power pack tank. In Load Manager Section, the tank added with three phase motor load

89

is applied on the model as in Figure 4.18. The load is set as distributed pressure along the tank leg. The load of the tank (with assumption the tank is full with hydraulic fluid) and motor is 90kg.
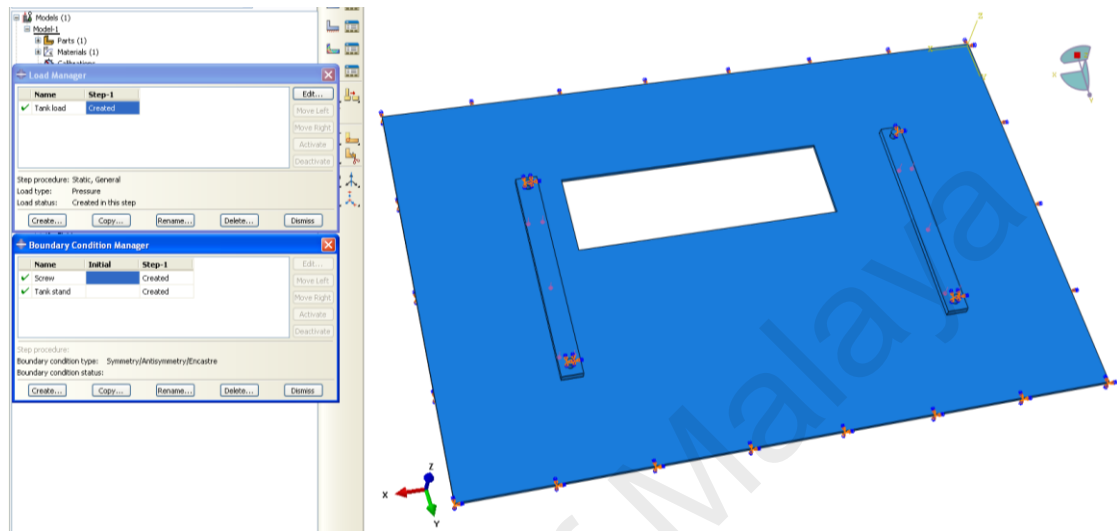
Figure 4.18 Boundary condition and loading for power pack stand.

The partitioning of the top part is easier to make as the model does not involved any circular shape. Again this is made to ensure the model can be meshed into Hexagonal type of meshing structure (indicate by green color as in Figure 4.19).
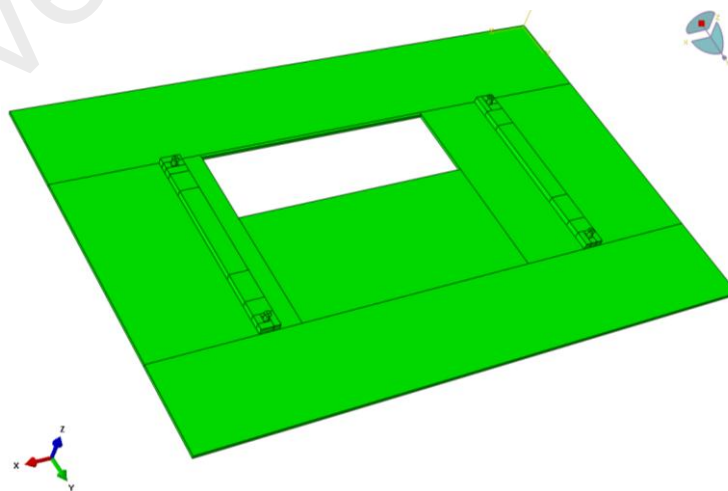
Figure 4.19 Partitioning strategy of power pack stand.

Then the model is meshed using seeding size of 0.005 as in Figure 4.20.
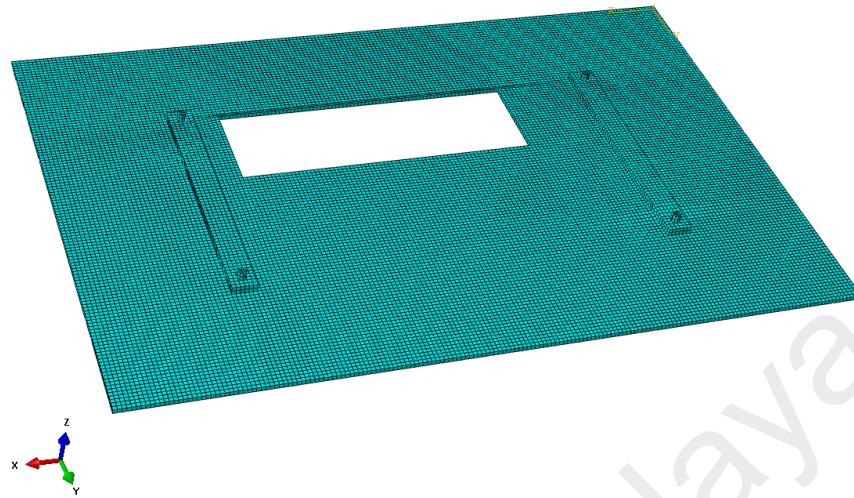
Figure 4.20 Meshing the power pack stand.

The analysis is submitted to post processing and the result is as in Figure 4.21 and Figure 4.22.
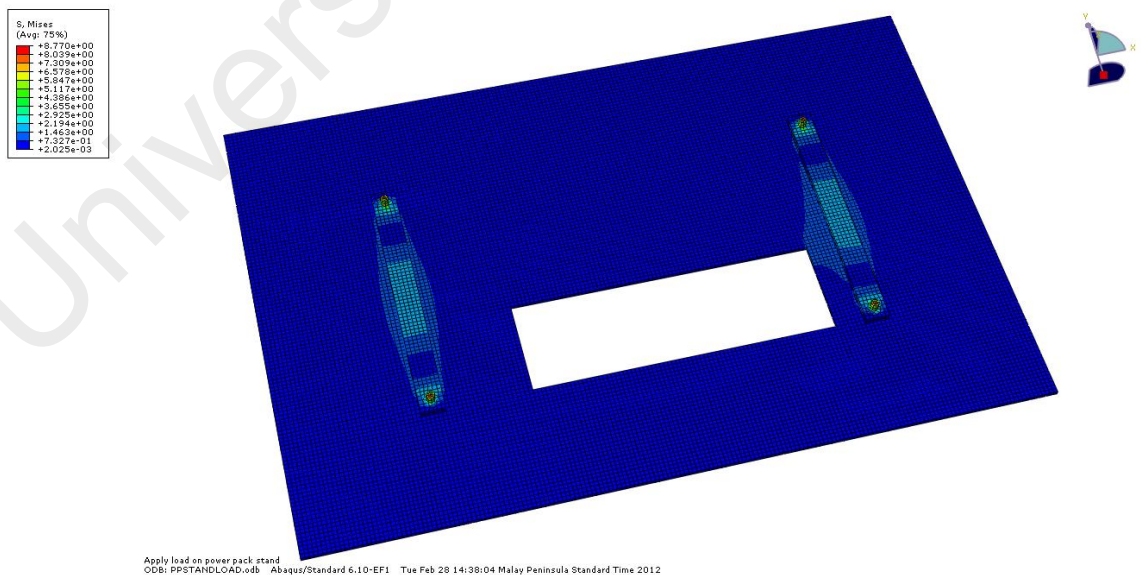
Figure 4.21 Contour plot of Misses stress on power pack stand.
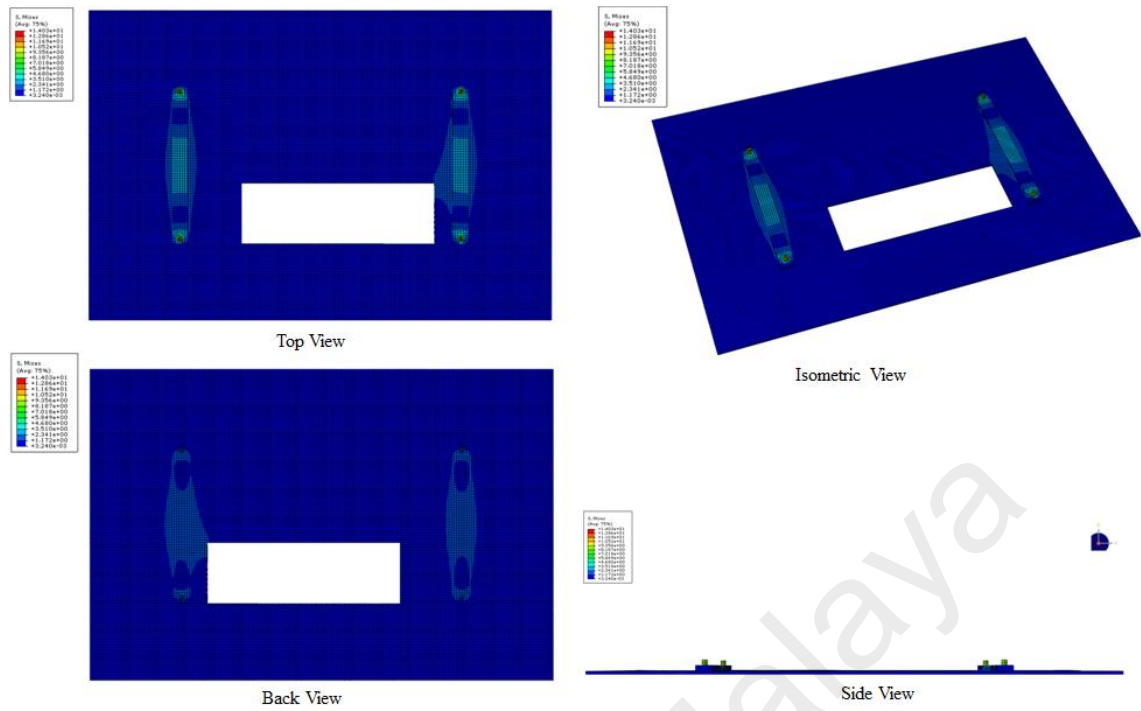
Figure 4.22 Contour plot of Misses stress of power pack stand (Top, Back, Side and Isometric view).

From the result, the maximum stress applied on the power pack stand when load applied is 8.770 MPa. The Factor of Safety is calculated as bellow;

Yield shear stress, $\sigma_y = 276$MPa

Maximum stress on power pack stand $= 8.770$MPa

$$\text{Factor of safety} = \frac{\text{Yield shear stress}}{\text{Maximum stress on component}} \tag{4.16}$$

$$= \frac{276 \times 10^6}{8.77 \times 10^6} = 31.4709$$

As the value of Factor of Safety is 31.4709 that is larger than 1.5, thus this power pack stand design can be used for fabrication.

4.3.9   FEA of Chassis

Analysis for test rig chassis is made to confirm safety for modification of the chassis when the flywheel spins during testing. Previously in structural analysis section, the value of corresponding pressure acting on the chassis is calculated. The value will be used in this analysis at loading section. The load acting on the chassis involved rotating load of the flywheel and drum brake. Therefore the analysis is a dynamic analysis. However, dynamic analysis can be treated as static analysis since dynamic analysis is for speed that changes through time. Hence the same approach is used to calculate the stress acting on the chassis. The chassis is modeled as in Figure 4.23 excluding the bell housing (red circle) since the chassis involved a lot of welding and it is important to make sure that the whole chassis structure is safe to be used.
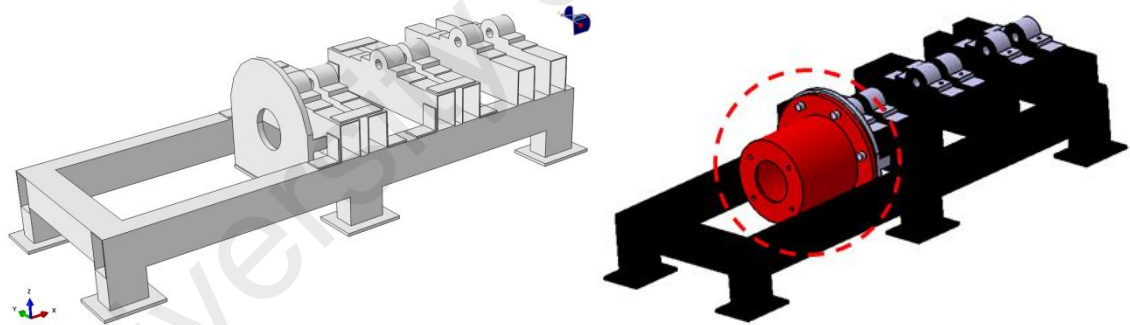
Figure 4.23 Simplified 3D model of test rig chassis.

The material used for the chassis is stainless steel 304 and the property value can be referred in Table 4.3. There are four load acting on the chassis. The value set for loading is given in Table 4.1.

Table 4.3 Value of load acting on test rig chassis.

Load	Pressure (MPa)
PR_A	0.3117
PR_B	0.0359
PR_C	0.0225
Pump	0.0600

There are two boundary conditions in this analysis. The first boundary condition is set at all 6 bases of the chassis while the second is at all 6 journal bearing base which is screwed on the chassis structure to hold the rotating shaft. The loading and boundary condition is shown in Figure 4.24.
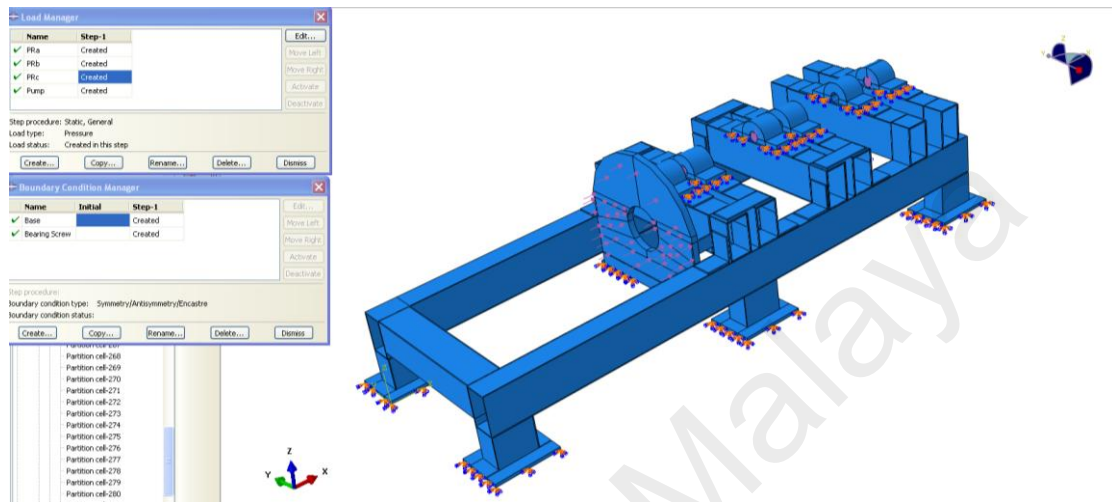
Figure 4.24 Boundary condition and loading for test rig chassis.

The assembly of chassis is set to be independent as modification can be made on the chassis later on meshing section. Next, the chassis is partition as in Figure 4.25 to obtain hexagonal structure.
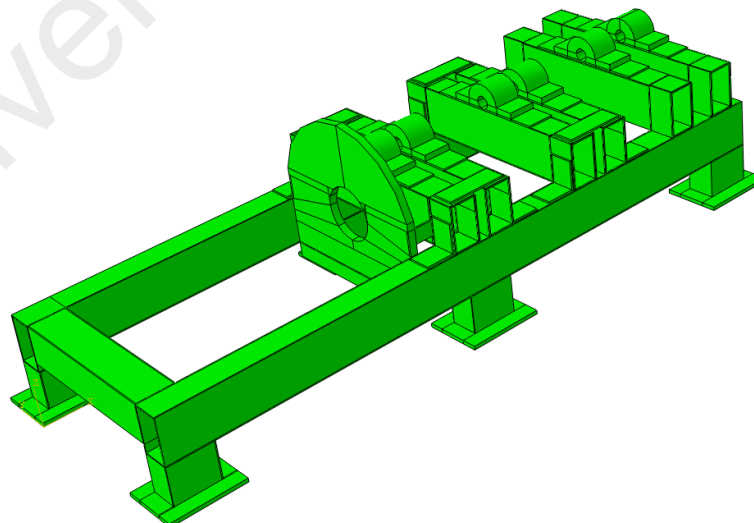
Figure 4.25 Partitioning strategy on test rig chassis.

After partitioning the chassis, the model is meshed using seeding size of 0.01. Due to the limitation of the student edition software, the seeding size is set to a larger value compared to previous analysis. The meshing result is as in Figure 4.26.
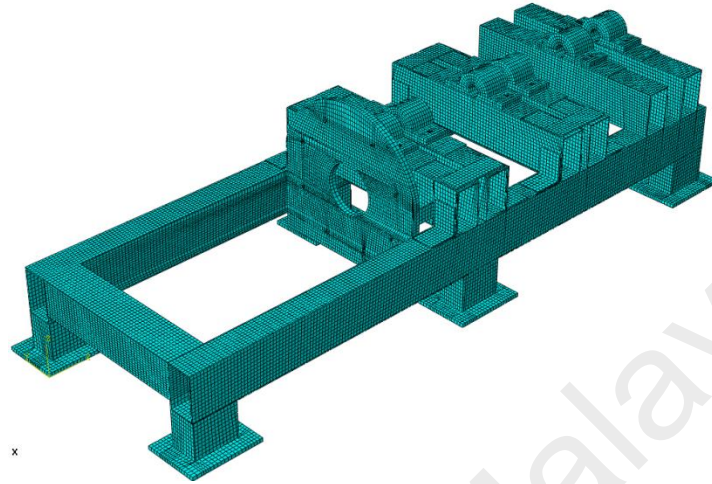
Figure 4.26 Meshing the test rig chassis.

After meshing is completed, Jobs is created and submitted for post processor. The maximum stress acting on the test rig chassis is 162 MPa (Figure 4.27).
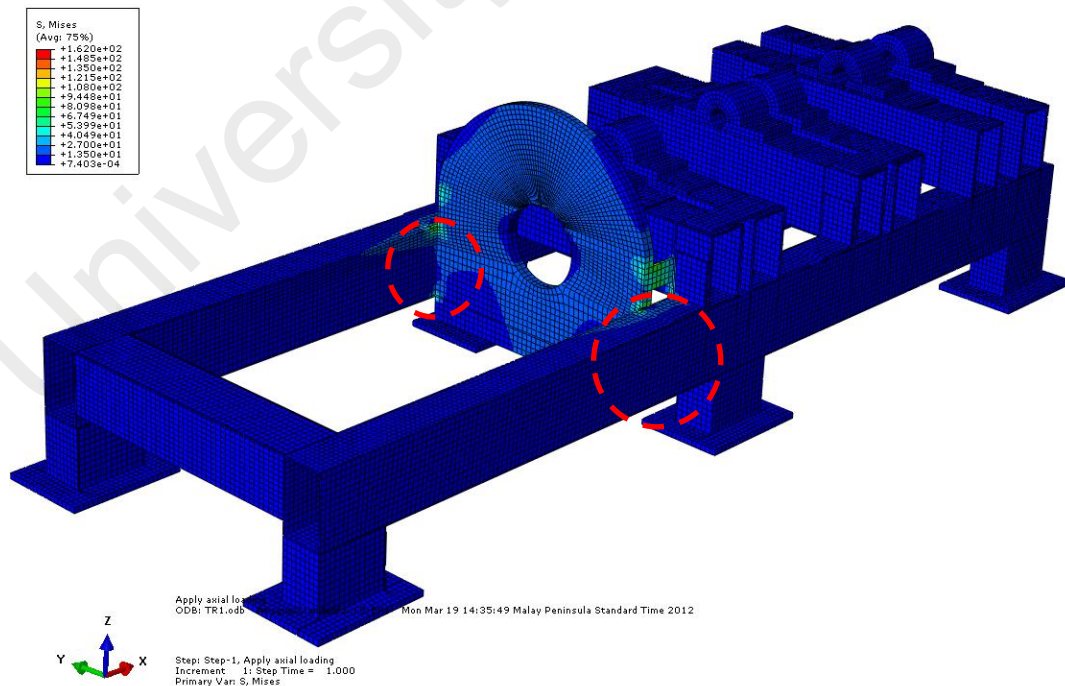
Figure 4.27 Contour plot of Misses stress on test rig chassis and welding location of bell housing plate (red circle).

Therefore the factor of safety is;

Yield shear stress, σ_y = 276MPa

Maximum stress on power pack stand = 162MPa

Factor of safety $\quad = \dfrac{\text{Yield shear stress}}{\text{Maximum stress on component}}$ (4.16)

$$= \frac{276\times10^6}{162\text{x}10^6} = 1.7037$$

The safety value is larger than 1.5. Observing Figure 4.28, the stress mostly concentrated at the part where the bell housing holding the pump. Note that this part is only an additional feature to strengthen the bell housing plate as the bell housing plate is welded onto the chassis body (red circle). Therefore, the modified design of test rig chassis is safe to be used for the test rig system.
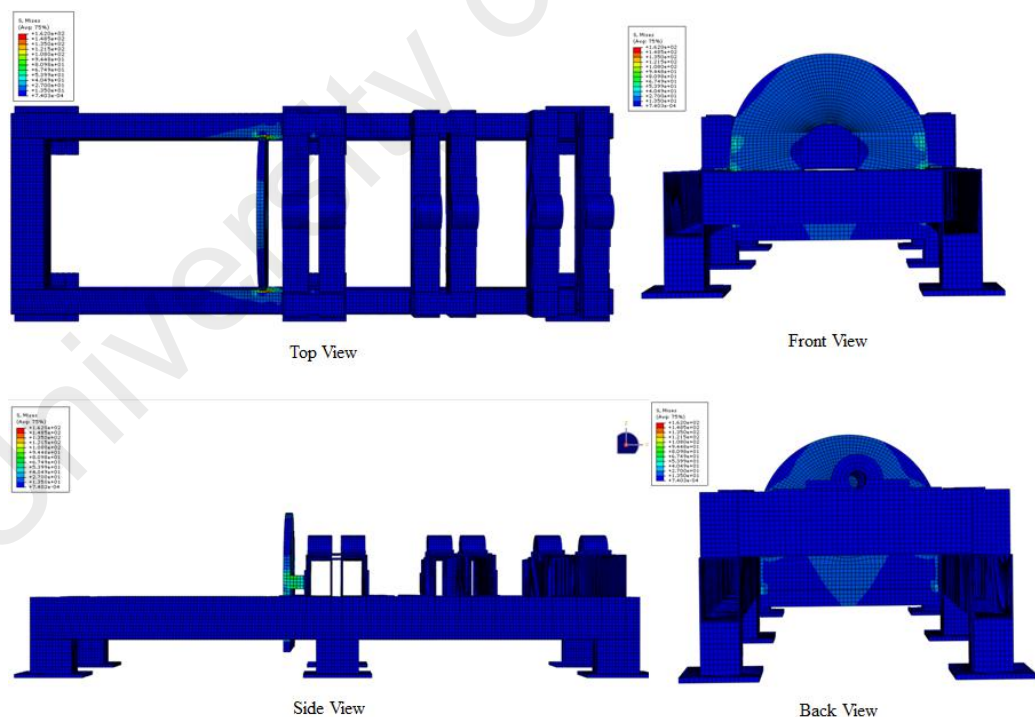
Figure 4.28 Contour plot of Misses stress of test rig chassis (Top, Back, Side and Isometric view).

After completing the analysis for all three models, the next step is to develop the hydraulic circuit for the test rig system and controller circuit to control the power pack and the axial piston pump in the test rig system.

4.4   Test Rig Hydraulic Diagram

The hydraulic circuit for test rig is designed based on the actual component on HRBS. Figure 4.29 shows the full schematic of the hydraulic circuit of the test rig system.
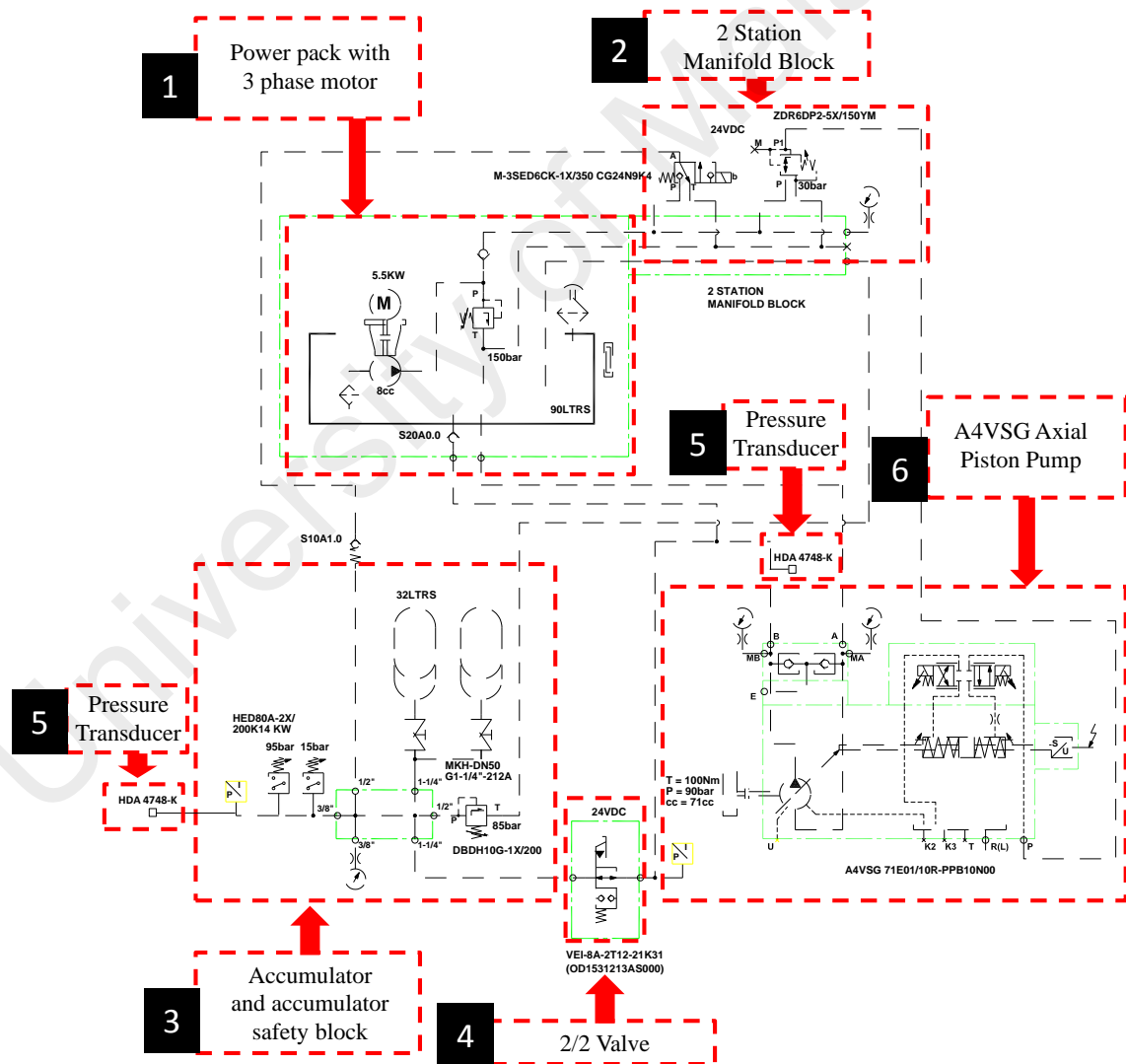
Figure 4.29 Hydraulic diagram of the test rig.

Generally, all hydraulic systems need a supply of fluid at constant pressure. Therefore, rapid fluctuations in rate of flow that can result in pressure drop which always occur in hydraulic systems should be avoided. Pressure drop may damage the pump and other parts as supply of fluid is not constant resulting void in the pipeline. In this system a variable flow rate of fluid is supplied at substantially constant pressure using self-regulating variable-delivery pump (Stringer, 1976). The power pack with 90 litre tank (Figure 4.30) in test rig system is used to provide start up power and provide constant hydraulic fluid supply. The three phase motor (M) equipped with the power pack is to charge the accumulator before the system starts to operate. A non-return valve is attached at the power pack to prevent backflow from the system to the axial piston pump. When the 3/2 valve is opened, axial piston pump flow rate at very low pressure is re-circulated to the power pack tank. It is very important to avoid backflow in order to protect the pump and also the whole system from damage (Stringer, 1976).

Power pack with 3 phase motor
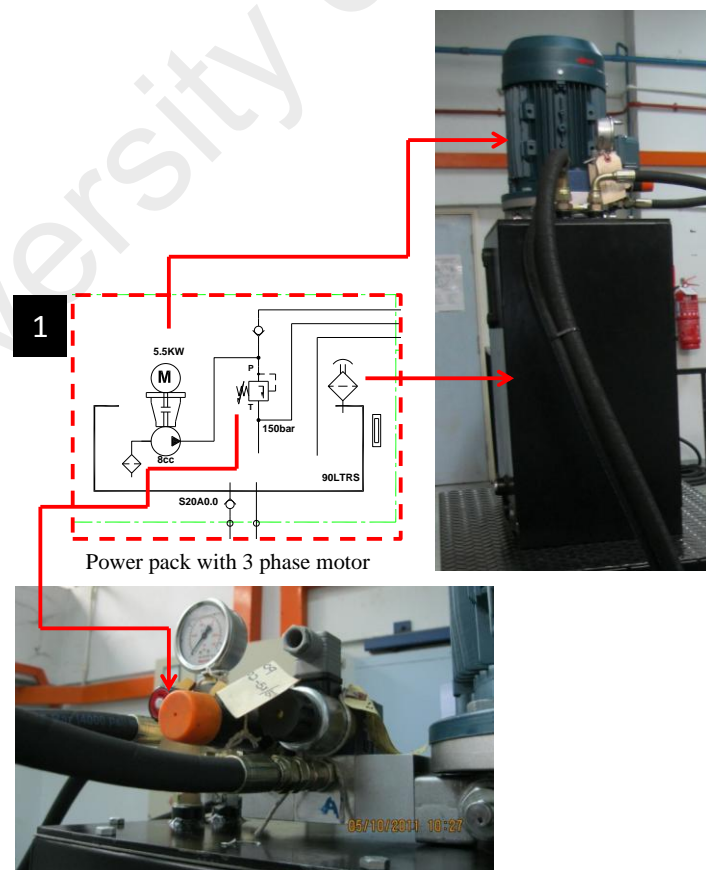
Figure 4.30 Power pack with 3 phase motor.

The hydraulic fluid flows from power pack to accumulator during charging. Before entering accumulator, the fluid will flow through station manifold block first (Figure 4.31). In the station manifold block, the switch ZDR6DP2-5X/150YM (Figure 4.31) will supply pilot pressure at 30 bars. The pilot pressure means that pressure at 30 bars is constantly being supplied to the system to avoid pressure drop. Next to the pilot pressure switch in Figure 4.31 is the 3/2 valve (M-3SED6CK-1X/350 CG24N9K4). Located at the top of power pack tank, the 3/2 valve is used during charging. During charging, the valve is open for hydraulic flow from power pack to accumulator.
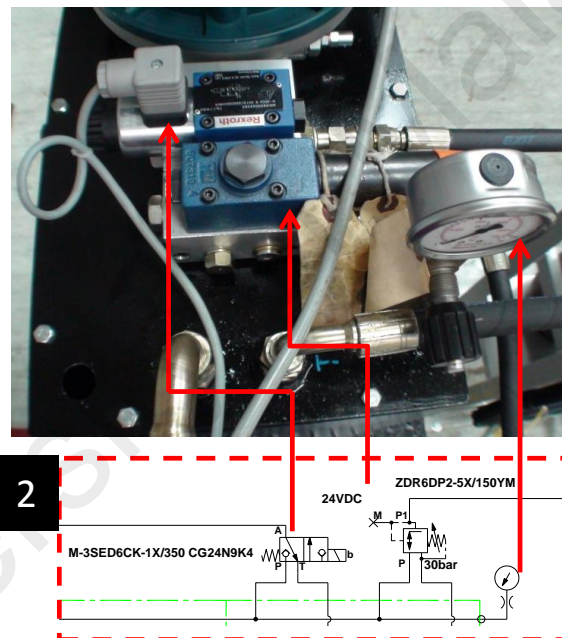
2 Station Manifold Block

Figure 4.31 Manifold block.

When the accumulator is full, the relief valve (Figure 4.32) will be activated. The relief valve (DBDH10G-1X/200) is set manually at 85 bars. Although the accumulator can be set at maximum 320 bars, in this study the pressure is set lower for safety reasons. The relief valve is applied together with axial piston pump. It is to protect accumulator from excessive pressure and to control filling and discharging of accumulator. The addition

of close valve in the system is to make sure that fluid does not flow all the time which will damage the pump. When the system is using high discharge pressure, a transmitter is used together with relief valve. The relief valve together with close valve at the discharge side is for safety precaution. The relief valve is positioned in the discharge line with a return line back to the suction line (Driedger, 1996).
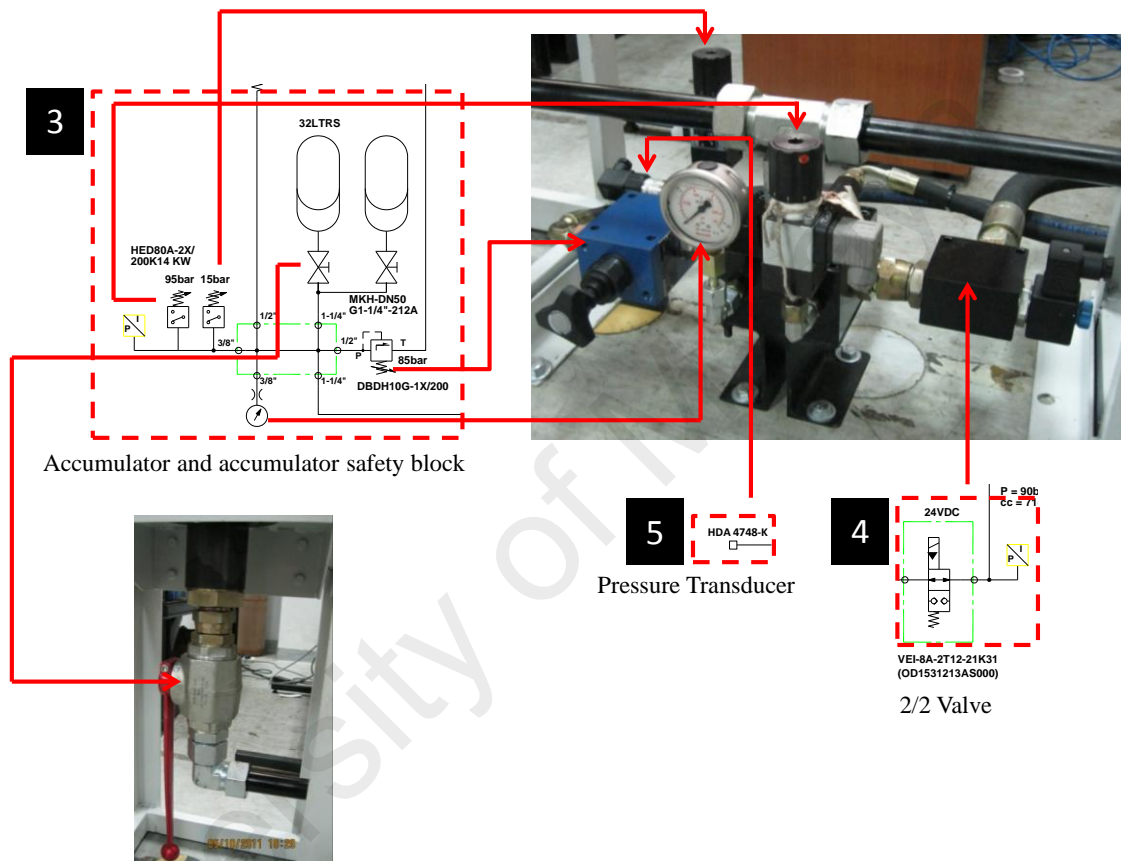
Figure 4.32 Accumulator safety block, pressure transducer and 2/2 valve.

Another valve located at this safety block is the 2/2 valve (VEI-8A-2T12-21K31). It is positioned at the end of the pipeline from the power pack. During charging from 0 to 85 bars, the 2/2 valve is open for fluid to flow into accumulator. Once the accumulator has fully charge meaning that the pressure has reach 85 bars, the relief valve will be activated and signalling the 2/2 valve to close down. As the 2/2 valve closes down, the system can start to operate in motor mode.

The accumulator safety block also includes two pressure switches for safety. The two pressure switch is for maximum pressure that the system can handle which is 95 bars; and 15 bars for minimum pressure. For minimum pressure switch, if the value went lower than 15 bars, signal will be sent to Host PC. Action must be taken by charging back the accumulator using power pack to fill the pipeline with fluid to avoid from void formation that might happen inside the pipeline when the pressure is low. For maximum pressure switch, switch will only function when the pressure suddenly exceeds 95 bars. When this happen the whole system will shut down immediately as a safety precaution.

During operations, the pressure in the system can be observed using the pressure transducer. The pressure transducer (HDA 4748) is attached near the pressure switch to measure the fluid flow in and out of the block right before the accumulator valve (MKH-DN50). As the charging of accumulator is completed at 85 bars, the test rig system can start to operate in motor mode. This is where the test rig simulates the behaviour of vehicle accelerating.

The fluid from accumulator flow to the axial piston pump (Figure 4.33) is through second pressure transducer located at the pump. The pressure transducer is only used to measure the pressure flowing to and from the pump. As the fluid flows inside the pump, a signal activates the proportional valve actuator to control the orifice opening of the directional valve. Hydraulic fluid moves from inlet port into the directional valve pushing the hydraulic cylinder (control member of a variable-displacement motor). The flywheel as in Figure 4.8 starts to spin and accumulator content decreases subsequently. As the accumulator content empties, signal is given to the axial piston pump to change the swash plate to pump mode. At this point the test rig simulates the vehicle behaviour during braking. When the vehicle brakes the accumulator accepts and stores fluid until

its pressure rises sufficiently. In the test rig system, the pressure rises inside the power pack tank. The regeneration cycle is completed and the same process is repeated again for a new cycle. After completing the hydraulic circuit, the controller circuit is designed to control the electrical part inside the system.
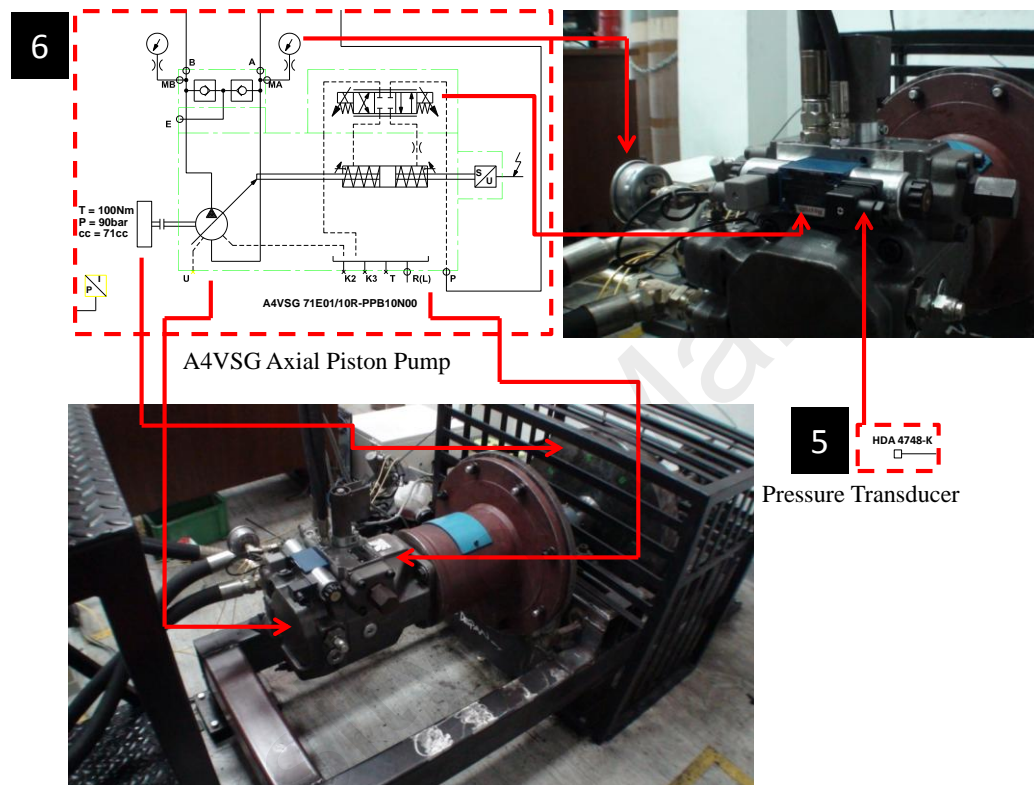
Figure 4.33 Axial piston pump and pressure transducer.

4.5   Test Rig Controller

The test rig controller is a simple controller to test operate the test rig in pump and motor mode. The circuit of the controller is presented in Figure 4.34. The controller is is divided into two sections; the first one as in Figure 4.35, function to supply power to the controller and also contains safety features. The left side of the circuit shows the wiring for pump (R,S,T, and N) and power pack motor (indicate by U1,V1 and W1). This controller connects the 3 phase power supply directly to the power pack motor.
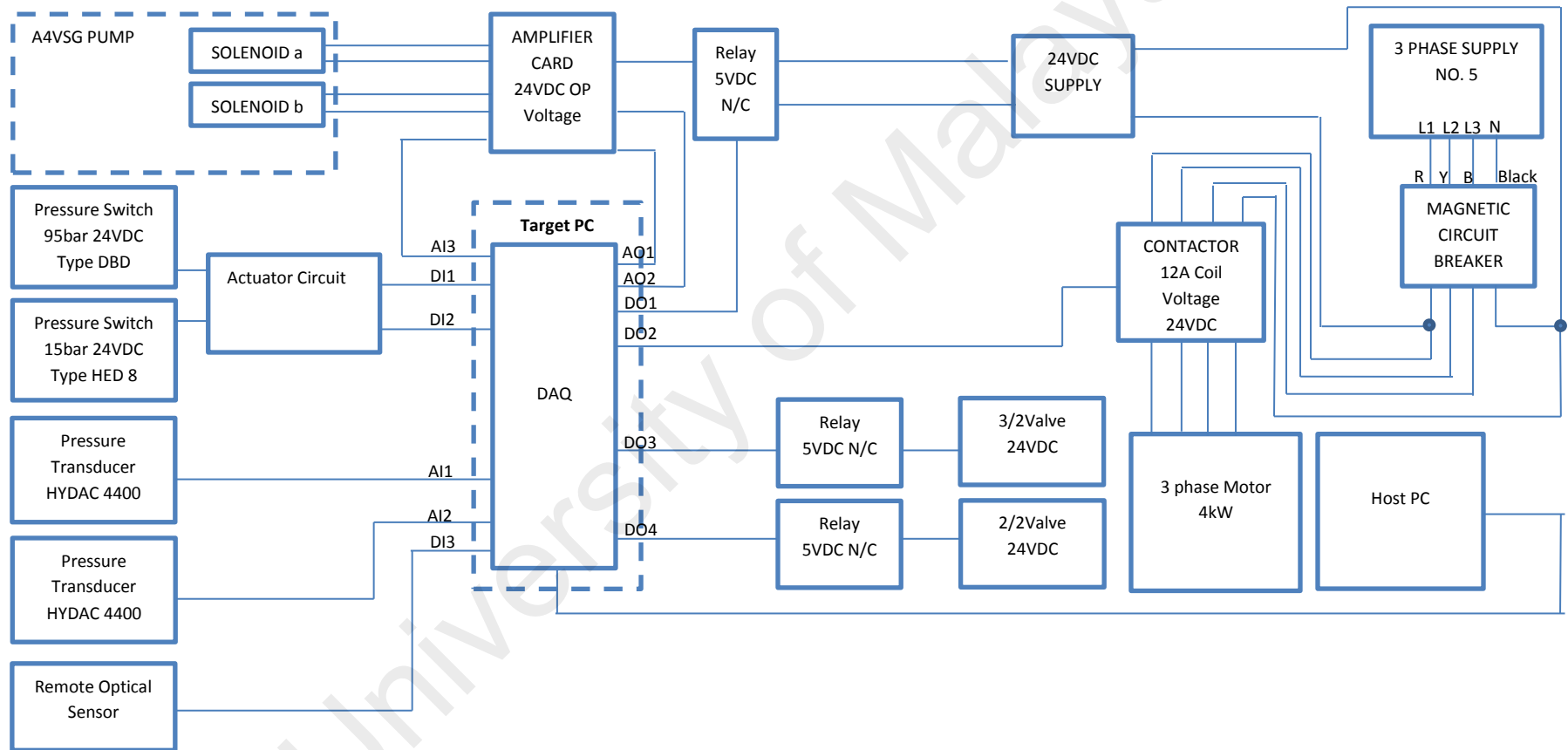
Figure 4.34 Test rig controller circuit.

In the middle of the circuit, the emergency button (ES1) is set in series. The emergency button is a must as some hydraulically operated machines may need to stop in open position to prevent damage to the equipment. However, there is another option from stoping the system in open position which is to charge the accumulator fully before the first cycle and continuing on the same step every new cycle until the machine shuts down. The fully charged accumulator will make sure the that system have stored energy ready to cycle the machine to open position in case of a power failure (Zones, 2012). Another safety feature is the addition of a circuit breaker, which is a normal practise when a controller is made. The circuit breaker is an interrupter differential residual current device with 4 poles function to cut the excessive input current from power supply to the rest of the controller part.

The thermal overload 7-10 A (MC1) is attached with contactor 24 V DC (Figure 4.35). The thermal overload has two functions; to break the circuit when current is over the limit and also to give warning by lighting the pilot lamp to warn the operator the situation. The thermal overload is connected to overload relay (OL1). When the three phase power is supplied to the controller box, the power pack motor starts first before the controller receives the power. The power pack motor can be controlled by operator through Host PC or automatic switch or manual control. This option is made available to tend to different needs during the commissioning test. The operator may be away from the Host PC and in this situation the manual control located at power pack motor can be useful.
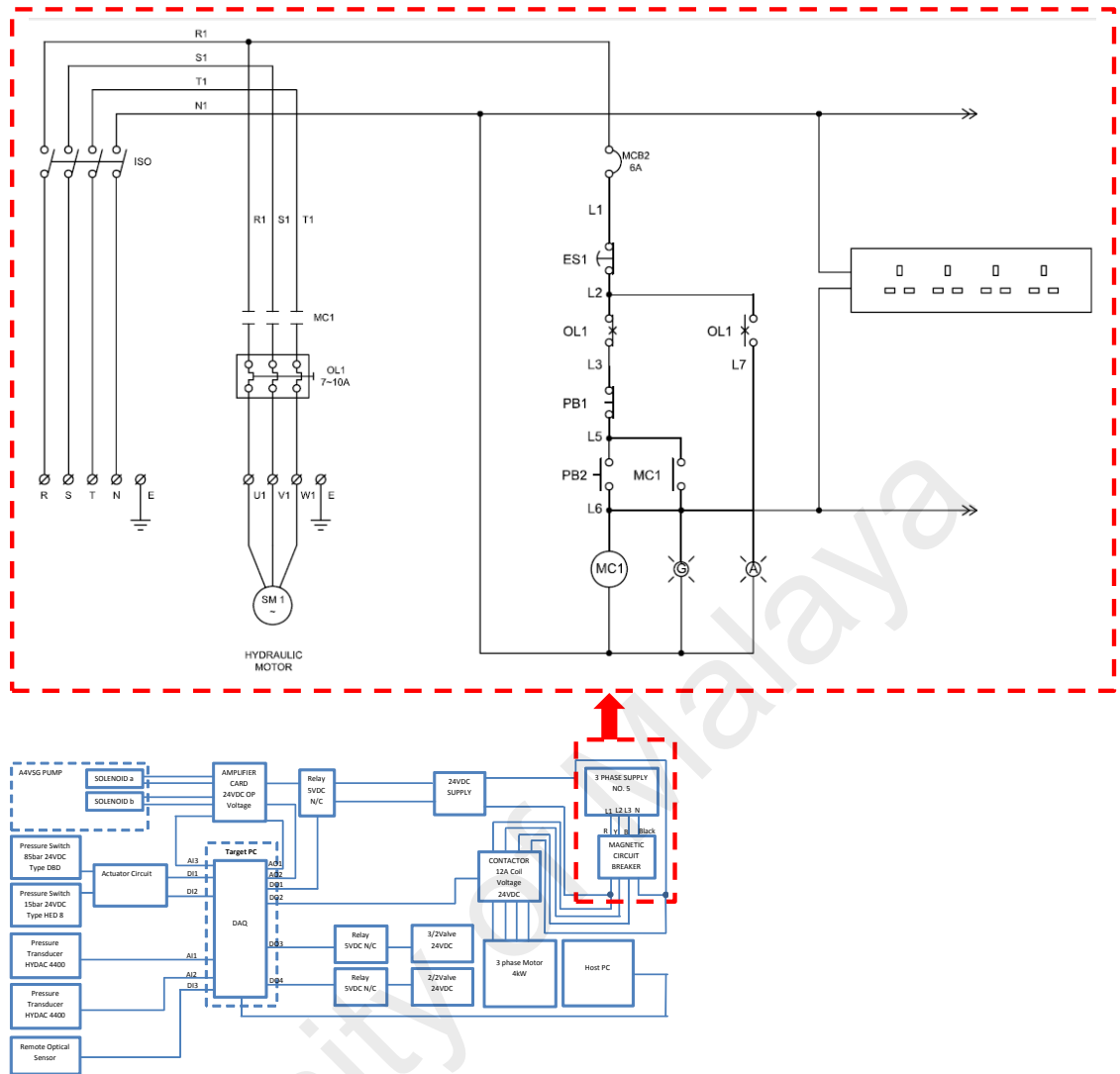
Figure 4.35 Power supply connection.

The second function of the controller (Figure 4.36) is to send input signals to the test rig system and output signals from test rig system to Host PC. The signal is process by DAQ card. Digital input D1 and D2 is set for pressure switch. The signal from remote optical sensor from digital input 3 (DI3) is sent back to Host PC for speed measurement in RPM. Analog input AI1 is referring to pressure transducer (pressure transducer 1) at accumulator while Analog input AI2 is for pressure transducer at axial piston pump (pressure transducer 2).

The third analog input (AI3) is for actual swash plate angle swivel. This input is for controlling the swash plate angle which will determine the opening orifice of the pump during operation. AI3 connects to the amplifier card. The amplifier card is used for adjusting the flow of variable displacement of the axial piston pump. For output signal, the digital output 1 (DO1) is used to supply 10 V to enable the DAQ card. The digital output 2 (DO2) is for contactor while digital output 3 (DO3) is to control 3/2 valve. Another valve which is the 2/2 is controlled by digital output 4 (DO4). The only one analog output (AO1) from the test rig is the swash plate angle. This analog output will show the angle of the swash plate inside the axial piston pump during operation.
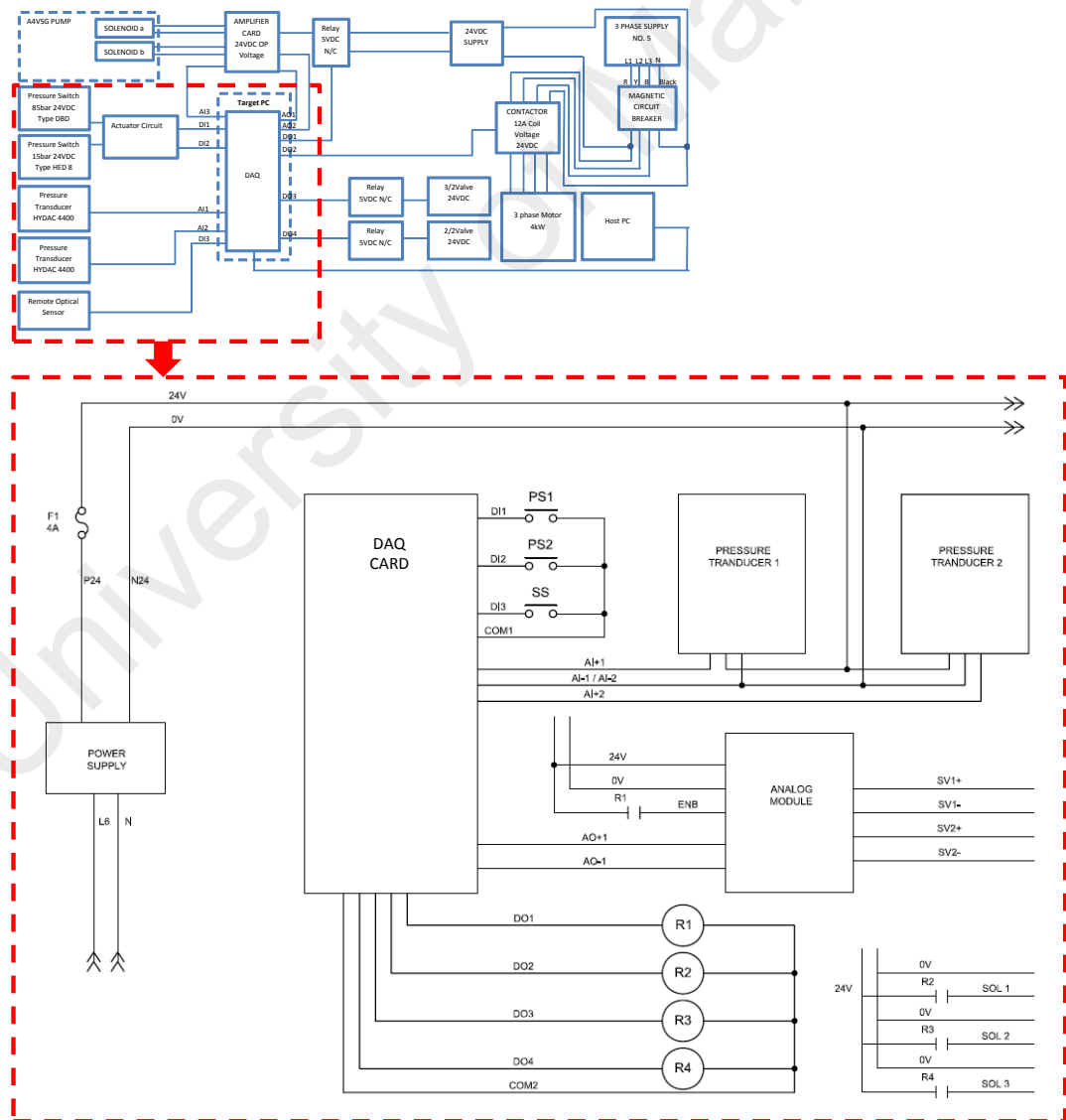
Figure 4.36 Input and output controller.

The integration of the controller to the test rig system is made to operate the test rig system. The wiring of the DAQ card inside the target PC computer is done and the other electrical components as in the controller circuit is wired and combined into one controller box as in Figure 4.37.
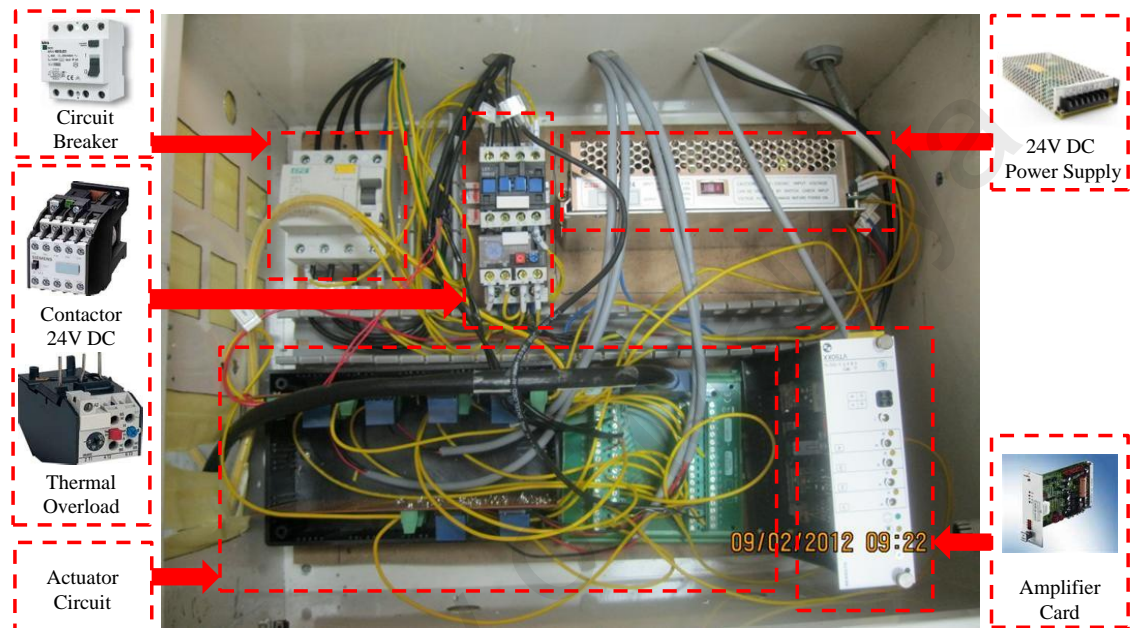
Figure 4.37 Test rig controller.

After completion of the controller, the physical test rig is fabricated and assembled. The next subchapter will describe the installation of physical test rig part.

4.6   Fabrication and Installation of Test Rig

The accumulator stand and power pack stand are fabricated and assembled together with the chassis. The modified chassis is attached with bell housing to hold the axial piston pump. To understand the whole picture of the test rig, the test rig system layout in Figure 4.38 is referred.

Figure 4.38 Test rig layout at lab.

There are 11 main components that are important for test rig configuration. The components are as in Figure 4.39.

Figure 4.39 Components on test rig.

The power pack (Figure 4.40) functions as a low pressure reservoir. Consists of a tank, regulator to control pressure supply and a motor to power the axial piston pump.

Figure 4.40 Power pack.

The axial piston pump (Figure 4.41) operates as a pump, capturing kinetic energy during braking. During acceleration the pump functions as a motor to spin the flywheel from stationary. The size of axial piston pump is 71cc/rev.

Figure 4.41 Axial piston pump.

The ROS (Figure 4.42) detected reflected pulse from a target consisting of T-5 Reflective Tape from rotating flywheel. ROS will calculate the frequency of flywheel rotating during experiment and transmit the output to target PC in RPM.
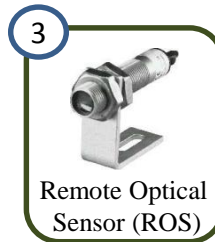
Figure 4.42 Remote optical sensor (ROS).

Flywheel (Figure 4.43) is attached to the chassis to imitate vehicle load. In this study the weight of flywheel is 108.33kg. The flywheel is a solid stainless steel cylinder fabricated using CNC milling.

Figure 4.43 Flywheel.

The disc brake (Figure 4.44) is a second-hand disc brake of a lorry. It is located at the end of the chassis structure at the opposite side of the axial piston pump. The disc brake provides friction for braking.
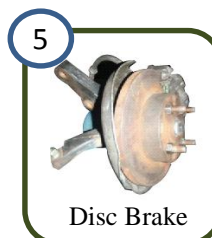
Figure 4.44 Disc brake.

Absorber pad (Figure 4.45) located at the base is to absorb vibration during cycle test and thus protect test rig structure.

Absorber Pad
at Base

Figure 4.45 Absorber pad.

Journal bearing (Figure 4.46) provides a frictionless environment to support and guide a rotating shaft. Couplings are used to provide linkage between shafts.

Journal
Bearing   Coupling   Shaft
& Housing
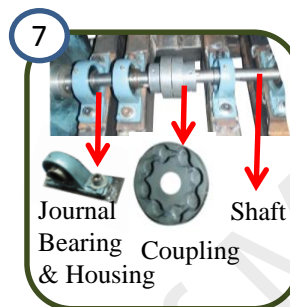
Figure 4.46 Journal bearing, coupling and shaft.

After each cycle, the flywheel will spin at high speed. When the Host PC sends the signal to stop the flywheel, the flywheel will still take time to stop spinning. To stop the flywheel immediately, the brake (Figure 4.47) is used to transmit braking signal.

Brake

Figure 4.47 Brake.

Pressure transducer (Figure 4.48) is used to convert pressure into an analog electrical signal. There are two pressure transducer attached to the test rig. The first one is located at accumulator safety block and the second is at axial piston pump.

Figure 4.48 Pressure transducer.

The accumulator safety block (Figure 4.49) is to protect the accumulator, shut-off the system if an emergency happens (pressure exceeds limit or backflow happen). It also serves as flow line to discharge hydraulic fluid from accumulators to axial piston pump and from power pack to accumulator.

Figure 4.49 Accumulator safety block.

The accumulator (Figure 4.50) stores energy from the pump during braking and releases pressure during acceleration. The accumulator is positioned vertically in the test rig system for testing. However, the accumulator is positioned horizontally on the lorry as this position is safer based on the crash analysis done by Khoo (Khoo, 2010).

Figure 4.50 Accumulator.

The fabrication and assembling of the whole test rig system in the lab took around 14 months to complete. The result of the completed system at the lab can be seen in two

views as in Figure 4.51. The next subsection shows the result of fabrication and assembled part of the test rig system by section which is; i) test rig structure, flywheel, shaft and connectors; ii) axial piston pump; iii) power pack and iv) accumulator.

Figure 4.51 Overview of test rig setup at lab.

4.6.1 Test Rig Structure, Flywheel, Shaft and Connectors.

A steel bar cage (Figure 4.52) is fabricated and assembled to cover the flywheel for safety during testing. During testing, the flywheel will spin at high speeds and this cage is made to hold the flywheel in case of any displacement during testing. The cage is affixed to the ground by extended anchor bolt.

Figure 4.52 Flywheel cage.

Figure 4.53 and Figure 4.54 is the top and side view of the chassis. The flywheel and the axial piston pump are attached to the chassis. The bell housing (red colour) is to hold the axial piston pump. To attach the bell housing, the bell housing plate is fabricated and welded onto the chassis.

Figure 4.53 Top view of the test rig chassis.

Figure 4.54 Side view of test rig chassis

The fabricated flywheel is assembled onto the chassis with support by shaft and journal bearing (Figure 4.55). The figure shows the flywheel without cage covering it. The shaft will rotate freely on journal bearing which will reduce friction when the shaft is spinning.

Figure 4.55 Flywheel on chassis.

The axial piston pump is connected to the shaft (Figure 4.56) by a custom made pump-shaft coupling. The coupling is fabricated using CNC milling to fit the pump shaft with the flywheel shaft.
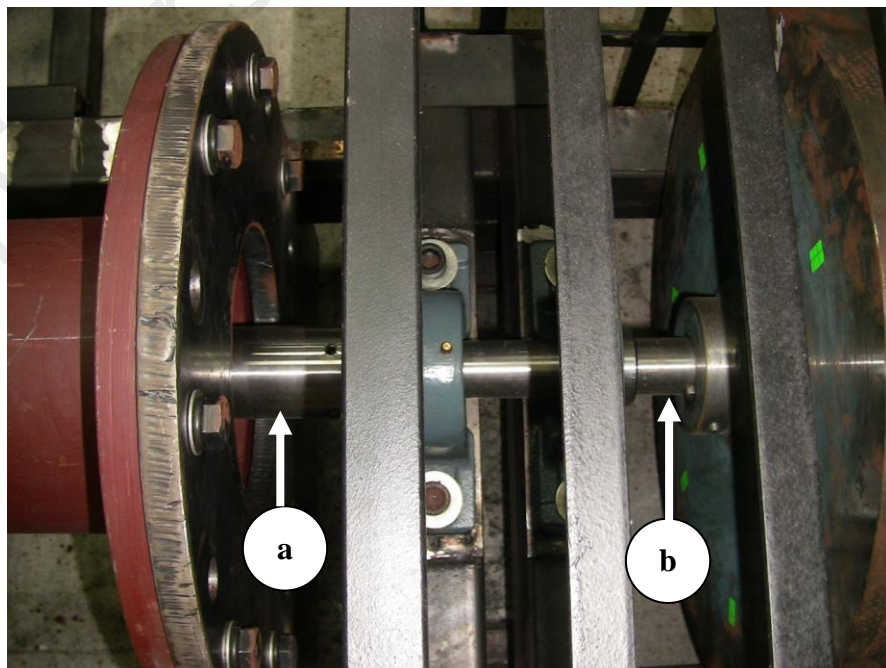
Figure 4.56 (a) Custom made pump-shaft coupling and (b) shaft.

The shaft of the flywheel length is not sufficient to cover the length from pump to drum brake. A shaft coupling (Figure 4.57) is added to extend the shaft length.
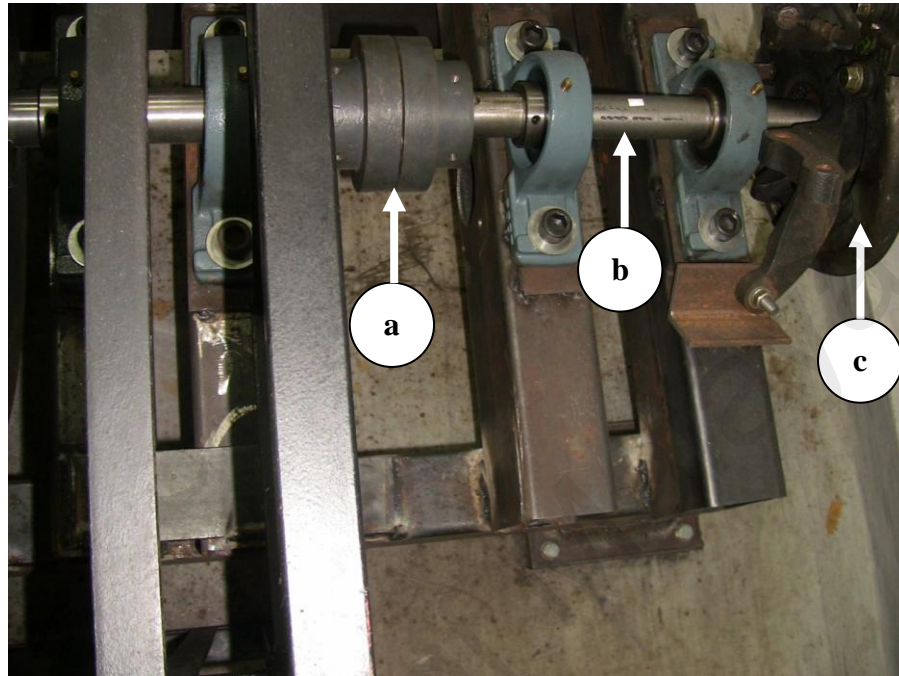
Figure 4.57 (a) Shaft coupling, (b) shaft (c) drum brake.

The test rig base is affixed to the ground with absorber pad (Figure 4.58) in between the base and the ground. Extended anchor bolt is used to fix the base to the ground. The next section will describe the axial piston pump installation on the chassis.

Figure 4.58 Test rig base with absorber pad.

4.6.2   Axial Piston Pump

The axial piston pump is a 71 cc pump. The swash plate can be used in two modes which is pump and motor mode. The dial indicator of the swash plate inside the pump can be viewed at the top of the pump (Figure 4.59).
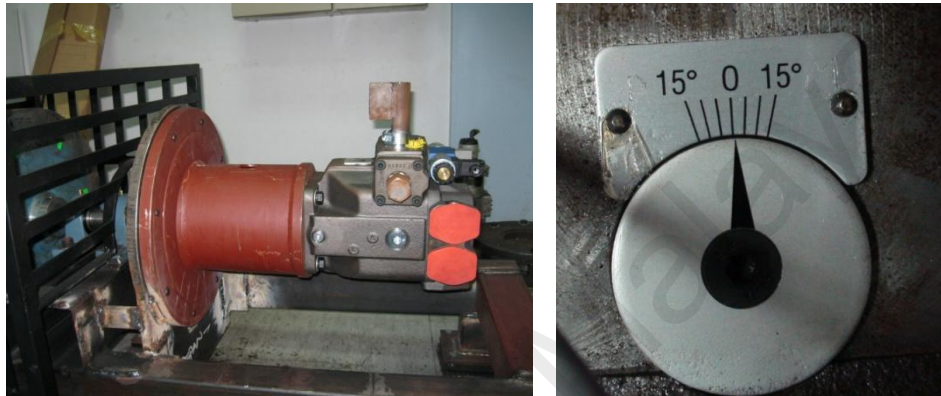
Figure 4.59 (Left) A4VSG Axial piston pump fixed on bell housing, (Right) Swash plate angle indicator, (-) Pump and (+) Motor.

The pump is held by bell housing. As mention before, the bell housing is fixed to the bell housing plate. The side of the plate is welded to the chassis body (Figure 4.60).
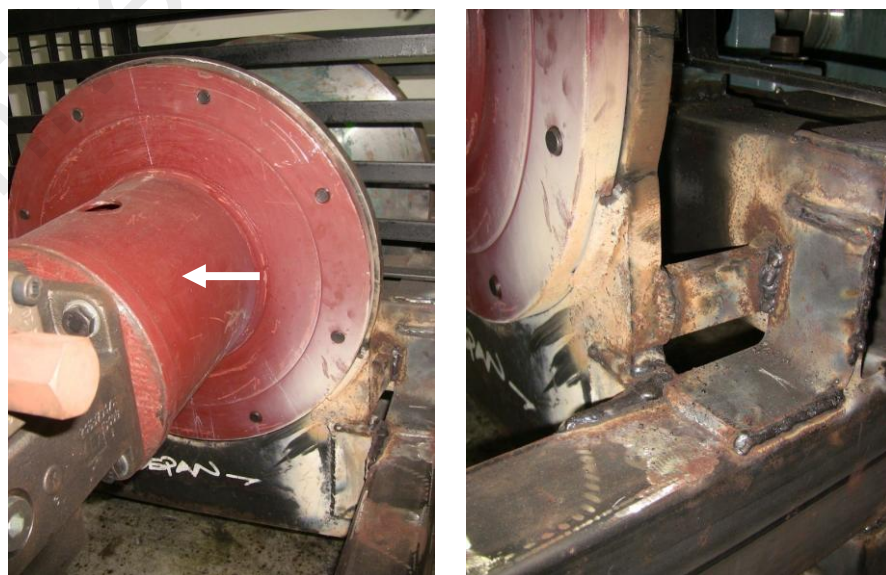
Figure 4.60 (Left) (a) Bell housing (Right) bell housing fixed on plate weld on test rig chassis.

The piping from power pack to pump is shown in Figure 4.61. In this picture on the right side, the whole pipeline to accommodate the system (from power pack to pump, from accumulator to pump and from pump to power pack) can be seen. The following section is about power pack and its installation on the test rig system.

Figure 4.61 Piping to axial piston pump (left) and to accumulator (right).

4.6.3 Power Pack

The power pack is assembled with the three phase motor to operate the pack. It is equipped with pilot pressure switch and 3/2 valve on top of the tank as in Figure 4.62.

Figure 4.62 (Left) Pressure regulator and valve, (Right) Motor to power axial piston pump.

The tank (Figure 4.63) with indicator on the side is used for temperature and flow measurement. When the power pack is used, temperature may rise above room temperature as the motor is a three phase motor and flow of hydraulic fluid in and out of the tank is continuous during testing.

Figure 4.63 (Left) Hydraulic reservoir, (Right) tank indicator.

The power pack stand with rectangular hole on the top side is for hydraulic piping (Figure 4.64) from power pack tank to and from axial piston pump.

Figure 4.64 Hydraulic piping underneath power pack.

The power pack is attached to the fabricated stand (Figure 4.65) by fixing the tank base to the top of the stand. After positioning the power pack and the stand near the pump, the stand leg is fixed to the ground using extended anchor bolt. Finally, the accumulator assembly on the system is shown in next section.
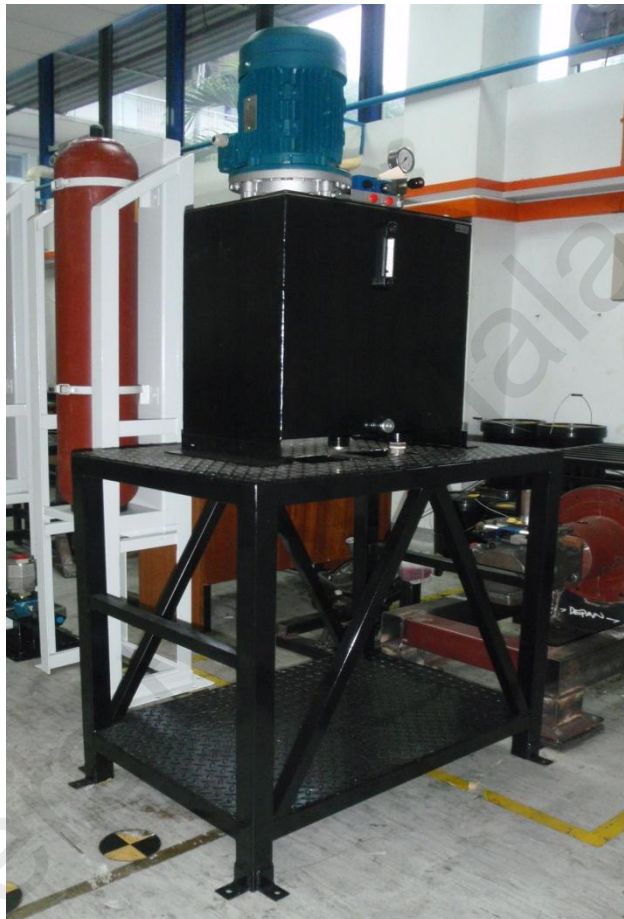
Figure 4.65 Power pack on fabricated stand.

4.6.4   Accumulator

There are two accumulator purchased for this study. However, only one accumulator is used as the power pack is used as low pressure tank and the accumulator is for high pressure tank. The accumulator is held vertically by accumulator belt which is attached together on the accumulator stand and the weight of the accumulator is supported by the stand support. This can be seen in Figure 4.66.

Figure 4.66 Accumulators on designed stand for horizontal positioning complete with (a) slot to hang belt (b) belt and clip (c) base for extended anchor bolt attachment to ground**.**

Accumulators are positioned above the accumulator safety block (Figure 4.67). The safety block is placed in the middle of the accumulator. In the case of future study, both accumulators can instantly be used as the pipeline is made for both of the accumulator.

Figure 4.67 (Left) Accumulators, (Right) accumulator safety block.

4.7   Conclusion

As the controller is ready and the fabrication and installation of the test rig is done following the hydraulic circuit and the test rig system layout, the test rig is now ready for commissioning test to evaluate the system performance.

CHAPTER 5

COMMISSIONING OF TEST RIG

5.1 Introduction

This chapter will discuss the testing done to evaluate the system performance. Before the commissioning test is conducted; a preliminary test is carried out check the flywheel setting. This test is also done to inspect the mechanical joints on test rig chassis when the flywheel is spinning. After pre-testing, the commissioning test is run. The commissioning test is necessary to define system behavior during operation. Different sets of testing have been conducted to see the effects of mode variation, angle variation and pressure variation.

5.2 Preliminary Test

In order to ensure that the flywheel is not run over the safe limit, the maximum safe speed, N is calculated. The calculation is done based on Equation (2.10).

$$N = 7425/D_{FW} \text{ rpm} \qquad \text{Eqn. (2.10)}$$

Where

N = maximum safe speed, rpm

D_{FW} = flywheel diameter, feet

Thus the maximum safe speed, N is;

N = 7425/1.6404

   = 4526 rpm

During commissioning test the flywheel speed must not exceed the safe speed which is 4526 rpm. Note, however, the experiment is carried out based on lorry mass; 5 ton (5000kg) and accelerating from stationary till 10km/h. For low speed (Lindzus & AG, 2010), 10km/h is selected as it is the minimum speed required for the accumulator to absorb energy from braking and for the vehicle to propel from stop. By calculating the braking energy of the lorry and again referring to Equation (2.9), the angular velocity is calculated as bellow;

$$\frac{1}{2}mv^2 = I\omega^2$$

Eqn. (2.9)

Where;

m = mass of lorry

v = speed of lorry

I = Total inertia on rotational axis

ω = angular velocity in rpm

Hence;

$$\left[\frac{\frac{1}{2}(5000)(2.7778^2)}{1000}\right] = \left[\frac{\frac{1}{2}(2.7665)(\omega^2)}{1000}\right]$$

$$\omega = \sqrt[2]{\frac{19290.4}{1.38325}}$$

    = 118.092 rad/s

    = 1127.695 rpm

Therefore the maximum angular velocity for commissioning test is set to 1127.695 rpm. The speed during testing must not exceed this value since the test rig is still new and a lot of improvements for safety need to be done if the speed of flywheel is higher. A 3 phase induction motor is attached to the flywheel shaft for the preliminary test. The purpose of the test run is to observe rotating conditions of the flywheel at high angular velocity. It is also for safety precaution and for welding inspection. An inverter is used to control the rotational speed of the motor while a Tachometer is used to measure rotational speed of the flywheel. List of equipment used in this pre-test is as below;

i.   Alliance 3-Phase Induction motor

The three phase motor is to supply power to rotate the flywheel. The motor is a 4.8 ampere motor. The motor shaft is coupled to the flywheel shaft using a coupling.

Figure 5.1 3 phase motor.

ii.   Tachometer- Testo 470

The tachometer is to measure the rpm of flywheel. It is an apparatus with a combination of optical and mechanical rpm measurements. Measuring Range is - +1 to 99,999 rpm.

Figure 5.2 Tachometer.

iii.   Inverter (Model SV022 LS)

To change a DC input voltage to a symmetrical AC output voltage of desired magnitude and frequency. In this pre-test, the output data from inverter is in frequency, Hertz. The inverter also used to control the rate of angular speed is in Hertz. The specification of the inverter is, 3HP/2.2KW.230V.

Figure 5.3 Inverter.

The setup of the preliminary test is shown in Figure 5.4. The motor is fixed to the chassis by screws. The brake pipeline is connected to the drum brake by a steel pipe. The positioning of the brake is limited and hence the brake is placed further away from the flywheel for testing as operator will push the brake to slow the flywheel speed.

Figure 5.4 Motor setup on test rig chassis.

During testing, operator is located further away from the rotating flywheel for safety precaution. The inverter used for controlling the speed of the flywheel is controlled manually by the operator. At this stage the test rig speed is controlled manually by adjusting the frequency of the inverter. The frequency is then converted to rpm by calculation and the results from testing are tabulated in Table 5.1. In Figure 5.5, the picture shows the actual condition during testing where the flywheel is spinning at full speed (inverter frequency is 30Hz at maximum (Figure 5.6)). A tachometer is used to measure the speed. The tachometer is set to measure using laser mode and the laser is pointed to a point on the flywheel which has been stick with a reflective tape. The test is run three times for confirmation and welding inspection.
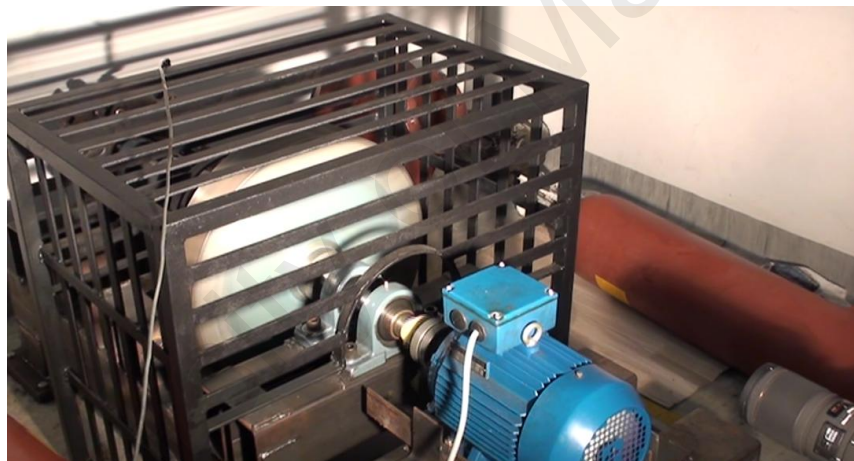
Figure 5.5 Flywheel rotates at full speed 2013 rpm.
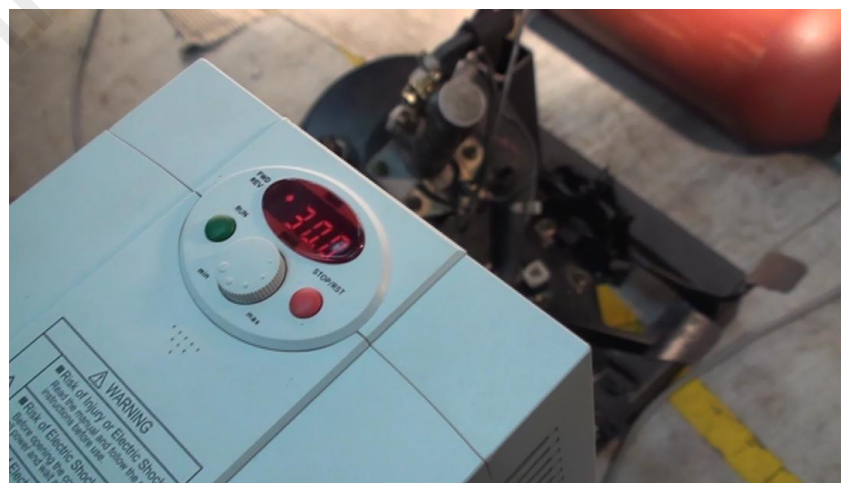
Figure 5.6 Inverter with maximum reading, 30Hz.

Table 5.1 Preliminary test result.

Frequency (Hz)	INPUT	Speed 1 (RPM)	Speed 2 (RPM)	Speed 3 (RPM)	OUTPUT (RPM)
0.000	0.000	0.000	0.000	0.000	0.000
2.000	120.000	119.500	120.000	118.300	119.267
4.000	240.000	240.500	244.500	242.400	242.467
6.000	360.000	362.400	367.600	360.600	363.533
8.000	480.000	494.900	502.200	493.300	496.800
10.000	600.000	620.100	626.400	620.000	622.167
12.000	720.000	758.800	772.400	754.500	761.900
14.000	840.000	897.300	908.000	891.100	898.800
16.000	960.000	1027.000	1043.000	1029.000	1033.000
18.000	1080.000	1160.000	1178.000	1168.000	1168.667
20.000	1200.000	1312.000	1323.000	1312.000	1315.667
22.000	1320.000	1436.000	1461.000	1446.000	1447.667
24.000	1440.000	1577.000	1590.000	1593.000	1586.667
26.000	1560.000	1733.000	1718.000	1732.000	1727.667
28.000	1680.000	1878.000	1840.000	1859.000	1859.000
30.000	1800.000	2014.000	2020.000	2006.000	2013.333

From the result in Table 5.1, the graph in Figure 5.7 is constructed.
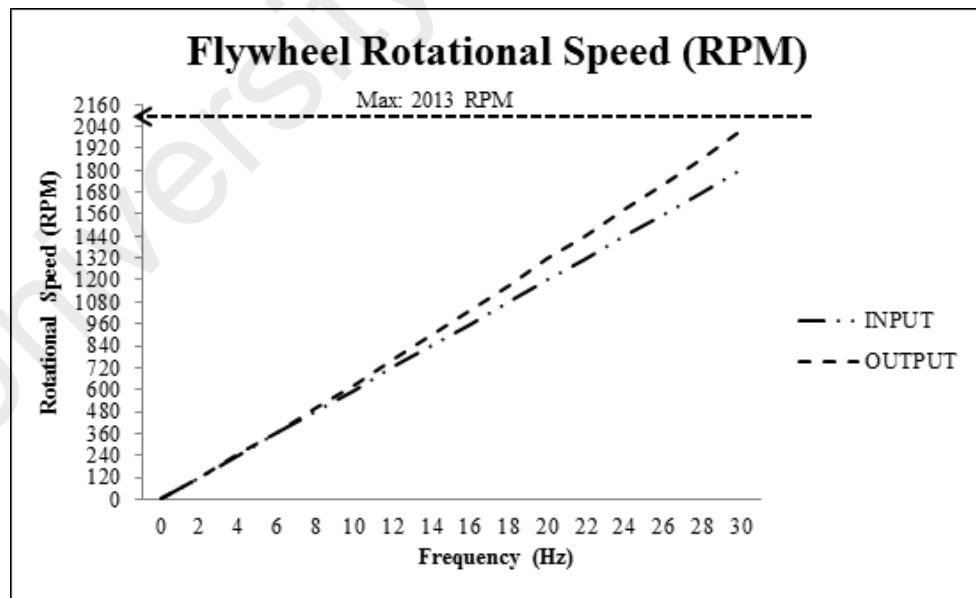
Figure 5.7 Graph Speed vs frequency.

The results display a difference reading between input (frequency value send by inverter) and output (actual speed of flywheel read by tachometer). This is probably due

129

to the inertia of the flywheel at high speed because at low speed the input speed is almost same with output speed. At this point the test objective has been achieved as the welding inspection done shows that the chassis is in good condition for commissioning test and the flywheel even after the flywheel spins at top speed, shaft and drum brake are aligned.

5.3   Commissioning Test

The test rig system consists of a fabricated stainless steel flywheel linked by shaft with a drum brake and an axial piston pump. The swash plate of the axial piston pump can be varied which allows variation on the flywheel speed. The power pack three phase motor is connected to main power supply to provide necessary reactive power for accumulator charging. Once the flywheel starts spinning, the axial piston pump can be driven as motor and the speed can be controlled by changing the swash plate. Pressure transducer allows the electrical power supplied from the axial piston pump to be monitored as an analogue signal by data acquisition system (DAQ CARD).

The speed (swash plate angle) and direction (negative as pump and positive as motor) of the axial piston pump can be controlled by analogue signal by voltage controlled oscillator and drive electronics. The voltage is changed to change the swash plate angle ($10V=15°$, $9V=13.5°$, $8V=12°$, $7V=10.5°$, $6V=9°$ and $5V=7.5°$). An optical sensor was used to generate analogue signal proportional to the flywheel speed. 180 litre of Shell Tellus VG46 is used to lubricate the whole system. The setup commissioning test is shown in Figure 5.8.
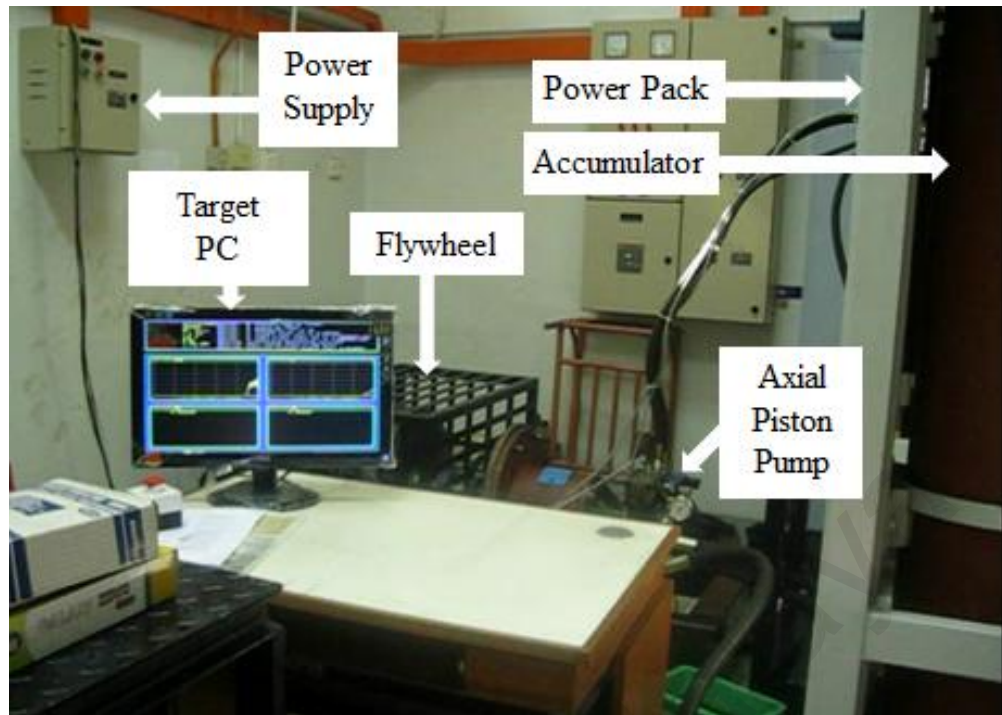
Figure 5.8 Commissioning test setup.

Currently, the test rig system is able to imitate the processes in actual HRBS. The two most important character in HRBS is; Motor Mode (energy releasing) and Pump Mode (energy recovery). The first test (Test 1) is to test the system in motor mode. The power pack is used to fully charge the accumulator (85 bars) before starting the test. After the accumulator is full, the controller sends the input signal thru DAQ card to the 2/2 valve. The valve will open and fluid flows to the axial piston pumps. At this rate the pump is in motor mode and functions to spin the flywheel. In actual situation on lorry, this stage is actually where the pump will act as motor and propel the vehicle from stop.

As the flywheel starts to spin, the speed results with variation of swash plate angle is collected by a speed sensor attached on the chassis near the flywheel as in Figure 5.9. The reading is collected and transferred to Excel file to construct a graph for analysis as in Figure 5.10.
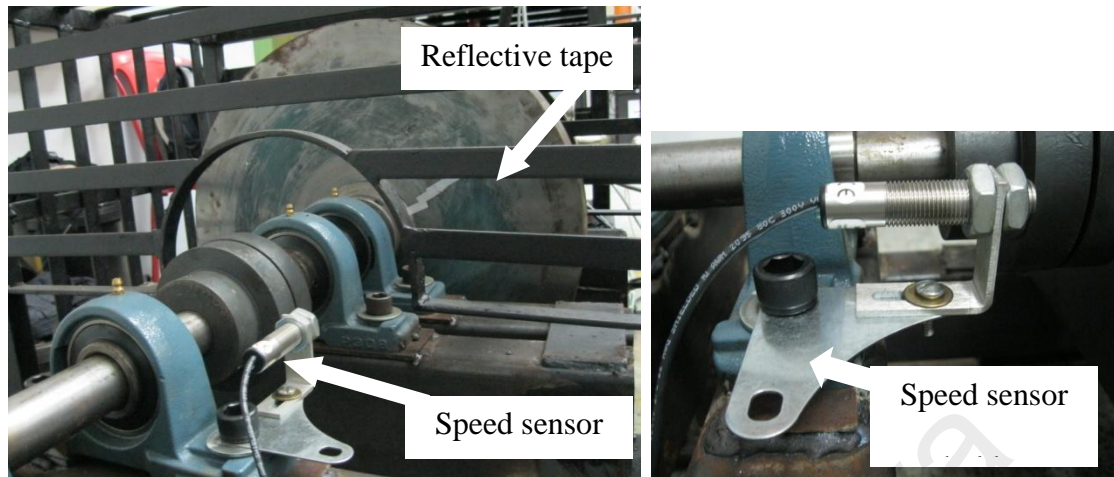
Figure 5.9 Speed sensor attachments on chassis.

The graph illustrates the success of the test rig system in operating in motor mode. The flywheel is run using different swash plate angles with fixed pressure (85bar). Observation on this graph can be concluded as follows; first, the speed is almost the same even when the swash plate angle varies and; secondly, the time for the flywheel to spin is different as can be seen from the fact that the smaller the angle of the swash plate, the longer the flywheel can spin. To further investigate this result, test number 2 and test number 3 were conducted.
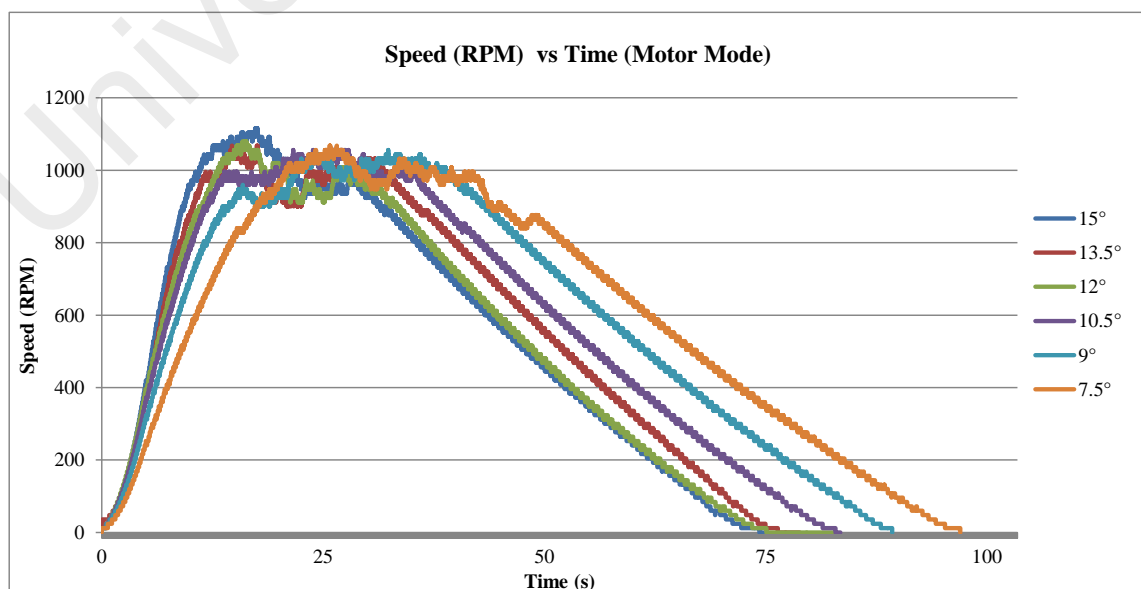
Figure 5.10 Test no. 1: Graph speed vs time (motor mode for various angle).

In test number 2, the swash plate angle effect on the speed of flywheel is investigated. The test proves that the angle variation does not really affect the speed of the flywheel. The result is shown in Figure 5.11. The system was unstable (Jefferson & Ackerman, 1996) at sampling data 15° because the flywheel was run at 15° first. The large fluctuations of accumulator are due to high power flow from power pack through the system. The swings of flywheel indicate the effective capturing of braking energy The accumulator pressure is characterized by large fluctuations (Hui & Junqing, 2010). Thus the propulsion of power was higher as the pressure from accumulator is higher since the accumulator is full from being charged by power pack. Once the test for 15° is completed, the system is run again in motor mode to spin the flywheel at swash plate angle 13.5°. At this point the system is already stable as the result from 13.5° until 7.5° shows the speed is almost at same range.

This test affirms the analysis result obtained from simulation done in past research. The average force exerted on the swash plate in x-axis (axis perpendicular with swash plate) remains constant as the swash plate angle increases (Norhirni, 2011). However, the average force exerted on the swash plate in z-axis increases proportionally with the swash plate angle. As the swash plate angle increases, it does not affect the total force exerted on the x-axis, because the swash plate angle effect is relatively small compared to the force caused by the hydraulic fluid flowing through the piston to the swash plate (Norhirni, 2011). Therefore, the swash plate angle does not affect the flywheel speed.
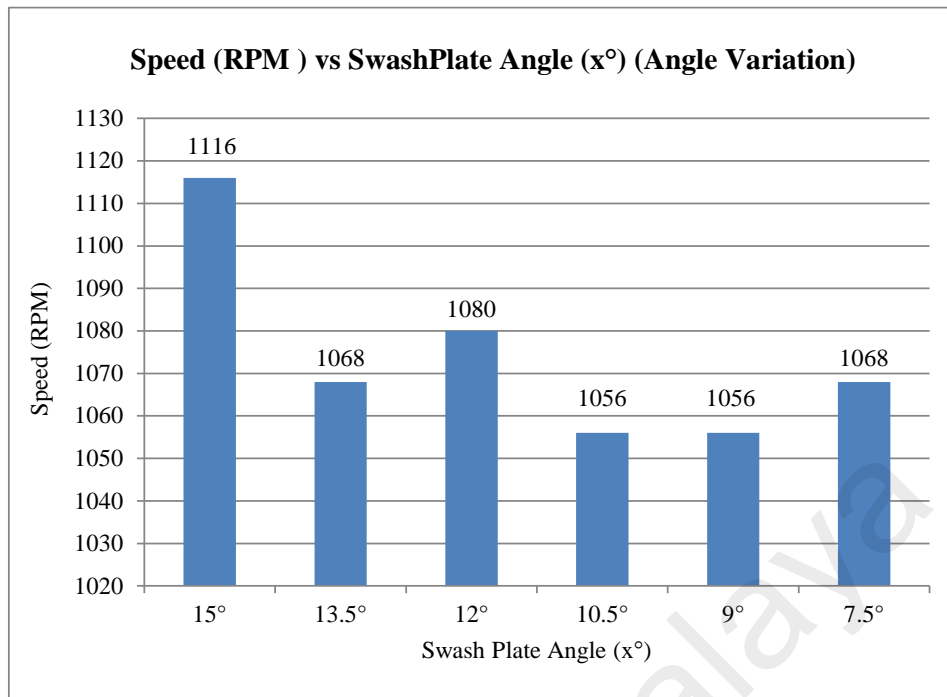
Figure 5.11 Test no. 2: Graph speed vs swash plate angle (angle variation).

The next test (test number 3) is to observe the effect of swash plate angle on the life span of the spinning flywheel. The result is shown in Figure 5.12. The trend shows that the smaller the opening of the swash plate (angle is small), the longer the flywheel can spin. This is because the opening orifice of the axial piston pump is smaller and so the fluid flow into the axial piston pump from the accumulator is slower. Therefore, flow of fluid in the system is longer as the swash plate angle opening is smaller. Test number 4 is conducted to determine whether the system can actually function as a HRBS. In this test the capability of the system to capture energy by pump (pump mode) and release energy to spin the flywheel (motor mode) is investigated.
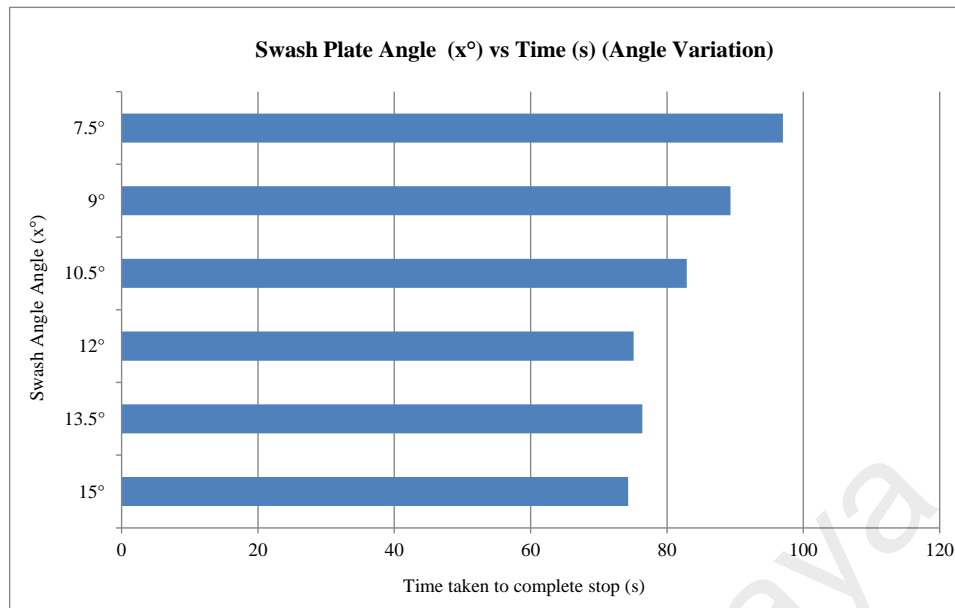
Figure 5.12 Test no. 3: Graph speed vs time (angle variation).

This test is very important as the result will determine the success of the test rig system to prove the HRBS concept design stated earlier in chapter 3. In this test the result is shown in Figure 5.13. The red line indicates noise signal as indication for improvement on controller side. However, for this study the noise reading has already been taken into consideration. The green line is the reading for pressure. From 0 to 125 second, the green line at zero reading means the pump is at zero displacement and at this rate the system accumulator is charged by power pack (Swing, 2008a). This is indicating 0 mode which mean the pump is off.
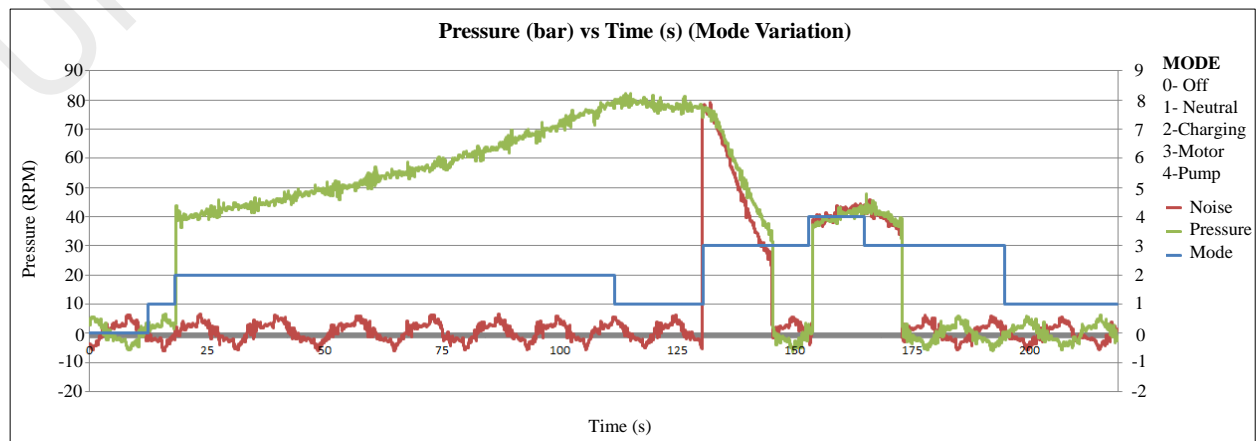
Figure 5.13 Test no. 4: Graph pressure vs time (mode variation).

The pressure starts to build up during charging mode from 20s until 110s. In commissioning test, during this stage the power pack is charging the accumulator. Whereas in actual situation the lorry starts braking and the accumulator starts to capture the energy. The axial piston pump will act as a pump at this stage and captured the kinetic energy from braking. When accumulator is full (85bar), the pressure is released thru 2/2 valve. The fluid flows from the valve to axial piston pump to spin the flywheel. The speed of flywheel at max speed for 85bar is 1016 which is almost equal to 10 km/h. For this speed (Lindzus & Contact, 2010), the vehicle can be propelled from a stop. By using this system, the lorry can propel form a stop without the use of fuel. This can save fuel usage and thus omit the emission since the engine is not used for propulsion.

Signal was sent by controller to the pump to change mode from motor mode (mode 3) to pump mode (mode 4). Here the brake is applied and the pump starts to capture kinetic energy. The fluid flows back to accumulator for charging and this time the charging is done by the pump and not from the power pack. When the mode changes from motor mode to pump mode (155s to 170s), the pressure drops during the interchange of motor mode to pump (145s to 155s). When the system pressure drops, the gas in the accumulator expands to release energy (Daines, 2012). Pressure drops happen due to the weakness of the controller where the controller signal is slower when delivering the input to the pump and therefore delay exists between the changes of mode. There is also a possibility that the fluid flowing at a length of time results in energy loss in pipeline (Zones, 2012).

However after the 10 second delays, the system manages to change from motor mode to pump mode (mode 4). The pressure captured in pump mode is lower than in motor mode. Here it can be seen that the energy capture during braking is less compared to

energy from power pack charging. As power pack charging is form the 3 phase motor, the accumulator can be charge to full. However, for pump mode, the ability of the system to capture energy during braking is proven but the amount of energy captured is lower because the flywheel weight small compared to a 5 ton lorry (actual HRBS condition). The heavier the weight of the vehicle, the more energy can be absorbed during braking (Lindzus & Contact, 2010).

Since the pressure captured is lower than the pressure from accumulator charged by power pack, it is noted that there may be a relation between pressure and life span of flywheel spin. This is because the flywheel only manages to spin for 25 seconds before the signal is sent to stop the test and the flywheel stops spinning. Therefore, test number 5 is conducted to verify this assumption on the relation between pressure and the life span of flywheel spin.

In this test, the control system is operated from minimum 50bar to 80bar. The error signal is define as the difference between the demand set of point (pressure variation) and the instantaneous rig power (Jefferson & Ackerman, 1996). The conditions of the system are set to constant and the pressure supply to the system is varied from 50bar to 80 bar. The result can be observed in Figure 5.14 and Figure 5.15
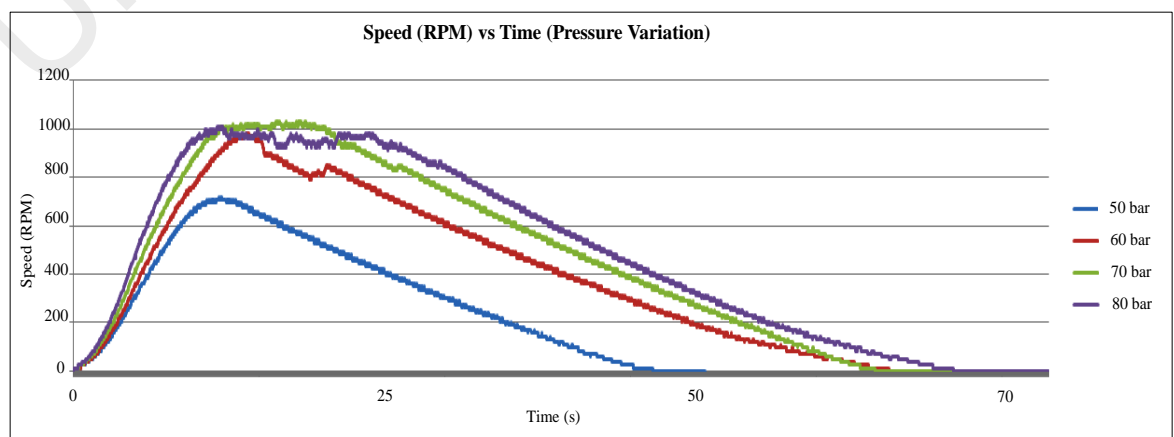
Figure 5.14 Test no. 5: Graph speed vs pressure (pressure variation).
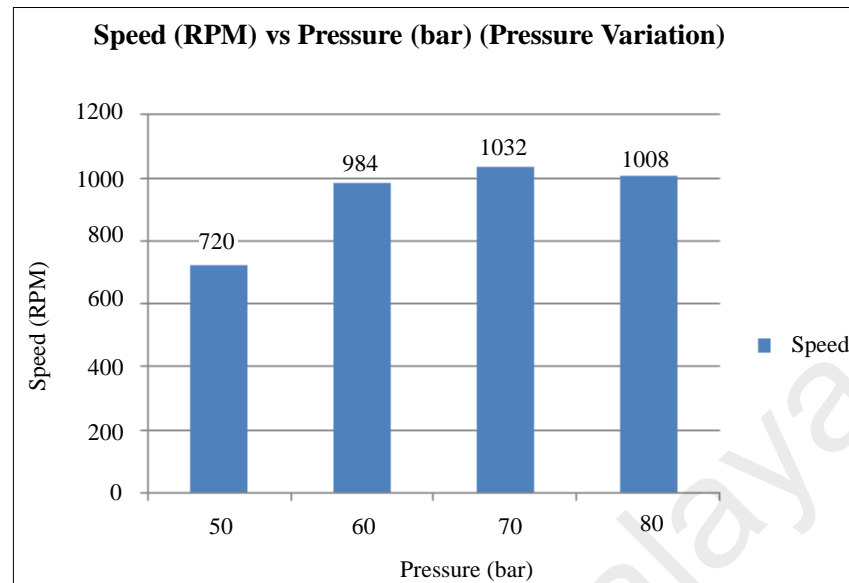
Figure 5.15 Test no.5: Graph speed vs pressure (maximum value of flywheel due to pressure variation).

The test were shows that as accumulator supplies more pressure to the system, it causes the flywheel to spin faster and longer. This can be related with Equation 2.2;

$$T = \frac{D \times P \times E_m}{2 \times \pi \times 1000} Nm \quad \text{(Kirschen, 1985)} \qquad \text{Eqn. (2.2)}$$

Where;

D= Displacement, cc/rev

P_F= Fluid pressure, kPa

E_m = Mechanical Efficiency

Whereby as the fluid pressure P_F increases, the torque of flywheel T, also increases and as the torque increases, the speed also increases as proven in Equation 2.1;

$$P_{out} = \frac{2\pi \times T \times N}{60} \, watt \qquad \text{(Kirschen, 1985)} \qquad\qquad \text{Eqn. (2.1)}$$

T = torque, Nm

N = speed, rpm

During this experiment, the maximum speed is only 1032 rpm. The speed value is smaller than the speed achieved during preliminary test which is 2013 rpm. Although the axial piston pump maximum speed is 3200 rpm, this does not affect the speed of flywheel as the factors which affect the speed is the amount of pressure supplied to the pump. The accumulator produces more fluid flow when the pressure is larger to expand pump output (Daines, 2012). Therefore to increase the flywheel speed, the pressure supplied by accumulator must be larger. It can also be observed that as the pressure supply increase, the system reaches it steady state at 70 bar.

5.4   Conclusion

In summary, the result obtained from all five tests can be very useful in designing a more accurate controller as part of improvements. In the next chapter, the conclusion will be drawn to summarize this study.

CHAPTER 6

CONCLUSION

6.1   Conclusion

This study presents a new design for a Hydraulic Regenerative Braking System (HRBS) for a 5 ton lorry and a test rig system to simulate the HRBS concept. The HRBS design is presented and verified thru a test rig system. A complete test rig system was setup and analysed analytically to evaluate its dynamic performance. The conclusions of this work based on the obtained results can be drawn as follows:

i.   A HRBS designed for minimal modification of an existing actual lorry is presented and design tested using a test rig system. Commissioning test of test rig shows that it can be used as a HRBS. This is shown through the tests performed and the results which show that the test rig has successfully captured energy during braking and released energy when accelerating (mode variation test).

ii.   The modification of the existing chassis has been successfully made and FEA has been done to check the strength of the chassis during operation. The accumulator stand and power pack stand has been successfully fabricated after FEA is done to determine the safety factor for both stands.

iii. Observation done on the commissioning test shows that when swash plate angle is varied, it is found that the it does not have any significant impact to flywheel speed because the effect of swash plate angle is small compared to force created by fluid flowing into the axial piston pump. However, the lifespan of flywheel spin can be prolonged when the swash plate angle is smaller.

iv.	It is also noted that the amount of pressure supplied by accumulator to the system is an important factor to control the speed of flywheel as the larger the pressure supplied, the faster the flywheel can spin.

v.	All the findings for pressure variation, swash plate angle variation and mode variation show that the test rig designed is able to perform as a HRBS.

## 6.2	Recommendation

It is hoped that in future this study can be extended and expanded into an actual prototype on a 5 ton lorry. The hydraulic regenerative braking system (HRBS) designed in this study is only at a beginning stage and there is more to be done to make this an economically viable and eco-friendly heavy commercial vehicle in stop & go operation to reduce fuel emission and fuel consumption. Several recommendations for improvement is list below;

i.	Based on the observation done on commissioning test, the controller can be further improved for more accurate data capture.

ii.	A used engine can be attached to the system to test the emissions of the system. By attaching the engine to the system, an actual test to check the emission from the system can be observed.

iii.	Addition of safety valve can be included in the test rig system and therefore the accumulator pressure can be increased to more than 85 bars (current study). By increasing the pressure of the accumulator, the flywheel can spin at a faster speed and more energy can be captured. The test rig can therefore be used to test at speeds higher than 10 km/h (current study).

RESEARCH OUTPUT

Journal Paper

    i.   **M. Z. Norhirni**, M. Hamdi, N.A. Mardi, N. Hilman, *Development Of A Test Rig For Hydraulic Regenerative Braking System (HRBS),* ASEAN Engineering Journal, June 2012 (Non-ISI).

    ii.   **M. Z. Norhirni**, M. Hamdi, S. Nurmaya Musa, L.H. Saw, N.A. Mardi, N. Hilman, *Design and Modelling of Swash Plate in Axial Piston Pump* (2011), Journal of Dynamic Systems, Measurement and Control, November 2011, Volume 133, Issue 6, 064505 (ISI).

Conference

    i.   **M. Z. Norhirni** and N. A. Mardi, *Feasibility study of Regenerative Hydraulic Braking System for Small Lorry Vehicle,* Regional Conference in Mechanical and Aerospace Technology, The 4th *RCMeAe2012*.

    ii.   **M. Z. Norhirni**, L.H. Saw and N. Hilman, *Simulation of crash analysis of parallel HHV based on High Precision Nonlinear FEA,* International Conference on Sustainable Mobility 2010.

    iii.   **M. Z. Norhirni**, L.H. Saw and N. Hilman, *Design and Development of Hydraulic Axial Piston Unit,* International Conference on Sustainable Mobility 2010.

iv. N. Hilman, L.H. Saw, M. Fadzil , M. Hamdi, **M.Z. Norhirni**, 2010, *Design and Evaluation of Regenerative Braking*, International Conference on Sustainable Mobility 2010**,** Kuala Lumpur, 1-3 December 2010.

v. N. Hilman, L.H. Saw, M. Hamdi and **M.Z. Norhirni** 2010. *Performance Evaluation of Parallel Hydraulic Hybrid Vehicle using EPA US06 Aggressive Drive Cycle Simulation.* Proceedings of the 5th AOTULE International Postgraduate Student Conference on Engineering, Bandung, Indonesia, 1-2 November 2010.

Awards

i. Bronze Medal **-** Malaysian Technology Expo 2011

Hydraulic Regenerative Braking System (HRBS) for Small Commercial Vehicle.

Name of PI   : Professor Dr. Mohd Hamdi Abd Shukor

Name of Team Member   : Dr. Noor Azizi b. Mardi

                        a. : Mohd Fadzil Jamaludin

                        b. : **Norhirni Binti Md Zahir**

                        c. : Mohamad Hilman Bin Nordin

                        d. : Bernard Saw Lip Huat

REFERENCES

A

Abuhaiba, M., & Olson, W. W. (2010). Geometric and Kinematic Modeling of a Variable Displacement Hydraulic Bent-Axis Piston Pump. Journal of Computational and Nonlinear Dynamics, 5.

Achten, P. A. J. A serial hydraulic hybrid drive train for off-road vehicles. Assigned by IFPE Staff, Innas BV.

B

Beer, F. P., Johnston, E. R., & Jr., J. T. D. (2006). Vector Mechanics for Engineers Statics and Dynamics,. Chapter 7.

Bitterlin, I. F. (2010). Flywheel Energy Storage: an alternative to batteries in UPS Systems (pp. 5-7,9).

Bitterlin, I. F. (2010). Flywheel Energy Storage: an alternative to batteries in UPS Systems (pp. 5-7,9).

BMW. (2007). Vision BM. Innovative Automotive Transmissions.

Boretti, A. (2010). Comparison of Fuel Economies of High Efficiency Diesel and Hydrogen Engines Powering A Compact Car With A Flywheel Based Kinetic Energy Recovery Systems. International Journal of Hydrogen Energy 35, 8417-8424.

Bracht, D. v., Ehret, C., & Kliffken, M. G. (2009). Hybrid Drives for Mobile Equipment An event. 2nd Symposium of the VDMA and the University of Karlsruhe (TH).

Burdekin, F. M. (2007). General principles of the use of safety factors in design and assessment. Engineering Failure Analysis, 14 X, 420–433.

Bylsma, W. (2003). Spreadsheet Accumulator Sizing for Hybrid Hydraulic Applications Using the Benedict-Webbrubin Equation of State. Tardec-Technical Report, 13942.

C

Carnago, R., Koch, S., Pawlik, B., & Smith, P. (2007). Challenge X: Regenerative Brake Pedal Design. University of Michingan.

Chan, K. H. (2010). Design and Development of Regenerative Braking Test Rig. Desertation.

Corporation, B. R. (2004). Variable Displacement Pump A4VSG. Spread Sheet.

D

Daines, J. R. (2012). Fluid Power. [Slide presentation].

Della, R. M., & Rand, D. A. J. (2001). Energy storage: A key technology for global energy sustainability. Journal of Power Sources, 100, 2–17.

Driedger, W. (1996). Controlling Positive Displacement Pumps. Hydrocarbon Processing.

G

Gholami, T., Lescheticky, J., & Pabmann, R. (2003). Crashworthiness Simulation of Automobiles with ABAQUS/Explicit. ABAQUS user conference.

Gould, R. R. (2010). Pumps. CFPE, VP engineering, Advanced Lifts Inc., St. Charles, Ill.

Group, M. (2012). What is FEA? http://www.mip-group.com/technical/fea-general.htm.

H

Handbook, E. s. (2012). Reference Tables -- Fluid Power Formulas. http://engineershandbook.com/Tables/fluidpowerformulas.htm.

Hoffma, E. G., & McCauley, C. J. (2001). Shop reference for Students and apprentices. Machinery's Handbook, IndustrialPress, 2

Horng, J.-H. (2008). Hybrid MATLAB and LabVIEW with neural network to implement a SCADA system of AC servo motor. Advances in Engineering Software, 39, 149–155.

Hui, S., & Junqing, J. (2010). Research on the system configuration and energy control strategy for parallel hydraulic hybrid loader. Automation in Construction, 19, 213–220.

Hui, S., Ji-hai, J., & Xin, W. (2009). Torque control strategy for a parallel hydraulic hybrid vehicle. Journal of Terramechanics, 46, 259–265.

Hui, S., Lifu, Y., Junqing, J., & Yanling, L. (2010). Control strategy of hydraulic/electric synergy system in heavy hybrid vehicles. Energy Convers Manage 52, 668–674.

I

Inc., R. F. P. (2012). Accumulator Operation and Applications. http://www.rhmfp.com/tech-tips/165-applyingaccumulators.

International, H. (2003). Bladder Accumulators Standard. Operating Manual.

ISUZU. (1999). [Manual]. ISUZU NKR.

J

Jefferson, C. M., & Ackerman, M. (1996). Flywheel Variator Energy Storage System Energy Conversion Management. Energy Conversion and Management, 37(Issue 10), 1481-1491.

K

Kaliafetis P., & et al. (1995). Modelling and simulation of an axial piston variable displacement pump with pressure control. Mechanical Machine Theory, 30(4), 599-612.

Kaliafetis, P. (1995). Modelling and simulation of an axial piston variable displacement pump with pressure control. Mechanical Machine Theory, 30(4), 599-612.

Khoo, J. H. (2010). Finite Element Analysis of Parallel Hydraulic Hybrid Vehicle. Department of Engineering Design and Manufacture, Faculty of Engineering, University of Malaya

Kim, S. D. (1987). A parameter sensitivity analysis for the dynamic model of a variable displacement axial piston pump. Proceedings of the institution of Mechanical Engineers,, 201, 235-243.

Kirschen, D. S. (1985). On-Line Efficiency Optimization of a Variable Frequency Induction Motor Drive. IEEE Transactions On Industry Applications 21(4).

L

Li, P. Y., Ven, J. D. V. d., & Sancken, C. (2007). Open Accumulator Concept For Compact Fluid Power Energy Storage ASME 2007 International Mechanical Engineering Congress and R&D Exposition.

Lin, T., Hu, Q. W. B., & Gong, W. (2010). Research on the energy regeneration systems for hybrid hydraulic excavators Automation in Construction 19 1016–1026.

Lindzus, E., & AG, B. R. (2010). HRB – Hydrostatic Regenerative Braking System: The Hydraulic Hybrid Drive from Bosch Rexroth. www.boschrexroth.com.

Lindzus, E., & Contact. (2010). HRB – Hydrostatic Regenerative Braking System: The Hydraulic Hybrid Drive from Bosch Rexroth. Bosch Rexroth AG.

M

McKillop, A. (2011). The Chinese Car Bomb.

N

Norhirni, M. Z. (2011). Load and Stress Analysis for the Swash Plate of an Axial Piston Pump/Motor. Journal of Dynamic Systems, Measurement and Control.

P

Pete. (2008). Hydraulic Accumulators.

R

Rexroth, B. (2011). Injection Molding Machines: Hybrid Injection Molding Machines.

Rexroth, E. M. (2012). Hydraulic-Training Axial Piston Unit. http://www.insanehydraulics.com/library/files/Hydraulic-Trainings-for-Axial-Piston-Units.pdf.

S

Saw, L. H. (2010). Simulation of crash analysis of parallel hydraulic hybrid vehicle based on High Precision Nonlinear Finite Element Analysis. Paper presented at the International Conference on Sustainable Mobility 2010, Kuala Lumpur, Malaysia.

Shenron. (2008). http://www.4x4truckstrailers.com/what-is-a-truck-differential.

Stecki, J., & Matheson, P. (2005). Advances in Automotives Hydraulic Hybrid Drives. Proceedings of the 6th JFPS International Symposium on Fluid Power, TSUKUBA

Stringer, J. (1976). Hydraulic systems analysis: An introduction The Macmillan Press LTD, 79-80.

Suzuki, Y., Koyanagi, A., Kobayashi, M., & Shimada, R. (2005). Novel applications of the flywheel energy storage system. Energy 30, 2128–2143.

Swing, R. (2008). Hydraulic Hybrid Vehicle Control System. [Desertation]. Department of Electrical and Computer Engineering, Colorado State University.

Swing, R. (2008a). Hydraulic Hybrid Vehicle Control System. Colorado State University.

Swing, R. (2008b). Hydraulic Hybrid Vehicle Control System. [Desertation]. Department of Electrical and Computer Engineering, Colorado State University.

T

Thompson, A. W. (1980). Automotive drive shafts. Philosophical transaction; Mathematical, Physical and Engineering Sciences, The Royal Society, 577-582.

V

Ven, J. D. V. d. (2009). Increasing Hydraulic Energy Storage Capacity: Flywheel-Accumulator International Journal of Fluid Power.

Vint, M. K., & Gilmore, D. B. (1988). Simulation of Transit Bus Regenerative Braking Systems Mathematics and Computers in Simulation 30 55-61.

Vista, B. (2011). http://pirate4x4.com/tech/billavista/PR-shaft/index.html.

Z

Zhai, P. S. (1978). Swash Plate type Axial Piston Pump Design. China, Coal Industry Publisher.

Zones, T. (2012). Hydraulic Accumulators. Hydraulics & Pneumatics.

ATTACHMENT

IDEA GENERATION

Development of a test rig for hydraulic regenerative braking system

Development

Idea: Flywheel system

Product to produce: HRBS system

HOW?

Understanding of flywheel system

Theory and idea generation for HRBS

Test rig to test the idea of HRBS

Can the system work as HRBS?

Can it regenerate energy by using the system designed?

Conclusion on HRBS system

Recommendation to improve system

Idea generation of the research.

GANTT CHART

	Task/ Month	1	2	3	4	5	6	7	8	9	10	11	12	13	14	15	16	17	18	19	20	21	22	23	24
1	Literature Review & Field Visit	█	█	█	█	█	█	█	█	█	█	█	█	█	█	█	█	█	█	█	█	█	█	█	█
2	Problem Analyzing	█	█																						
3	Concept design of test rig system			█	█																				
4	Design specification of test rig system				█	█	█																		
5	Mathematical modelling and simulation							█	█																
6	3D modelling of test rig mechanical parts										█	█	█												
7	Purchasing pump and accumulator			█	█	█	█	█	█	█	█	█	█	█	█	█									
8	Finite element analysis of parts										█	█	█	█											
9	Fabrication of test rig structure													█	█	█									
10	Controller integration															█	█								
111	Trouble shoot test rig system																	█	█						
12	Test rig functional testing																			█	█	█			
13	Report writing & completion of study																					█	█	█	█

	Milestone/Month	1	2	3	4	5	6	7	8	9	10	11	12	13	14	15	16	17	18	19	20	21	22	23	24
1	Completion of test rig specification						█																		
2	Completion of detail design of test rig											█													
3	Completion of test rig structure															█									
4	Experimentation																					█			
5	Thesis write-up																								█

Gantt chart for Design and Development of Hydraulic Regenerative Braking System

FLOWCHART

```
        ┌─────────────────────────────────┐
        │   Literature review & Field visit│
        └─────────────────────────────────┘
                      │
        ┌─────────────────────────────────┐
        │       Problem analyzing          │
        └─────────────────────────────────┘
                      │
        ┌─────────────────────────────────┐
        │   Concept design of test rig system│
        └─────────────────────────────────┘
                      │
        ┌─────────────────────────────────┐      ┌──────────────────┐
        │ Design specification of test rig │─────▶│ Planning material│
        │            system                │      │   requirement    │
        └─────────────────────────────────┘      └──────────────────┘
                      │                                    │
        ┌─────────────────────────────────┐               │
        │   Mathematical modeling & simulation│            │
        └─────────────────────────────────┘               │
                      │                                    │
        ┌─────────────────────────────────┐               │
        │ 3D Modeling of test rig mechanical parts│        │
        └─────────────────────────────────┘               │
                      │                                    │
        ┌─────────────────────────────────┐               │
        │   Finite Element Analysis of parts│             │
        └─────────────────────────────────┘               │
                      │                                    │
        ┌─────────────────────────────────┐               │
        │   Fabrication of test rig structure│◀────────────┘
        └─────────────────────────────────┘
                      │
        ┌─────────────────────────────────┐
        │     Controller integration       │
        └─────────────────────────────────┘
                      │
        ┌─────────────────────────────────┐
        │   Trouble shoot test rig system  │
        └─────────────────────────────────┘
                      │
   ┌──────────────┐   No    ◇───────────────◇
   │ Modification │◀────────   Functioning?
   └──────────────┘         ◇───────────────◇
                                   │ Yes
        ┌─────────────────────────────────┐
        │    Test rig functional testing   │
        └─────────────────────────────────┘
                      │
              ◇───────────────◇
                  Objectives
                  achieved?
              ◇───────────────◇
                      │
        ┌─────────────────────────────────┐
        │ Report writing & completion of study│
        └─────────────────────────────────┘
```

Flow chart of study for Development of Hydraulic Regenerative Braking System.

SUPPLIER LIST

No.	Item	Contact
1.	Hydropneumatic Bladder Accumulator	Hydac
2.	A4VSG Axial Piston Pump, A4VSO Axial Piston Pump, Piping for HRBS System, Power Pack, Accumulator Safety Block, Bell Housing, Relief Valve.	Bosch Rexroth Sdn Bhd (41112-D) 11, Jalan Astaka U8/82, Bkt. Jelutong, 40150 Shah Alam, Selangor Darul Ehsan, Telephone +603 78448000 Telefax +603 78454800 www.boschrexroth.com.my
3.	Speed Sensor.	DAG Technlogies, No 12A, Jalan 17/155C, Bandar Bukit Jalil, 57000 Kuala Lumpur. Tel: (+603) 8994 9590 Fax: (+603) 8994 9591 E-mail: hotline@dagtech.com.my
5.	DAQ Card.	National Instruments, Virtual Instruments Sdn Bhd. Wisma Kemajuan, Jalan 19/1, Suite L 2-1, Level 2, 46300 Petaling Jaya, Selangor. Tel: +603-7948 2000 Fax: +603-7955 2000
6.	Journal Bearing, Coupling.	Power Hardware & Trading Sdn Bhd 130, Jalan SS 24/2, Taman Megah, 47301 Petaling Jaya, Selangor Tel: 03 78049888 Fax: 03- 78040728
7.	Brake, Disc Brake.	Power Hardware & Trading Sdn Bhd 130, Jalan SS 24/2, Taman Megah, 47301 Petaling Jaya, Selangor Tel: 03 78049888 Fax: 03- 78040728
8.	Vacuum generator	Pusaco Industrial Supplies SDN BHD No. 12 Jalan PJU3/48, PJU3, Sunway Damansara, 47810 Petaling Jaya, Selangor Tel: 03-7880 8899 Fax: 03-7880 4488
9.	Vacuum generator	Pusaco Industrial Supplies SDN BHD No. 12 Jalan PJU3/48, PJU3, Sunway Damansara, 47810 Petaling Jaya, Selangor Tel: 03-7880 8899 Fax: 03-7880 4488

10.	Flywheel Material	N.S Machinery Enterprise Lot 35, Section 92 & 92A, Batu 3 ½ , Jalan Sg. Besi, 57100 Kuala Lumpur. Tel: 03- 7839608 Fax: 03- 7809 155
11.	Flywheel Fabrication	In house, Workshop Jabatan Rekabentuk dan Pembuatan, Fakulti Kejuruteraan, University of Malaya
12.	Accumulator & Power Pack stand.	Monzir Design Productions Sdn Bhd. 811122-H No. 74, Jalan BK 5/8B, Bandar Kinrara, 47100 Puchong, Selangor Darul Ehsan Tel : 03-80700807 Fax : 03-80700329 Email: sales@monzirdesign.com Website : www.monzirdesign.com
13.	Hydraulic Oil- Shell tellus VG 46, 20 Litre.	EP Marketing Enterprise 29-3A, Jalan Puteri 2/3, Bandar Puteri, 47100 Puchong, Selangor, Malaysia. Tel: +603-8063 5168 Fax: +603-8063 5169 Mobile: +60 16 626 1162 (Hugo Phang)
14.	Inverter SV022 LS 3HP/2.2KW.230V	Speed Drive & Automation Sdn Bhd, No. 29, Jalan BP 6/3, Bandar Bukit Puchong, 47100 Puchong, Selangor. Tel: 603- 806 13212, 016-335 5575 Fax: 603- 806 15668 Email: speeddrv@streamyx.com
15.	5 Tonne Lorry	Soon Lee Car Auto Part, No. 3& 5, Lrg Perusahaan 1, Kimpalan Ind. Park, 68100 Kuala Lumpur. Tel: 03-6186 8588
16.	Chassis material	Power Hardware & Trading Sdn Bhd 130, Jalan SS 24/2, Taman Megah, 47301 Petaling Jaya, Selangor Tel: 03 78049888 Fax: 03- 78040728
17.	Plate for Bell Housing, Flywheel Cage, Metal Work for Test Rig Structure.	SH Bina, Blok D6, T4-8, Taman Melati, 53100 Kuala Lumpur. Tel: 013-388 5008 (En. Suhaimi)

COSTING

No.	Item	Qty	Price per item	Price
1.	Axial Piston Pump	1	19,500.00	19,500.00
2.	Accumulator		3,864.00	7,728.00
3.	Amplifier card with holder	1	8,430.00	8,430.00
4.	Valve, manifold block and accessories for installation		2,300.00	2,300.00
5.	DAQ Card.	1	4,840.00	4,840.00
6.	Inverter SV022 LS	1	980.00	980.00
7.	Bell housing	1	1,050.00	1,050.00
8.	Vacuum generator	1	182.25	182.25
9.	Shell tellus	6	159.00	954.00
10.	Cage	1	560.00	560.00
11.	Flywheel and coupling		1,700.00	1,700.00
12.	ROS sensor	1	915.00	915.00
			TOTAL	49,139.25

CONVERSION UNIT

1 mph=0.4470 m/s

kph: s x RPM= 1.5708m x 2000RPM= 3140 m/min= 3.14 km/min

1 rpm = 1/min = 1/(60s) = 1/60 Hertz $\approx$ 0.01667 Hz

1 rpm= 2π rad·min^{-1}= $2\pi/60$ rad·s^{-1}= 0.1047 rad·s^{-1} $\approx$ 1/10 rad·s^{-1}

Test   :   Gas Analyzer
Place   :   Sunway
Date   :   23/7/09
Time   :   4.00 pm
Test equipment :   DynoJet
                :   Automobile Emission 4/5 Analyzer -Autochek
Type of fuel   :   Gasoline
Objective   :   To test the lorry engine

1st Gear 1 Run

	RPM		
	1000	2000	3000
CO2 (%)	1.97	2.93	4.67
CO2 (%)	0.01	0.02	0.04
HC (ppm)	6	8	11
O2 (%)	17.28	16.37	16.32
LAMBDA	3.0	3.0	3.0
AFR	25.0	25.0	25.0

1st Gear 2 Run

	RPM		
	1000	2000	3000
CO2 (%)	1.44	1.84	3.66
CO2 (%)	0.01	0.01	0.02
HC (ppm)	5	5	6
O2 (%)	14.06	18.34	16.31
LAMBDA	3.0	3.0	3.0
AFR	25.0	25.0	25.0

2nd Gear 1 Run

	RPM		
	1000	2000	3000
CO2 (%)	2.87	3.90	2.94
CO2 (%)	0.01	0.02	0.03
HC (ppm)	4	6	5
O2 (%)	17.91	16.45	14.68
LAMBDA	3.00	3.00	3.00
AFR	25.0	25.0	25.0

2nd Gear 2 Run

	RPM		
	1000	2000	3000
CO2 (%)	3.19	3.60	0.02
CO2 (%)	0.01	0.01	0.01
HC (ppm)	0	0	2
O2 (%)	18.3	16.7	20.88
LAMBDA	3.00	3.00	0.00
AFR	25.0	25.0	25.0

3rd Gear 1 Run

	RPM		
	1000	2000	3000
CO2 (%)	2.94	2.08	2.07
CO2 (%)	0.61	0.02	0.02
HC (ppm)	9	11	13
O2 (%)	16.35	15.5	15.05
LAMBDA	3.00	3.00	3.00
AFR	25.0	25.0	25.0

3rd Gear 2 Run

	RPM		
	1000	2000	3000
CO2 (%)	3.19	0.00	0.01
CO2 (%)	0.01	0.00	0.00
HC (ppm)	0	3	2
O2 (%)	18.3	21.08	21.09
LAMBDA	3.00	3.00	0.00
AFR	25.0	5.0	5.0

4th Gear 1 Run

	RPM		
	1000	2000	3000
CO2 (%)	2.36	2.57	2.23
CO2 (%)	0.01	0.01	0.02
HC (ppm)	3	3	5
O2 (%)	18.78	18.33	14.07
LAMBDA	3.00	3.00	2.76
AFR	25.0	25.0	25.0

4th Gear 2 Run

	RPM		
	1000	2000	3000
CO2 (%)	1.58	2.76	5.83
CO2 (%)	0.01	0.02	0.03
HC (ppm)	4	2	0
O2 (%)	18.7	17.54	15.27
LAMBDA	3.00	3.00	3.00
AFR	25.0	25.0	25.0
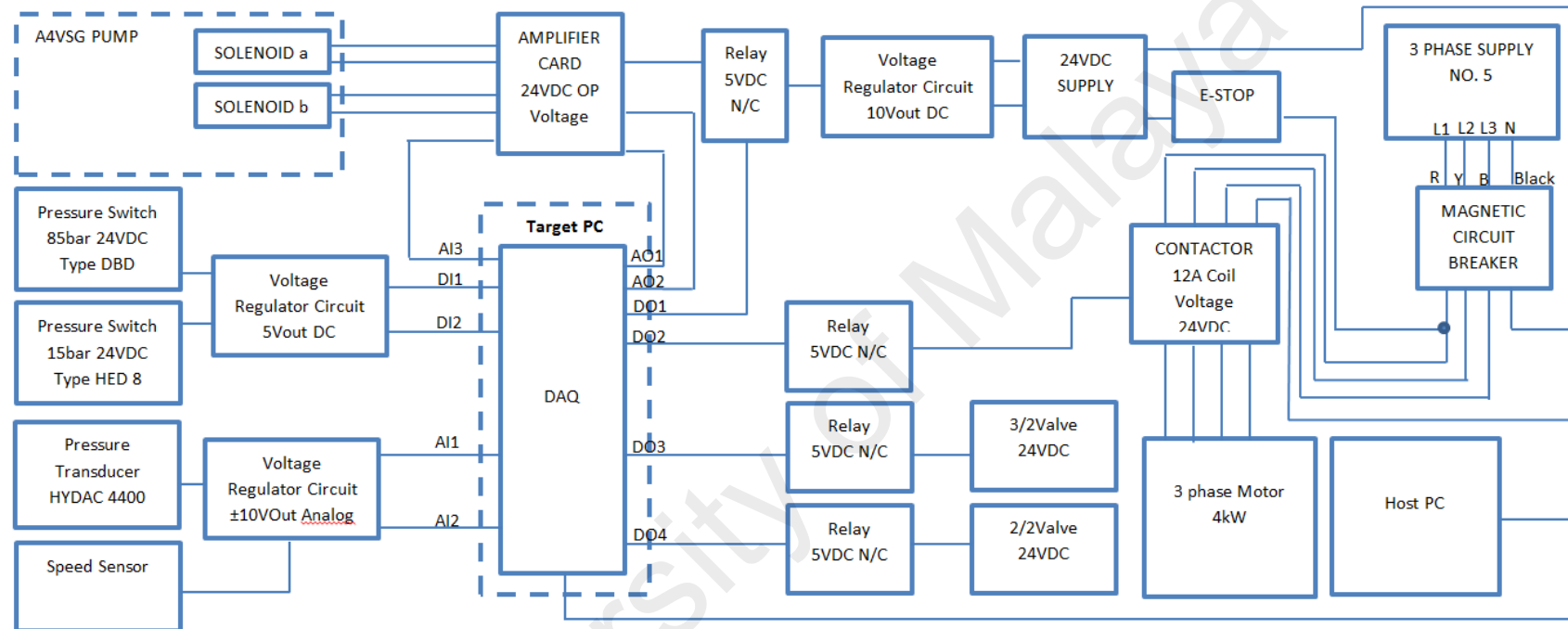
Input	Signal	Descriptions
Digital Input 1 (DI1)	0V, 5V	85 bar P switch
Digital Input 2 (DI2)	0V, 5V	85 bar P switch
Analog Input 1 (AI1))		Pressure Transducer
Analog Input 2 (AI2)		Speed Sensor
Analog Input 3 (AI3)	0 to 6V	Actual swivel angle "x"

Output	Signal	Description
Digital Output 1 (DO1)	0V, 5V	Supply 10V as enable
Digital Output 2 (DO2)	0V, 5V	Contactor
Digital Output 3 (DO3)	0V, 5V	3/2 Valve
Digital Output 4 (DO4)	0V, 5V	2/2 Valve
Analog Output 1 (AO1)	0 to ±10 V	Swash plate angle
Analog Output 2 (AO2)		Ramp time

BRAKING ENERGY OF LORRY

BRAKING ENERGY OF FLYWHEEL

RPM	ω, rad/s	Flywheel Energy
420	43.9880	3.86853
440	46.0827	4.24574
460	48.1773	4.64049
480	50.2720	5.05278
500	52.3667	5.48262
520	54.4613	5.93000
540	56.5560	6.39492
560	58.6507	6.87739
580	60.7453	7.37741
600	62.8400	7.89497
620	64.9347	8.43007
640	67.0293	8.98272
660	69.1240	9.55291
680	71.2187	10.14065
700	73.3133	10.74593
720	75.4080	11.36875
740	77.5027	12.00912
760	79.5973	12.66704
780	81.6920	13.34249
800	83.7867	14.03550
820	85.8813	14.74604
840	87.9760	15.47414
860	90.0707	16.21977
880	92.1653	16.98295
900	94.2600	17.76368
920	96.3547	18.56194
940	98.4493	19.37776

Velocity, V (km/h)	v(m/s)	Braking energy, J (5000kg)
0	0	0
2	0.5556	0.7716
4	1.1111	3.0864
6	1.6667	6.9444
8	2.2222	12.3457
10	2.7778	19.2901
12	3.3333	27.7778
14	3.8889	37.8086
16	4.4444	49.3827
18	5.0000	62.5000
20	5.5556	77.1605
22	6.1111	93.3642
24	6.6667	111.1111
26	7.2222	130.4012
28	7.7778	151.2346
30	8.3333	173.6111

RPM	ω, rad/s	Flywheel Energy
0	0.0000	0
20	2.0947	0.00877
40	4.1893	0.03509
60	6.2840	0.07895
80	8.3787	0.14035
100	10.4733	0.21930
120	12.5680	0.31580
140	14.6627	0.42984
160	16.7573	0.56142
180	18.8520	0.71055
200	20.9467	0.87722
220	23.0413	1.06143
240	25.1360	1.26319
260	27.2307	1.48250
280	29.3253	1.71935
300	31.4200	1.97374
320	33.5147	2.24568
340	35.6093	2.53516
360	37.7040	2.84219
380	39.7987	3.16676
400	41.8933	3.50887

960	100.5440	20.21112	1500	157.1000	49.34354
980	102.6387	21.06202	1520	159.1947	50.66814
1000	104.7333	21.93046	1540	161.2893	52.01029
1020	106.8280	22.81645	1560	163.3840	53.36998
1040	108.9227	23.71999	1580	165.4787	54.74721
1060	111.0173	24.64107	1600	167.5733	56.14199
1080	113.1120	25.57969	1620	169.6680	57.55431
1100	115.2067	26.53586	1640	171.7627	58.98418
1120	117.3013	27.50957	1660	173.8573	60.43159
1140	119.3960	28.50083	1680	175.9520	61.89654
1160	121.4907	29.50963	1700	178.0467	63.37904
1180	123.5853	30.53598	1720	180.1413	64.87908
1200	125.6800	31.57987	1740	182.2360	66.39667
1220	127.7747	32.64130	1760	184.3307	67.93180
1240	129.8693	33.72028	1780	186.4253	69.48448
1260	131.9640	34.81680	1800	188.5200	71.05470
1280	134.0587	35.93087	1820	190.6147	72.64247
1300	136.1533	37.06248	1840	192.7093	74.24778
1320	138.2480	38.21164	1860	194.8040	75.87063
1340	140.3427	39.37834	1870	195.8513	76.68864
1360	142.4373	40.56259			
1380	144.5320	41.76438			
1400	146.6267	42.98371			
1420	148.7213	44.22059			
1440	150.8160	45.47501			
1460	152.9107	46.74698			
1480	155.0053	48.03649			

Data from

BOSCH

ø350
ø301
ø140
ø96
10

234
26
70
10
140

ø140
ø350
ø450

M16
M12
ø18
400
180
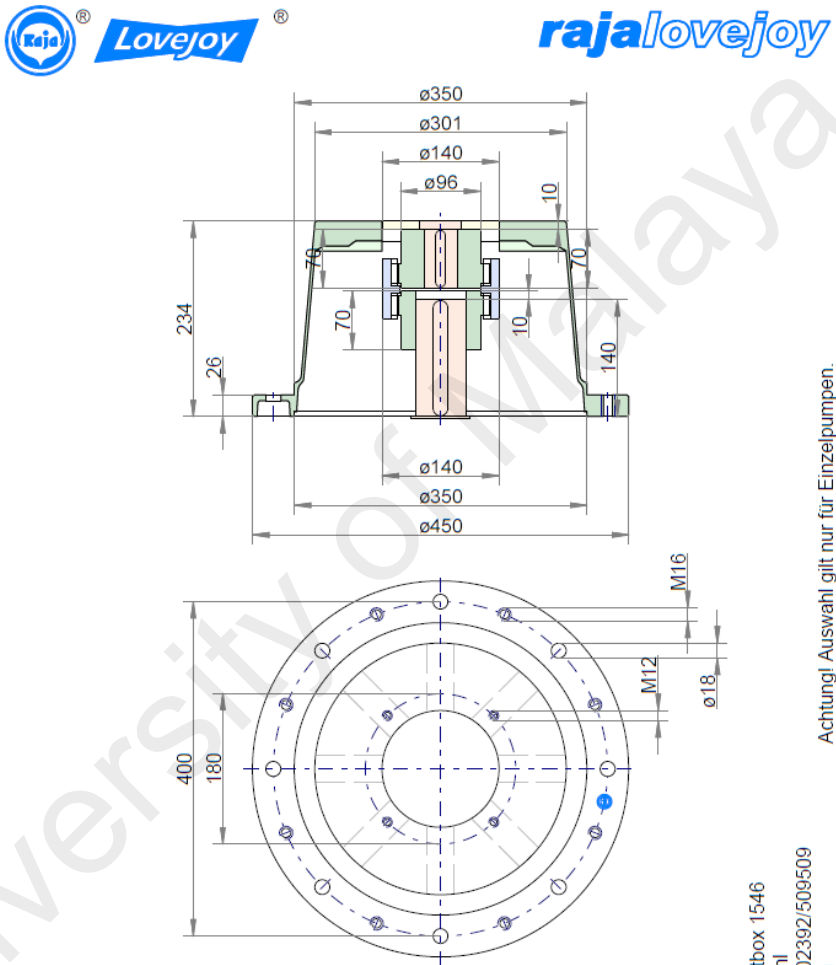
Achtung! Auswahl gilt nur für Einzelpumpen.

Pumpe	Rexroth A4VSG NG 71 Welle P
IEC (50Hz)-Motor	1500 RPM 37.00 kW 225S IM B5/V1 ø450
Raja-Pumpenträger	RV450/234/270
Raja-Dämpfungsflansch	ohne
Raja-Kupplung	Dentex B65.60H7-40H7 Si
Zubehör	ohne / ohne